A STUDY OF THE OXYGEN ELECTROCHEMISTRY OF RUTHENIUM AND IRIDIUM

THESIS PRESENTED FOR THE

Ph. D. DEGREE

OF THE

NATIONAL UNIVERSITY OF IRELAND

by

Denis Noel Buckley, B.Sc.

Department of Chemistry

University College, Cork

SEPTEMBER 1975

ACKNOWLEDGEMENTS

I am indebted to my supervisor, Dr. L.D. Burke, for his excellent direction at every stage of the work without which this thesis would not have been possible.

I wish to thank especially Mr. J. K. Mulcahy and Dr. S. Venkatesan for invaluable assistance with the diagrams. My sincere gratitude also to Dr. S. Corkery, to Mr. S. Downey and his technical staff and to all my colleagues in the Department.

I gratefully acknowledge a Maintenance Grant for Research from the Irish Government.

Finally, I wish to thank most sincerely Miss Marie McSweeney for doing such a superb job of typing the manuscript in such a short time.

ABSTRACT

This thesis is concerned with an investigation of the anodic behaviour of ruthenium and iridium in aqueous solution and particularly of oxygen evolution on these metals. The latter process is of major interest in the large-scale production of hydrogen gas by the electrolysis of water.

The presence of low levels of ruthenium trichloride ca. 10^{-4} mol dm^{-3} in acid solution give a considerable increase in the rate of oxygen evolution from platinum and gold, but not graphite, anodes. The mechanism of this catalytic effect was investigated using potential step and a.c. impedance technique. Earlier suggestions that the effect is due to catalysis by metal ions in solution were proved to be incorrect and it was shown that ruthenium species were incorporated into the surface oxide film. Changes in the oxidation state of these ruthenium species is probably responsible for the lowering of the oxygen overvoltage. Both the theoretical and practical aspects of the reaction were complicated by the fact that at constant potential the rates of both the catalysed and the uncatalysed oxygen evolution processes exhibit an appreciable, continuous decrease with either time or degree of oxidation of the substrate.

The anodic behaviour of iridium in the oxide layer region has been investigated using conventional electrochemical techniques such as cyclic voltammetry. Applying a triangular voltage sweep at 10 Hz, 0.01 to 1.50 V increases the amount of electric charge which the surface can store in the oxide region. This activation effect and the mechanism of charge storage

is discussed in terms of both an expanded lattice theory for oxide growth on noble metals and a more recent theory of irreversible oxide formation with subsequent stoichiometry changes. The lack of hysteresis between the anodic and cathodic peaks at ca. 0.9 V suggests that the process involved here is proton migration in a relatively thick surface layer, i.e. that the reaction involved is some type of oxide-hydroxide transition. Lack of chloride ion inhibition in the anodic region also supports the irreversible oxide formation theory; however, to account for the hydrogen region of the potential sweep a compromise theory involving partial reduction of the outer regions of iridium oxide film is proposed. The loss of charge storage capacity when the activated iridium surface is anodized for a short time above ca. 1.60 V is attributed to loss by corrosion of the outer active layer from the metal surface.

The behaviour of iridium at higher anodic potentials in acid solution was investigated. Current-time curves at constant potential and Tafel plots suggested that a change in the mechanism of the oxygen evolution reaction occurs at ca. 1.8 V. Above this potential, corrosion of the metal occurred, giving rise to an absorbance in the visible spectrum of the electrolyte (λ_{max} = 455 nm). It is suggested that the species involved was IrO_2^{2+}. A similar investigation in the case of alkaline electrolyte gave no evidence for a change in mechanism at 1.8 V and corrosion of the iridium was not observed. Oxygen evolution overpotentials were much lower for iridium than for platinum in both acidic and alkaline solutions.

CONTENTS

Page

CHAPTER I : INTRODUCTION

1.1. The electrical double layer 1

1.2. Electrical potentials across interfaces 2

1.3. Interfacial tension and the potential of zero-charge 6

1.4. Differential capacitance and the structure of the double layer 8

1.5. Equilibrium electrode potential and the thermodynamics of electrode processes 13

1.6. Electrode kinetics 17

1.7. The mechanism of electron transfer 22

1.8. Consequences of the Butler Volmer equation 24

1.9. The oxygen electrode 27

1.10. Oxide filmson noble metals 28

1.11. Oxide filmson active metals 34

1.12. The role of oxide films in the oxygen evolution reaction 36

1.13. The mechanism of oxygen evolution 39

1.14. Ruthenium and iridium as substrates for oxygen evolution 42

CHAPTER II : EXPERIMENTAL

2.1. Galvanostatic methods 44

2.2. The basic potentiostatic method 48

Page

2.3. Error associated with solution resistance 53

2.4. Automatic compensation of solution iR error ... 58

2.5. Electrodes and cells 62

CHAPTER III : RUTHENIUM

3.1. Anodic oxide films on ruthenium 68

3.2. The anodic properties of thermally-prepared ruthenium dioxide films 72

3.3. Oxygen evolution and corrosion 75

3.4. Investigation of oxygen evolution at noble metal electrodes in the presence of ruthenium salts 77

Results

3.5. Charging curve experiments 78

3.6. Potential-step experiments 80

3.7. A.c. polarography and potential sweep measurements 86

3.8. Effect of pH 89

3.9. Effect of electrode material 90

3.10. Discussion 93

CHAPTER IV : IRIDIUM

Part 1: The Oxide Film Region

4.1. Oxide films on iridium 98

4.2. The reversibility of the oxide formation and reduction reactions 100

Page

4.3. The present investigation 101

Results

4.4. Charging curves 102

4.5. Cyclic voltammetry 103

4.6. The activation process 108

4.7. The deactivation process 111

4.8. Visual observation of the electrode 114

4.9. Increase in oxide charge at higher potentials ... 115

4.10. Impedance measurements 117

Discussion

4.11. The expanded lattice and irreversible oxide theories 117

4.12. Hysteresis 121

4.13. The mechanism of the activation process 122

4.14. The ratio of anodic to cathodic charge.. 123

4.15. Deactivation at anodic potentials 124

4.16. The effect of added chloride ion 125

4.17. The hydrogen region 126

4.18. Comparison with related work 128

CHAPTER V : IRIDIUM

Part 2: The Oxygen Evolution Region

5.1. The corrosion of iridium 132

5.2. Oxygen evolution on iridium 136

Page

5.3. The present investigation 137

Results

5.4. The time variation of current 138

5.5. Tafel plots 138

5.6. Effect of electrolyte 142

5.7. Corrosion 142

5.8. The solution species 147

5.9. The effect of chloride ion 147

Discussion

5.10. Oxygen evolution mechanisms 150

5.11. Processes occurring at lower potentials 151

5.12. Processes occurring at higher potentials 152

REFERENCES 157

APPENDICES

Appendix 1 168

Appendix 2 169

CHAPTER I

INTRODUCTION

In the field of electrochemistry interest is often centred on phase boundaries and in particular on the interface between a metal and an electrolytic solution. The properties of the electrolyte near the interface differ from those in the bulk of the solution. There is normally an electric field across the interface, the magnitude and direction of which depends not only on the metal and the electrolyte but also on any current which may be flowing from one phase to the other. If a current is flowing a change in mechanism from ionic conduction through the electrolyte to electronic conduction through the metal occurs at the interface and is accompanied by chemical changes. These chemical changes may consist of any of a wide variety of electrochemical reactions. Examples include the electrodeposition of metal by reduction of the corresponding ions, the corrosion of metal from the electrode surface, and the oxidation of water with the formation of oxide species on the electrode surface and the evolution of oxygen gas. This thesis is concerned particularly with the latter type of reaction. However, some appreciation of the properties of the aqueous electrolyte/metal interface is prerequisite to an understanding of any electrode process in aqueous solution. A survey of these properties will therefore be given in this chapter.

1.1. The Electrical Double Layer

Under equilibrium conditions in the bulk of the electrolyte the time-averaged forces experienced by a particle such as an ion or a water molecule are isotropic. The positive and negative ions are equally distributed so that in any macroscopic region of the electrolyte there is overall electroneutrality and there is no overall preferred orientation of dipoles.

A different situation arises, however, near the interface between the electrolyte and the metal. Here a particle interacts with both the metal and the electrolyte and the forces it experiences are therefore, in general, anisotropic - those in the direction of the phase boundary are different from those in the direction of the bulk electrolyte. Thus both positive and negative ions in the interphase region will experience net forces and so a build-up of charge occurs on the electrolyte side of the boundary. This charge build-up induces an equal and opposite charge on the metal so that electroneutrality of the interphase region as a whole (both sides of the interface) is preserved. However, since each side is charged, an electric field exists across the interface. Due to their dipolar character, water molecules at the interface tend to align themselves with this field. Indeed, even in the absence of an electric field, these water molecules tend to orient themselves in a preferred direction due to the assymmetry of the forces acting on them. Thus arrays of charged particles and oriented dipoles exist at the interface. This situation is usually referred to as the electrical double layer (or simply as the double layer), a term derived from an early model of the interphase.

1.2. Electrical Potentials Across Interfaces

The double layer at a metal/electrolyte interface may be discussed in terms of two fundamental aspects, an electrical aspect and a structural aspect. The electrical aspect is concerned with the magnitude of the excess-charge density on each phase and the electrical potential difference across the interface.

Consider the problem of measuring the potential difference across the interface. This measurement may be attempted by means of a potential-detecting device such as a high impedance voltmeter. However both terminals of the meter are composed of metal and, even if this metal is the same as that of the electrode under investigation, at least one other phase boundary must still be created, i.e. a contact between a meter terminal and the solution, in order to obtain a deflection. Now this new interface will also have a potential difference associated with it which will be included in the measurement. Therefore it is found that whereas the intention was to measure the potential across one interface, the best that can be achieved is a measurement of the sum of the potentials across two interfaces. If the problem is pursued further[1] it is found that, in general it is not possible to measure the potential across a single metal/electrolyte boundary.

Even though it may not be experimentally determinable, it is useful to analyse the difference in electrical potential across a metal/electrolyte interface in some detail. In more precise terms, this may be defined as the difference in electrical potential between a point in the bulk of the metal and a point in the bulk of the electrolyte. In a general context the electrical potential of any point is defined as the energy required to overcome electrical forces in transporting unit positive charge from infinity in vacuum to the point. If this definition is applied in an experiment to determine the potential of a point in the bulk of either the metal or the electrolyte, the resulting potential is called the Galvani potential or the inner potential. However, the experiment is purely hypothetical because the test charge will not only disturb the charge

distribution in the interior of the phase but will also experience forces of a chemical nature. If the Galvani potential of the metal is ϕ_m and that of the electrolyte is ϕ_s then the Galvani potential difference ($\Delta\phi$) between them is defined as

$$\Delta\phi = \phi_m - \phi_s$$

This is a measure of the absolute electrical potential difference across the interface. Again it is not an experimentally determinable quantity since Galvani potential is defined by a hypothetical experiment.

The problem of interaction between the test charge and the phase material is avoided if the potential is defined at a point not within the phase but close to the surface and just outside the range of interference forces. The Volta or outer potential (ψ) is defined as the work required to transport unit positive charge from infinity to such a point. According to Grahame[2] it may be defined alternatively in the case of a metal as the potential of a cavity in the metal with a small exterior opening.

The Volta potential differs from the Galvani potential if a potential difference exists between the interior and the surface of the phase, as is often the case. This difference in potential[3] is called the surface potential or dipole potential (χ). It occurs, for example, when there is orientation of polar solvent molecules on the surface or when the centre of gravity of positive charge does not coincide with that of negative charge on the surface of the metal. Thus

$$\phi = \psi + \chi$$

The Volta potential difference ($\Delta\psi = \psi_m - \psi_s$) is measurable.[4] ($\psi_m$ is the Volta potential of the metal and ψ_s that of the electrolyte). However this is generally not the absolute potential difference across the interface since ψ does not refer to a point in the bulk phase. It is related to $\Delta\phi$ by the expression

$$\Delta\phi = \Delta\psi + \Delta\chi \qquad 1.2.1.$$

where $\Delta\chi = \chi_m - \chi_s$, (m referring to metal and s to electrolyte).

Changes in potential difference across a single interface can be measured even though the absolute value of potential difference cannot. The potential across an interface may vary if, for example, current is passed and this variation may be measured by observing the potential between the electrode under investigation (the working electrode) and a non-polarizable reference electrode through which the current also passes. An example of such an electrode is found in two electrode polarography where the calomel electrode functions as both anode and reference electrode, its potential remaining essentially constant for the passage of small currents. Alternatively the current may be passed between the working electrode and a counter-electrode which may be subject to considerable polarization, if the potential is measured against a third electrode (reference electrode) through which no current is passed. Thus when referring to the potential (E) of an electrode, what is meant is the potential of a cell consisting of that electrode and some standard reference electrode.

1.3. Interfacial Tension and the Potential of Zero-charge

One property which yields considerable information on the structure of the double layer is the interfacial tension. This property of interfaces bears the same relationship to surface as pressure does to bulk volume. It may be defined as the increase in surface energy per unit increase in surface area. Work has to be done against interfacial tension in order to change the area of the interface just as it has to be done against pressure to change the volume of the bulk phase.

The interfacial tension of a liquid/liquid interface is easily measured[6] but that of a solid/liquid interface is not. This had led to an emphasis on the use of mercury as an electrode material in double layer investigations. Mercury is preferred for other reasons also: a liquid surface is more reproducible; fresh surface can be continuously exposed by the use of a dropping mercury electrode, thus reducing contamination problems; and the aqueous electrolyte/mercury interface is ideally polarizable (i.e. it passes no current) over a fairly wide range of potentials. This interface may therefore be regarded as a relatively simple one, the study of which helps in understanding the behaviour of more complex interfaces. If the interfacial tension (γ) of an aqueous-HCl/mercury interface is plotted against potential (E), a graph of the type shown in Figure 1.1 is obtained. This is called an electrocapillary curve after the method of measurement.[6] A maximum of interfacial tension called the electrocapillary maximum (e.c.m.) is observed at a particular potential E_o. It can be shown[5] by thermodynamic arguments that at constant temperature (T) pressure (P) and composition (c)

$$\left(\frac{\delta\gamma}{\delta E}\right)_{T,P,c} = - q^m$$

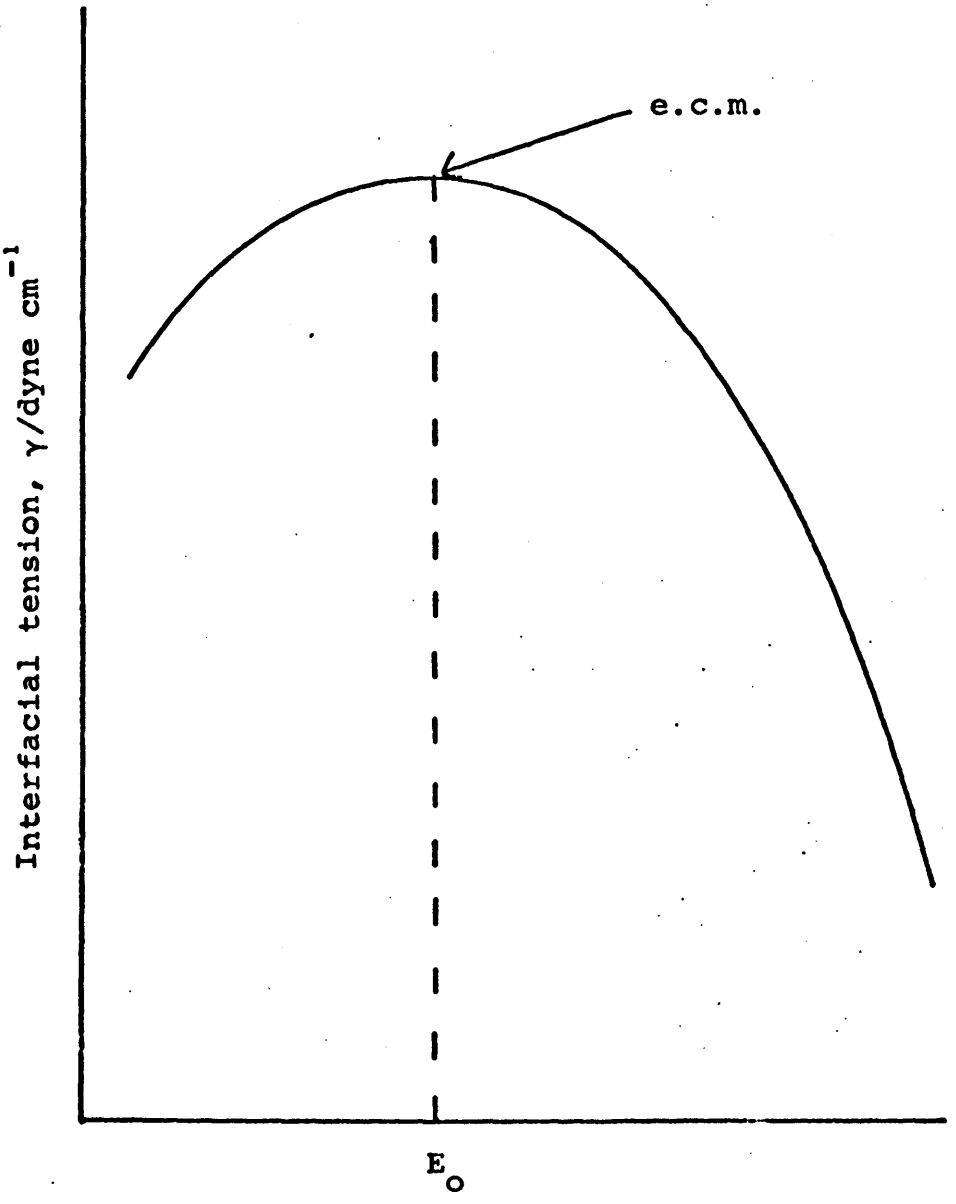

FIGURE 1.1 : A Typical Electrocapillary Curve

where q^m is the charge density on the electrode. Thus the slope of the γ versus E curve (Figure 1.1) at any value of E is the charge density (q^m) on the electrode at that potential. In particular, since the slope at E_o is zero, there is zero-charge density on the electrode at this potential. It is therefore known as the potential of zero-charge (p.z.c.) and is a fundamental reference point in studies of electrified interfaces.[2] At the p.z.c. the Volta potential difference across the interface is zero ($\Delta\psi = 0$) and therefore from equation 1.2.1

$$(\Delta\phi)_{p.z.c.} = (\Delta\chi)_{p.z.c.}$$

Thus the potential difference across the interface is not necessarily zero at the p.z.c.

1.4. Differential Capacitance and the Structure of the Double Layer

Information about the structure of the double layer may also be obtained from capacitance measurements. The differential capacitance of the interface is defined

$$C = \left(\frac{\delta q^m}{\delta E}\right)_{\substack{\text{constant} \\ \text{composition}}}$$

As already stated q^m may be obtained by differentiation of the γ versus E curve and C may therefore be obtained by a further differentiation. Alternatively it may be measured electrically, usually by alternating current methods which are particularly useful in the case of solid electrodes.

Various models of the double layer have been proposed to explain the variation of capacitance and interfacial tension with potential. The degree of success of particular models in this regard will not be discussed here in detail but the modern qualitative picture based on a model by Grahame[2,7] will be described.

The double layer may be considered in terms of three main regions: (a) the metallic phase, (b) an inner layer of a few molecular diameters in thickness, and (c) an outer or diffuse layer which extends from the inner layer into the bulk solution. In general there will be an excess charge density q^m on the metal which may be negative (an excess of electrons) or positive (a deficiency of electrons). This charge will reside at the surface of the metal in a very thin layer that for practical purposes may be regarded as two-dimensional. The quantitative value of q^m has well-defined thermodynamic significance[8] and may be estimated from measurements of interfacial tension as described earlier.

As indicated in Figure 1.2,the region of the electrolyte nearest the metal is called the inner layer (alternatively the compact, rigid, Helmholtz or Stern layer). It contains water molecules and sometimes other neutral molecules adsorbed on the electrode surface. Some sites on the electrode surface may, on occasion, be occupied by specifically adsorbed ions, particularly anions. The locus of the centres of these ions is called the Inner Helmholtz Plane (IHP), also called the Helmholtz Plane. The charge density resulting from ions in the IHP is usually denoted by q^i and the distance of the IHP from the metal surface by x_1, which is approximately equal to the radius of the ion which is specifically adsorbed. There is not general agreement on the detailed nature of the forces of interaction between the ions and the

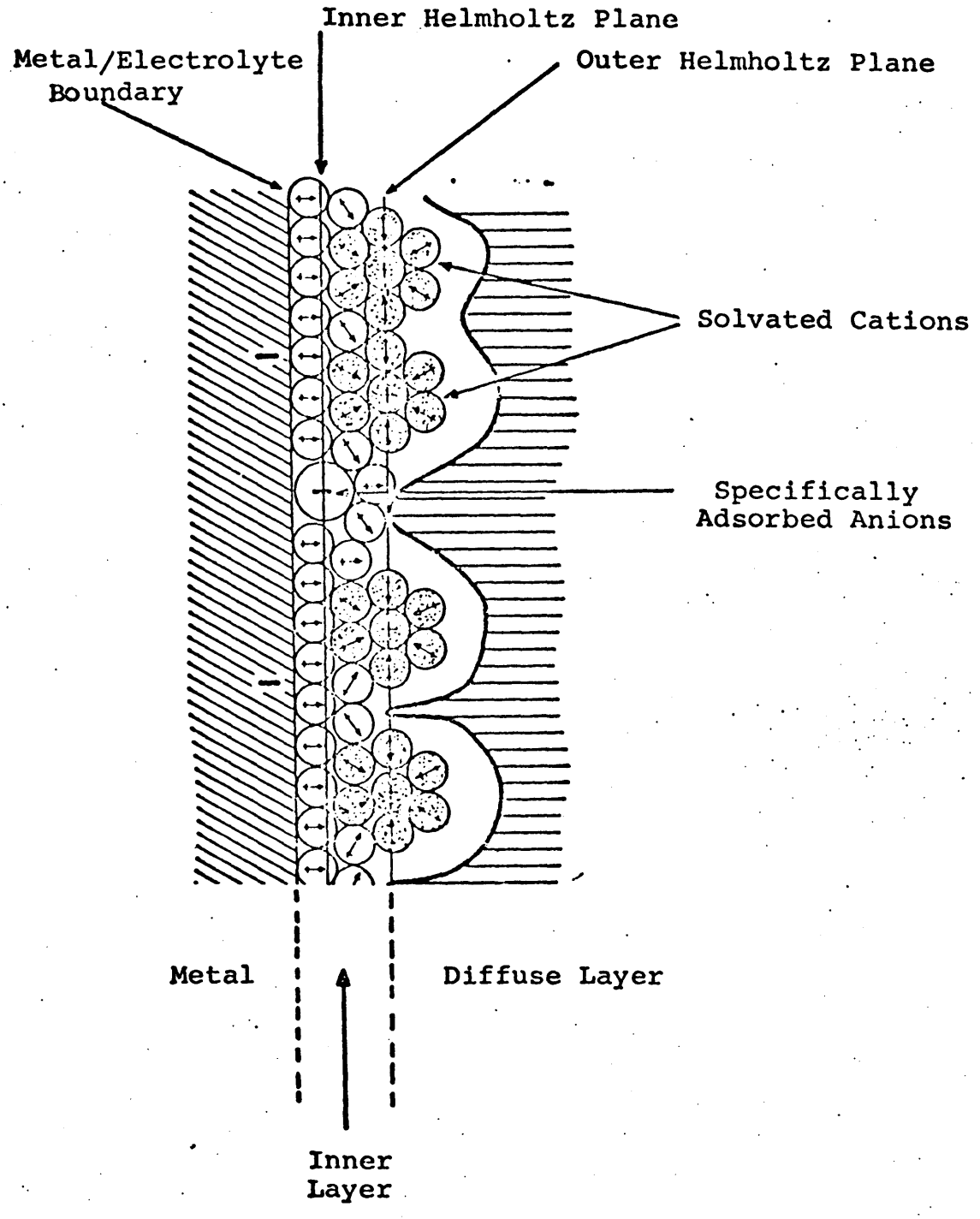

FIGURE 1.2 : Model of the Electrical Double-Layer.

metal which bring about specific adsorption. However experiments seem to suggest that some ions are specifically adsorbed while others are not. Whether or not an ion is specifically adsorbed depends on the properties of the individual ion. Some authors[2,9] have postulated a covalent bond between the ion and the electrode surface. More recently, however, doubt has been thrown on this explanation and both electrical image energy[10] and the degree and type of ionic solvation[11,12] have been suggested as the controlling factors.

Regardless of the mechanism of specific adsorption, it is generally agreed that,before an ion can penetrate into the inner layer and be adsorbed at the IHP, it must lose its solvation sheath,at least in the direction toward the metal. If the interaction with the metal is not strong enough to bring about desolvation, the hydrated ion may be adsorbed at a distance x_2 from the metal ($x_2 > x_1$) as indicated by the shaded clusters in Figure 1.2. As pointed out earlier, the electrode itself is hydrated so that the hydrated ions adsorbed at the electrode are generally regarded as separated from the metal surface by this inner solvent layer. The locus of the centres of these ions is called the outer Helmholtz plane (OHP) and sometimes the Gouy Plane. Unlike the specific adsorption in the IHP, ions in the OHP are held at the electrode by simple coulombic forces which are independent of chemical properties but depend rather on the ionic charge. This is sometimes called non-specific adsorption.

Not all of the non-specifically adsorbed ions are located on the OHP. Rather there is a gradual transition from the concentration in the OHP to the equilibrium concentration in the bulk solution and this transition region is called the diffuse layer. The diffuse character of this layer is due to thermal agitation which provides

a disordering influence opposed to the ordering effect of the coulombic forces. The net effect is an "ionic atmosphere" similar to that surrounding an ion in bulk solution. In fact the behaviour may be described by equations[13] which greatly resemble the Debye-Hückel equations for an electrolyte. The excess charge density in the diffuse layer (q^d) is expressed in units of charge per unit area of interface but is really three-dimensional. It is essentially the total excess charge on a column of solution of unit cross-sectional area extending from the OHP into the bulk solution.

The interfacial region as a whole must be electrically neutral and therefore the charge on the metal must be balanced exactly by the total charge (q^s) on the solution side of the interface, i.e.

$$q^m = -q^s = -(q^i+q^d)$$

Since the thickness of the inner layer is extremely small (a few molecular diameters), the thickness of the entire double layer is essentially given by the thickness of the diffuse layer. The perturbation of charge distribution in the electrolyte which occurs inside the diffuse layer dies out quite rapidly with increasing distance from the electrode surface. For example 99.99% of the diffuse layer perturbation occurs[14] within a thickness of less than 10 nm in the case of 10^{-1}M electrolyte; the thickness increases with decreasing concentration and in the case of 10^{-6}M electrolyte is of the order of 1 μm. Thus the double layer at a metal/electrolyte interface is relatively thin.

1.5. Equilibrium Electrode Potential and the Thermodynamics of Electrode Processes

The discussion so far has been concerned with the properties of the interface under conditions where there is no charge transfer across it. However charge transfer occurs across many metal/electrolyte interfaces and the resulting chemical transformations are a prime concern of electrochemistry. Whether or not a particular charge transfer process occurs depends both on thermodynamic and on kinetic factors, i.e. it depends both on the free-energy difference between initial and final states and on the existence or non-existence of a mechanism with a free energy of activation low enough for the process to occur. The thermodynamic aspects are discussed in this section and the kinetic aspects in Section 1.6.

The free energy change occurring when a charged species transfers from one phase to another depends both on chemical and electrical factors. The chemical potential (μ_i) of an uncharged species s_i in a particular phase, at temperature T and pressure P, is defined[15] by the expression

$$\mu_i = \left(\frac{\delta G}{\delta n_i}\right)_{T,P,n_j}$$

where G = the free energy of the phase
n_i = the no. of moles of s_i in the phase
n_j = the no. of moles of any other component in the phase

and is a measure of the work expended per mole in bringing the species from an infinitely dilute gaseous phase into the given phase. For the analogous transfer of charged particles work must be expended to overcome not only the dispersion and chemical forces but also the electrical ones. The total work is measured by a quantity (introduced

by Guggenheim[1]) known as the electrochemical potential ($\bar{\mu}$). It is related to the chemical potential (μ) by the equation[16]

$$\bar{\mu} = \mu + zF\phi \qquad 1.5.1.$$

where z = charge on particle in units of electronic charge
F = Faraday's constant
ϕ = Galvani potential of the phase.

Whether or not the net transfer of a charged species A is possible on thermodynamic grounds depends on the electrochemical potential of A in each of the phases involved.

For an interface at equilibrium the free energy change associated with the transfer process

$$dG = 0$$

and this condition is satisfied when

$$\bar{\mu}_A^m = \bar{\mu}_A^s \qquad 1.5.2.$$

where $\bar{\mu}_A^m$ and $\bar{\mu}_A^s$ represent the electrochemical potential of A in the metal and electrolyte phases, respectively. The species A may be an ion or an electron. An example of the former case is Cu^{2+} in the process

$$Cu^{2+} + 2e^- \rightleftharpoons Cu$$

at a copper electrode in aqueous electrolyte. An example of a process where A is an electron is

$$H^+ + e^- \rightleftharpoons \tfrac{1}{2}H_2$$

at a platinum electrode in aqueous electrolyte. Using equation 1.5.1 to substitute for $\bar{\mu}$ in equation 1.5.2

$$\mu_A^m + z_A F\phi^m = \mu_A^s + z_A F\phi^s$$

where the superscripts m and s represent metal and electrolyte respectively. Therefore,

$$\Delta\phi = \phi^m - \phi^s = -\frac{\mu_A^m - \mu_A^s}{z_A F} = -\frac{\Delta\mu_A}{z_A F}$$

i.e. the difference in Galvani potential ($\Delta\phi$) between the metal and the electrolyte is exactly balanced by the corresponding difference ($\Delta\mu_A$) in the chemical potential of A.

As discussed in Section 1.2 it is not possible to measure the potential of an electrode with respect to the electrolyte but it is possible to measure it with respect to a reference electrode. What is being measured then is really the potential of an electrochemical cell. If the equations of the half-reactions corresponding to the electrode processes of this cell are combined, the result is the equation of the overall chemical reaction which will occur if current is drawn from the cell. If this current is small so that the reaction can occur reversibly the electrical work done on the external circuit must equal the free energy decrease in the cell due to reaction. Thus

$$\Delta G = -w = -nFE$$

where w = electrical work done,
n = number of electrons transferred in the overall cell reaction,
F = Faraday's constant,
E = potential difference between the electrodes,
ΔG = free energy change of the reaction.

This relationship may also be expressed in terms of chemical potential, viz.

$$\sum_i \nu_i \mu_i = \Delta G = -nFE \qquad 1.5.3.$$

where ν_i are the stoichiometric factors of the components in the equation of the cell reaction with positive ν_i for products and negative ν_i for reactants. If the actual direction of spontaneous reaction is as written, ΔG will be negative and so positive E is obtained; likewise if the reaction cannot occur spontaneously as written negative E is obtained. If the convention[17] (Stockholm, 1953) of writing the reaction in the direction corresponding to reduction at the test electrode is adopted, the sign obtained for electrode potential will be the actual polarity of that electrode when measured with respect to the reference.

Since the chemical potential of any species in a given phase depends on its activity, the potential of any cell depends on the activities of the potential-determining species. Since conditions at the reference electrode are constant by definition, only changes in the activity of potential-determining species at the test electrode need be considered. The chemical potential (μ) of a species of activity **a** in a given phase is

$$\mu = \mu^{o} + RT \ln a \qquad 1.5.4.$$

where μ^{o} = the chemical potential of the species at unit activity. If equation 1.5.4 is substituted in equation 1.5.3. we obtain

$$E = E^{o} + \frac{RT}{nF} \sum_{j} \nu_j \ln a_j$$

where E = the potential of the test electrode
E^{o} = the standard potential of the test electrode (i.e. the potential at unit activity of potential-determining species s_j at the electrode)

and ν_j is positive for oxidants and negative for reductants.

This relationship between electrode potential and concentration of electroactive species is known as the Nernst equation.

Electrode potentials are frequently quoted with respect to the hydrogen electrode (HE). This consists of platinized platinum immersed in an aqueous solution through which hydrogen gas is bubbled at 1 atmosphere pressure. The electrode reaction is

$$2H^+_{(aq)} + 2e^- \rightleftharpoons H_2$$

The potential of the hydrogen electrode varies with pH according to the Nernst equation. Since the potential of the oxygen electrode varies with pH in a similar manner, a hydrogen electrode in the same solution as the working electrode is often used as a reference in oxygen electrochemistry. Alternatively potentials may be quoted with respect to the standard hydrogen electrode (SHE), i.e. with respect to a hydrogen electrode in a solution of unity hydrogen-ion activity (pH = 0).

1.6. Electrode Kinetics

If a reaction is feasible on thermodynamic grounds, kinetic factors determine whether or not it can occur. Any electrochemical reaction at the metal/electrolyte boundary involves an electron transfer process. Sometimes the reaction will involve more steps than one, not all of which necessarily involve electron transfer. The rate-determining step may be either chemical (involving no electron transfer) or electrochemical (electron transfer). The rate constant for an electron transfer step is dependent on the potential of

the electrode. This may also affect the rate of a chemical step indirectly by changing the concentration of intermediates at the electrode surface. Thus a change from one rate-determining step to another may occur as a result of changing the potential. Therefore, an understanding of the effect of potential on electron transfer processes is central to electrode kinetics.

Consider a simple electron transfer between the metal and a species A in solution bringing about the transformation

$$A + e^- \longrightarrow B \qquad 1.6.1.$$

Let $\vec{\Delta G}_z^{o*}$ be the standard free energy of activation for the cathodic process (i.e. transfer of an electron from the metal to A) when there is zero potential difference across the interface. Then, in terms of the transition state theory, the rate of electron transfer to A is

$$\vec{v}_z = \frac{kT}{h} a_A \exp\{-\frac{\Delta G_z^{o*}}{RT}\} \qquad 1.6.2.$$

where k = Boltzmann's constant
T = Temperature in degrees Kelvin
h = Planck's constant
a_A = Activity of A at interface
R = Gas constant

Since a charge transfer process is involved the standard free energy of activation $\vec{\Delta G}^{o*}$ depends on the potential across the interface. Let the solid line in Figure 1.3 represent the free energy profile when there is zero potential across the interface and let the broken line represent the corresponding profile in the presence of a positive potential $\Delta\phi$ on the metal with respect to the solution. As the discussion is concerned only with

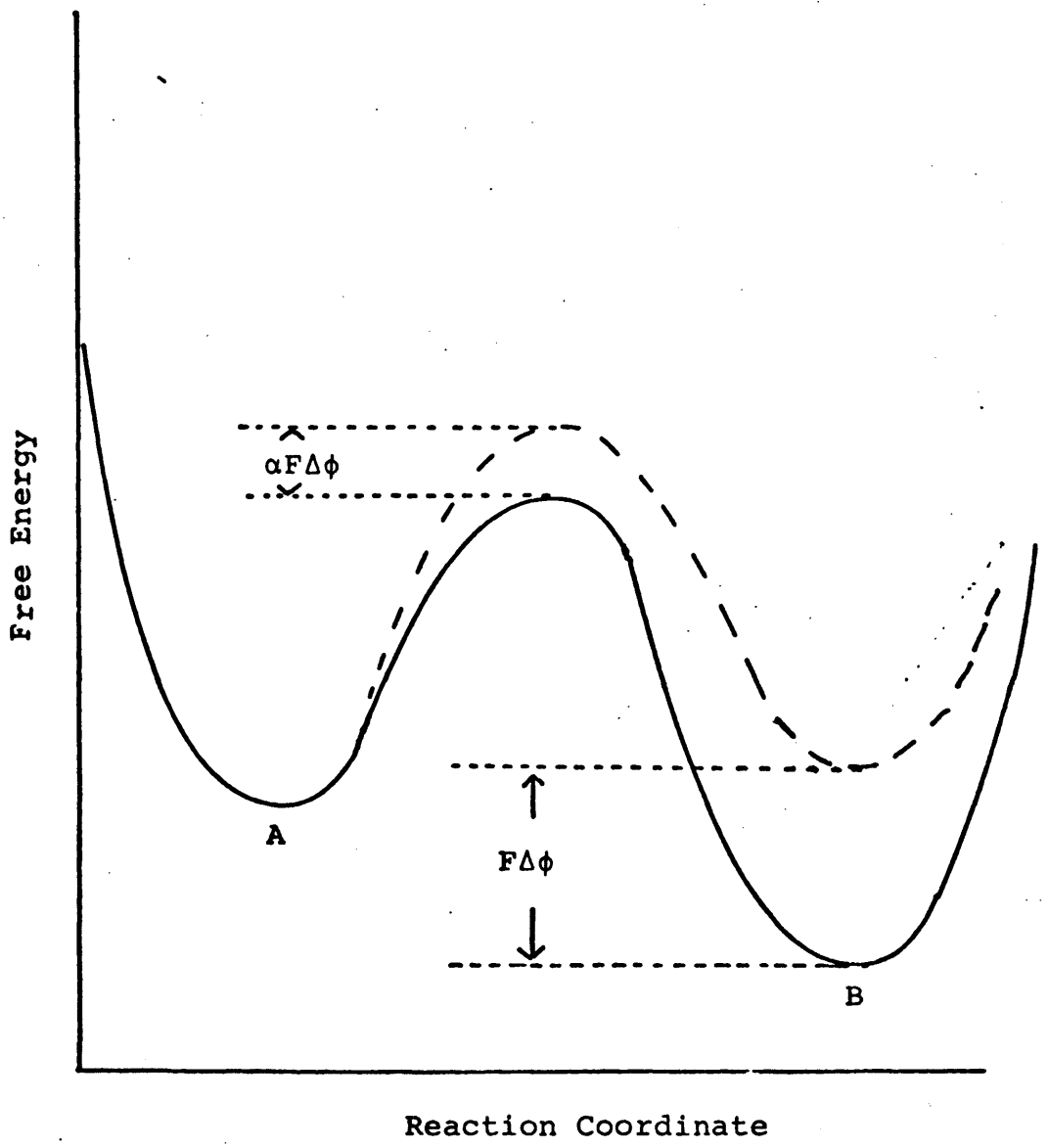

FIGURE 1.3 : Free energy profile for an electron-transfer reaction at a metal/electrolyte interface.

changes in free energy of activation the standard free energy of the reactants may be depicted as equal in both cases. Then since the conversion of reactant to product involves the transfer of an electron, the standard free energy of the product will be increased by $F\Delta\phi$. The change in the standard free energy of the transition state is expected to be intermediate to that of reactant and product and will be represented as $\alpha F\Delta\phi$ where $0<\alpha<1$. Thus

$$\vec{\Delta G}^{o*} = \vec{\Delta G}_z^{o*} + \alpha F\Delta\phi \qquad 1.6.3.$$

and therefore the rate of electron transfer to A under the influence of the potential difference $\Delta\phi$ can be written

$$\vec{v}_e = \frac{kT}{h} a_A \exp\{-\frac{\vec{\Delta G}^{o*}}{RT}\}$$

and on substitution from 1.6.3 and 1.6.2

$$= \vec{v}_z \exp\{-\frac{\alpha F\Delta\phi}{RT}\}$$

This rate $\vec{v}_e$ is the number of moles of electrons transferred per unit time per unit area of the interface. Thus, the cathodic current density

$$\vec{i} = F\vec{v}_e$$

$$= F\vec{v}_z \exp\{-\frac{\alpha F\Delta\phi}{RT}\} \qquad 1.6.4.$$

(In the remainder of this discussion "current density" is abbreviated to "current").

A similar treatment may be applied to the anodic reaction, i.e. electron transfer from B to the electrode.

As seen from Figure 1.3 the standard free energy of activation in this case is

$$\overleftarrow{\Delta G}^{o*} = \overleftarrow{\Delta G}_z^{o*} - (1-\alpha)F\Delta\phi$$

and therefore the anodic current

$$\overleftarrow{i} = F\overleftarrow{v}_z \exp\{\frac{(1-\alpha)F\Delta\phi}{RT}\}$$

When no net current is flowing across the interface a dynamic equilibrium exists where the cathodic current $\vec{i}_{\Delta\phi_e}$ is exactly balanced by the anodic current $\overleftarrow{i}_{\Delta\phi_e}$

$$|\vec{i}_{\Delta\phi_e}| = |\overleftarrow{i}_{\Delta\phi_e}| = i_o \qquad 1.6.6.$$

where i_o is termed the exchange current density. Under these (equilibrium) conditions there is a potential $\Delta\phi_e$ on the electrode with respect to the solution. The overpotential η of the electrode when its potential is $\Delta\phi$ with respect to the solution is defined

$$\eta = \Delta\phi - \Delta\phi_e \qquad 1.6.7.$$

i.e. it is a measure of how far removed the potential is from its equilibrium value. If a net current i is flowing across the interface

$$i = \vec{i} - \overleftarrow{i} = F\vec{v}_z \exp\{-\frac{\alpha F\Delta\phi}{RT}\} - F\overleftarrow{v}_z \exp\{\frac{(1-\alpha)F\Delta\phi}{RT}\}$$

Here the cathodic current is taken as positive since it corresponds to the forward direction of reaction 1.6.1 which is written as a reduction in accordance with the Stockholm convention.[17] Substituting for $\Delta\phi$ from 1.6.7

$$i = \vec{F}v_z \{\exp\ (-\frac{\alpha F\Delta\phi_e}{RT})\}\ \{\exp\ (-\frac{\alpha F\eta}{RT})\}$$

$$- Fv_z \{\exp\ \frac{(1-\alpha)F\Delta\phi_e}{RT}\}\{\exp\ \frac{(1-\alpha)F\eta}{RT}\}$$

But from equations 1.6.4 and 1.6.5.

$$\vec{i}_{\Delta\phi_e} = \vec{F}v_z \exp\{-\frac{\alpha F\Delta\phi_e}{RT}\}$$

$$\overleftarrow{i}_{\Delta\phi_e} = \overleftarrow{F}v_z \exp\{\frac{(1-\alpha)F\Delta\phi_e}{RT}\}$$

Therefore

$$i = \vec{i}_{\Delta\phi_e} \exp\{-\frac{\alpha F\eta}{RT}\} - \overleftarrow{i}_{\Delta\phi_e} \exp\{\frac{(1-\alpha)F\eta}{RT}\}$$

Substituting from equation 1.6.6

$$i = i_o (\exp\{-\frac{\alpha F\eta}{RT}\} - \exp\{\frac{(1-\alpha)F\eta}{RT}\}) \quad 1.6.8.$$

Equation 1.6.8 is often referred to as the Butler-Volmer equation. It shows how the current density across the interface depends on the overpotential.

1.7. The Mechanism of Electron Transfer

In the derivation of equation 1.6.8 the actual mechanism of electron transfer was not discussed. This will now be considered. Because of the small mass of electrons their wave properties sometimes manifest

themselves and one consequence of this is that electrons may have a finite probability of being found in classically forbidden regions. Thus electrons can tunnel through potential energy barriers which they could not otherwise overcome. It can be shown by an approximate calculation[18] that in the case of an electron traversing an energy barrier of 1 eV (96.45 kJ $mole^{-1}$) and of width 0.5 nm, the probability of electron tunnelling is much greater than that of overcoming the barrier at 25°C. Since this barrier is of the same order as those thought to be involved at the electrode surface, it would appear that electron transfer in electrochemical reactions occurs by a tunnelling mechanism.

The probability of occupation P(E) of an electronic state of energy E in the metal is given by the Fermi distribution function.

$$P(E) = \frac{1}{1 + \exp\{(E-E_f)/kT\}}$$

where k = Boltzmann's constant
T = temperature in degrees Kelvin
E_f = the Fermi level of the electrons and corresponds to the electrochemical potential $\bar{\mu}_e$ of electrons in the metal.

This implies[19] that most of the free electrons in the metal have energies which differ from E_f by less than kT. The corresponding energy (E_r) of an electron in solution is the energy required in the process

$$A + e^- \longrightarrow B$$

where A and B are as in equation 1.6.1 and the electron is brought from vacuum at an infinite distance from the

solution. Both A and B undergo changes in configuration due to vibrations and rotations with corresponding changes in the value of E_r. A condition for electron tunnelling is that it occur between states of equal energy.[20] Thus for the reaction to occur the configurations of A and B must be such that E_r is equal in energy to an appreciably populated electronic state in the metal, i.e. one having an energy within about kT of E_f. Furthermore, according to the Franck-Condon principle[21] the instantaneous configuration of A and B must remain constant during the electron transfer process so that a given value of E_r corresponds to a precisely defined arrangement of atoms in A and an identical one in B. Thus electron tunnelling can occur only when the electron acceptor (A) or donor (B) is in a suitably excited state and we may regard the energy involved in this excitation as the activation energy assumed in Section 1.6. Since a change in potential difference across the interface changes the relative values of E_f and E_r, this activation energy is potential dependent.

1.8. Consequences of the Butler Volmer Equation

Equation 1.6.8 refers to a simple one-electron transfer process. However electrochemical reactions often involve several steps one of which is usually rate-determining. If n electrons are transferred in the reaction and if the rate-determining step must occur ν times for the overall reaction to occur once, the current-overpotential relationship may be expressed[22] in a more general form of the Butler-Volmer equation.

$$i = i_o \{\exp(-\frac{\alpha n F \eta}{\nu RT}) - \exp\frac{(1-\alpha) n F \eta}{\nu RT}\} \qquad 1.8.1.$$

Some limiting cases of equation 1.8.1 will now be considered.

(1) At large positive η the first exponential term is neglibibly small so that

$$i = -i_o \exp\{\frac{(1-\alpha)nF\eta}{\nu RT}\}$$

$$\ln |i| = \ln i_o + \frac{(1-\alpha)nF\eta}{\nu RT}$$

$$\therefore \quad \eta = \frac{\nu RT}{(1-\alpha)nF} \ln i_o + \frac{\nu RT}{(1-\alpha)nF} \ln i$$

$$= a + b \log_{10} |i| \qquad 1.8.2.$$

where

$$a = \frac{2.303\ \nu RT}{(1-\alpha)nF} \log_{10} i_o$$

$$b = \frac{2.303\ \nu RT}{(1-\alpha)nF}$$

Equation 1.8.2 is known as the Tafel equation and indicates a linear relationship between overpotential and log $|i|$ at high overpotential. Experimentally this is often so at overpotentials greater than about 100 mV. A graph of η versus log i is often referred to as a Tafel plot. From such a plot the coefficients a and b may be obtained and these in turn yield values of i_o and $(1-\alpha)/\nu$. Similarly at large negative overpotentials a Tafel plot is obtained from which i_o and α/ν may be evaluated.

(2) If the exponents in equation 1.8.1 are expanded only the first two terms need be considered if

$$\eta << \frac{\nu RT}{\alpha nF}$$

Thus

$$i = i_o \{1 - \frac{\alpha n F \eta}{\nu RT} - 1 - \frac{(1-\alpha) n F \eta}{\nu RT}\}$$

$$= - \frac{i_o n F \eta}{\nu RT}$$

and therefore

$$\eta = - \{\frac{\nu RT}{i_o n F}\} i$$

This shows that overpotential is proportional to current at low overpotential. (The negative sign arises because anodic overpotential and cathodic current are both taken as positive). The proportionality constant corresponds to an ohmic electrical resistance

$$R_c = \frac{\nu RT}{i_o n F} \qquad 1.8.3.$$

and has been designated[23] the charge-transfer resistance. If R_c is large, a small current will cause an appreciable overpotential whereas if R_c is small the potential will not change appreciably from its equilibrium value when a small current is passed. Thus the charge-transfer resistance is a measure of the polarizability of an electrode. Equation 1.8.3. shows that the greater i_o, the less polarizable is the electrode.

1.9. The Oxygen Electrode

The oxygen electrode as first used by Grove[24] consisted of a piece of platinized platinum gauze immersed in an acid solution. Oxygen was bubbled over the gauze and the potential was measured against a hydrogen electrode in the same solution. Grove showed that current could be drawn from this combination of electrodes. He also showed that if current was passed through a cell consisting of two platinum electrodes in acid solution oxygen was evolved at the anode and hydrogen at the cathode.

The electrode reaction for the oxygen electrode in acid solution is

$$\tfrac{1}{2}O_2 + 2H^+ + 2e^- \rightleftharpoons H_2O$$

If this is coupled with a hydrogen electrode

$$H^+ + e^- \rightleftharpoons \tfrac{1}{2}H_2$$

the overall reaction requiring the transfer of two electrons is

$$\tfrac{1}{2}O_2(g) + H_2(g) \rightleftharpoons H_2O\ (l)$$

The standard potential E of the oxygen electrode is therefore given (see Section 1.5) by

$$E^o = -\frac{\Delta G_f^o(H_2O,l)}{2F}$$

where $\Delta G_f^o(H_2O,l)$ is the standard free energy of formation of liquid water. The accepted calorimetric value[25] for $\Delta G_f^o(H_2O,l)$ is -238 kJ mole^{-1} (-56.9 kcal mole^{-1}) which according to equation 1.9.1 yields a value E^o = 1.229 volts. With a few notable exceptions where unusual activation conditions were employed,[26,27,28] the

attainment of this theoretical potential has not been achieved experimentally for the oxygen electrode; a typical value[29] for the observed rest potential* on platinum in oxygen-saturated solution is 1.06 V. Low values are also reported for gold[30] (0.98 V), palladium[31] (0.87 V), rhodium[32] (0.93 V), iridium[33] (1.02 V), ruthenium[34] (0.85 V) and osmium[34] (0.87 V) in oxygen-saturated solution. Application of a small anodic current to a platinum electrode in acid solution eventually leads to a relatively steady potential (Figure 1.4) of about 1.6 V. Thus the overpotential for oxygen gas evolution is about 0.37 V. Similarly high overpotentials are obtained with other noble metals although all (notably those at ruthenium and iridium) are not as high as those at platinum.

These low rest potentials and high oxygen evolution overpotentials indicate that the oxygen electrode does not behave in a reversible manner. Owing to its great importance in fuel cell research, considerable effort has been expended by electrochemists in investigations into the cause of this irreversibility. A large amount of experimental fact has been uncovered as a result and a wide variety of explanations has been put forward even though no generally agreed mechanism has evolved.

1.10. Oxide Films on Noble Metals

It was realised at an early stage that noble metals are not truly inert to oxygen-saturated electrolytes. In 1898 Mond, Ramsey and Shields[35] concluded from measurement of the heat evolved during the adsorption

*Unless otherwise stated, potentials are referred to a hydrogen electrode (HE) in the same solution.

of oxygen on platinum black that a layer of $Pt(OH)_2$ was formed on the platinum surface. Clear evidence for the presence of adsorbed oxygen films on noble metals is obtained from constant current charging curves. Figure 1.4 shows the variation with time of the potential of a platinum electrode in deaerated acid solution under galvanostatic conditions. At times less than t_A a constant cathodic current is passed; the current is reversed at t_A and again at t_E (i.e. the region AE corresponds to anodic current and the other regions to cathodic current). Information on the processes occurring at the electrode surface may be obtained from an examination of this curve.

In the region to the left of A hydrogen gas is being evolved from the electrode. The electrode is covered by a film of adsorbed hydrogen atoms and these are oxidized when the current is made anodic. As the hydrogen coverage of the surface decreases the potential increases (the region AB) slowly to a value of about 0.4V at which point the surface is free of adsorbed hydrogen. The only charge stored by the surface when its potential changes through the region BC is that involved in charging the double layer capacitance[36]; hence the potential rise through BC is rapid. The potential changes much less rapidly through CD; here a faradaic process occurs, i.e. electrochemical formation of an oxide film on the surface of the platinum. This process is virtually complete at D and the potential is relatively constant over the region DE which corresponds to oxygen gas evolution.

When the current is subsequently made cathodic (E), the above sequence occurs in reverse. There is an initial rapid fall in potential which then levels

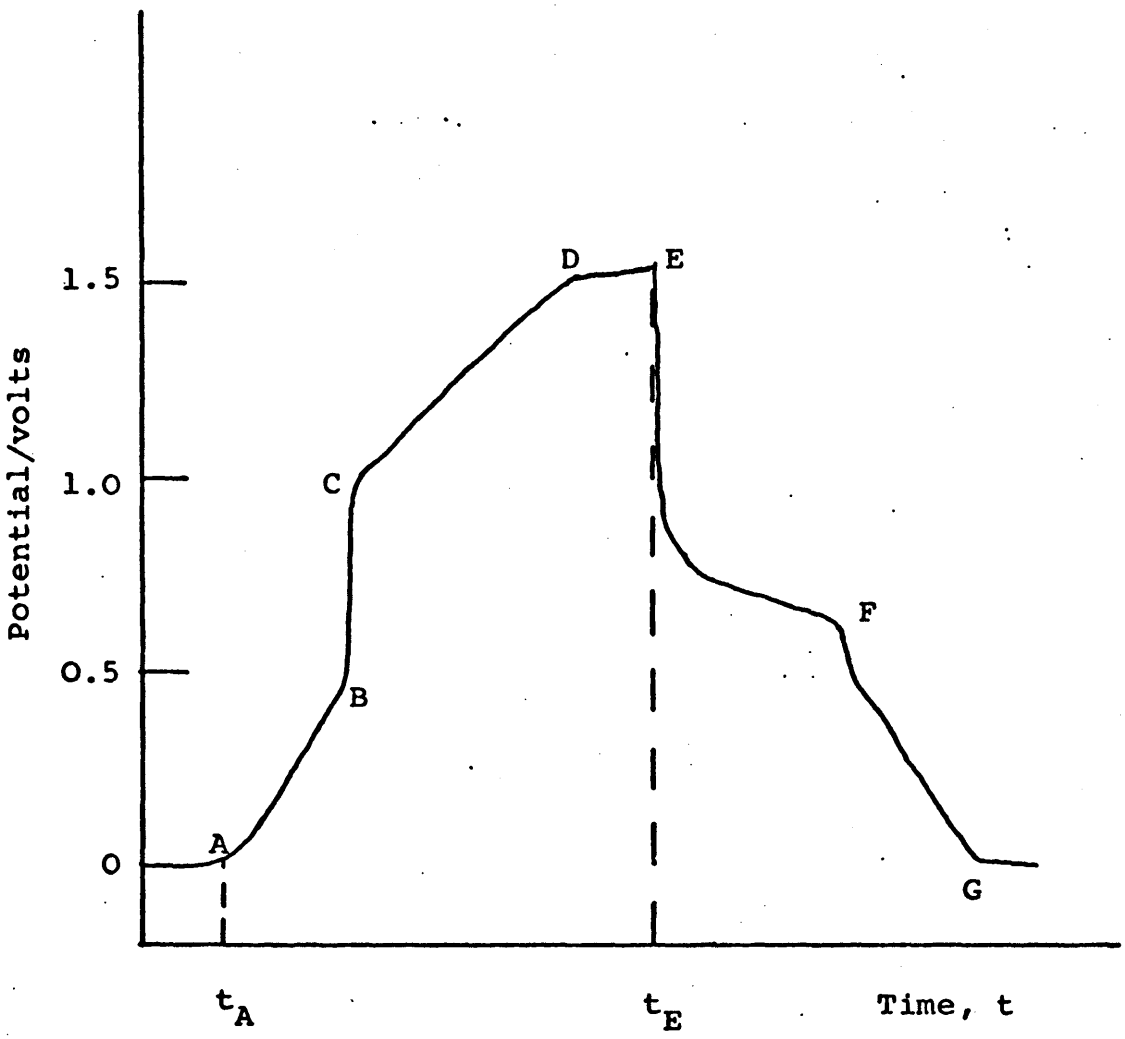

FIGURE 1.4 : A typical charging curve for a platinum electrode in deaerated acid solution.

off to a plateau at ca. 0.7V over which most of the oxide reduction occurs. When the oxide film has been stripped from the surface (point F) the potential again falls, first through a short double layer region and then more gradually with hydride film formation until hydrogen gas evolution begins at OV (point G). Note that formation and oxidation of the hydride film occurs over the same potential range (0-0.4V) but that the oxide species formed over the range 0.8V-1.6V is not substantially reduced until the potential falls to about 0.7V. Thus, like the related oxygen evolution and reduction reactions, the formation and reduction of oxide films on platinum is an inherently irreversible process.

If a constant current (I) is used, the quantity of electricity (Q) passed across the interface in any time interval (t) is

$$Q = It$$

According to Faraday's laws the amount of oxide or hydride formed on the surface is therefore proportional to the corresponding time interval on the charging curve. Thus, the quantity $Q_H = It_{AB}$ is proportional to the capacity of the surface for adsorbed hydrogen and if it is assumed that there is monolayer coverage[37] at OV, it may be used as a measure of surface area. The corresponding measure of oxide capacity, $Q_a = It_{CD}$ is usually about twice Q_H and, assuming two electrons are transferred per adsorbed oxygen atom (compared with one per hydrogen atom), this indicates that there is approximately monolayer oxide coverage of the surface.

The ratio Q_a/Q_c (where $Q_c = It_{EF}$) tends to vary with the experimental conditions. Various values have been reported; in general those obtained from fast

charging techniques[38,39] (i.e. high current density) tend to be close to unity whereas those obtained at low current densities[40,41] correspond to $Q_a > Q_c$. The latter behaviour has been ascribed[40] to incomplete reduction of the surface oxide film at potentials anodic to the hydrogen region. However,some authors[39] have suggested that the effect is due to dissolution in the metal during the anodic polarization,of oxygen which is not readily removed on cathodization. This is supported by evidence in the literature[42,43] that oxygen may be dissolved in bulk platinum.

A technique known as cyclic voltammetry[44] is also commonly used in the study of oxide films. The potential of the working electrode is varied potentiostatically in a triangular manner and the resulting current is plotted against potential. Regions corresponding to both hydride and oxide formation and reduction may be distinguished. Integration of area under the curve in the relevant regions gives the quantities Q_H, Q_a and Q_c (since potential is a linear function of time). Optical techniques such as ellipsometry[45] yield further information on oxide films. Ellipsometry is based on the changes produced on the polarization state of a beam of light reflected from the electrode surface. Reddy, Genshaw and Bockris[46] found that films adsorbed on platinum from oxygen-saturated solution could not be detected ellipsometrically but, if the electrode was anodically polarized, measurable changes occurred at 0.98V.

It is generally agreed that platinum electrodes, in contact with oxygen saturated solution or anodically polarized, have surface oxygen species. However, there is controversy as to the exact structure of the film. Some workers[47,48,49] postulate that it is composed of

oxides of platinum. Anson and Lingane[48] chemically stripped the oxide films formed under various conditions and analysed the solutions spectrophotometrically. From their results they concluded that two oxides, PtO and PtO_2 are present in the ratio of 6:1. Others[50,51,52] however favour the theory that the film consists of adsorbed oxygen atoms. Some evidence for this is afforded by an observed[52,53] square root relationship between the partial pressure of oxygen and the amount of oxygen adsorbed on the platinum surface as measured by cathodic stripping techniques.

The discussion so far has been confined largely to platinum because work on the oxygen electrode has tended to concentrate on this metal. However, the techniques described have also been used in examining other noble metal substrates. Charging curves[54] and cyclic voltammetry[55] suggest that about a monolayer of oxide is formed on an anodically polarized palladium electrode before oxygen evolution begins. Butler and Drever[54] concluded that this consists of PdO which is converted to a monolayer of PdO_2 as oxygen is evolved. With very strong anodization they observed that an oxide several layers deep could be formed. It was concluded from rest-potential studies[32] that rhodium, in contact with oxygen-saturated acid solution, adsorbs about a monolayer of oxygen under open-circuit conditions. An oxide film also begins to form anodically[55,56] at potentials above 0.6 V, and about monolayer thickness is obtained before oxygen evolution begins. This film is not readily reduced, the oxide reduction region in the subsequent cathodic polarization extending into the hydrogen region. Bold and Breiter[56] found that $Q_a > Q_c$ and attributed this to the strong resistance to

reduction of the adsorbed film. Gold is reported[52] to adsorb very little oxygen from oxygen-saturated acid solutions but on anodic polarization an oxide, which appears to be the phase oxide, Au_2O_3, is formed[55,57,58] at potentials greater than 1.36V. On subsequent cathodic polarization, the potential falls to about 1.2V before substantial reduction of this oxide begins. Most observers reported $Q_a = Q_c$ indicating complete reduction of the oxide.[40,59] Charging curves for osmium-plated platinum wires were obtained by Khomchenko et al[60] but the results were complicated by corrosion of the metal which occurs above 0.88V. The anodic behaviour of ruthenium and iridium is discussed in detail in later chapters.

1.11. Oxide Films on Active Metals

Oxide films formed on metals at anodic potentials very often inhibit or completely prevent corrosion of the metal. The so-called "valve metals" have a tendency to form a protective high-resistance oxide film on anodic polarization to the exclusion of all other electrode processes. Typical valve metals include tantalum, niobium, aluminium, zirconium, hafnium, tungsten, bismuth and antimony. Tantalum provides an extreme example where an oxide film is nearly always present on the metal and anodic polarization in aqueous solutions of almost any electrolyte causes this film to grow thicker.[61] Other anodic processes such as oxygen evolution are almost entirely inhibited even though there may be a potential difference of some hundreds of volts across the film. With other valve metals such as zirconium, considerable oxygen evolution may occur but the evidence suggests that this is due to flaws in the

film.[61] The rate-determining step in the growth of these oxides is the migration of ions through the oxide film already formed. The electric fields involved are usually extremely high (about 10^{-7}V cm^{-1}) and oxide-formation current, i, is found to depend on the field, E, according to the relationship[62]

$$i = A \exp BE \qquad 1.11.1.$$

where A and B are constants.

Iron is the most common member of a group of metals (including also nickel and chromium) which undergo an active-passive transition at a particular potential. In the active state the metal dissolves according to the reaction

$$Fe \longrightarrow Fe^{z+} + z\bar{e}$$

and usually z = 2. This gives rise to a corrosion current. However, above a particular potential the corrosion reaction is inhibited by the formation of an oxide film on the surface and so the corrosion current decreases to a very low level. This decrease in current with increasing potential may be quite sharp and the potential at which it occurs is known as the Flade potential.[63] The value is given by Franck[64] as 0.58V against a hydrogen electrode in the same solution independent of pH for pH < 4. This does not correspond to the equilibrium potential of any known oxide of iron. It is about 0.6V anodic to the reversible potential of either Fe/Fe_2O_3 (-0.040V) Fe/FeO (-0.060V) or Fe/Fe_3O_4 (-0.082V).[65] It has been deduced[65] from experimental evidence that the current for passive film formation on iron is related to the

field across the film according to equation 1.11.1. This would suggest that, as for the valve metals, ionic movement through the oxide under the influence of a high electric field is rate-determining.

According to Vetter[67] corrosion of metals in the passive state is not due to pores in the oxide but must be considered as the dissolution of the non-porous passive layer in the electrolyte. If the metal is to persist in the passive state the oxide film must be replenished as quickly as it is lost by corrosion. The discrepancy between the Flade potential and the reversible oxide potential may thus be explained[68,69] in terms of the overpotential associated with a rate of oxide growth sufficient to maintain a film on the surface of the metal.

From measurements of the rate of oxide growth on platinum Ord[70] has concluded that the anodic oxidation of platinum meets the basic requirements for a process limited by the field in the oxide layer. This suggests that the same basic mechanism may be responsible for the anodic oxidation of metals as dissimilar as tantalum, iron and platinum spanning a range of oxide film thickness from thousands of angstroms to monolayer coverage.

1.12. The Role of Oxide Films in the Oxygen Evolution Reaction

The maximum thickness to which an oxide film may grow depends on the maximum potential which can be applied across the film. The latter is determined by the occurrence of other electrochemical reactions as the potential is raised, oxygen evolution being the most common. The conditions under which this reaction

may occur are summarized by Vermilyea.[71] Evolution of oxygen gas is thermodynamically possible at potentials greater than 1.23V. As outlined earlier, however, a large overpotential is generally observed so that the reaction requires a potential of 1.5 to 2.0V. If there are pores in the oxide film rapid oxygen evolution can occur in this potential region and it may not be possible to raise the potential much higher so that the thickness of the oxide film is effectively limited (cf. zirconium (Section 1.11)). The behaviour of a pore-free film depends on whether or not electrons can pass through it. Two categories of film may be distinguished:

(1) Electronically conducting films. Oxygen is evolved at potentials in the range 1.5V to 2.0V on oxide covered metals (e.g. passive iron) where the oxide is a good electronic semiconductor.

(2) Electronically insulating films. If the band-gap of the insulator is large, a large potential drop may be sustained by this type of film since no electrons can pass through it. The field can thus rise to a value sufficient for ionic migration across the film and oxide growth can proceed indefinitely. In the following cases, however, electrons can transfer across a film of electronically insulating oxide.

(a) If the band-gap of the insulator is not sufficiently large {less than 3 eV (289.4 kJ mol^{-1})} tunnelling of electrons from the valence band to the conduction band may occur in the presence of the high electric field (ca. 10^{-7}V cm^{-1}) required for ionic transport. For instance, if the band-gap is 2 eV (192.9 kJ mol^{-1}) and if the electric field is 10^{7}V cm^{-1}, the

distance required for electron tunnelling from the top of the valence band to an empty state in the conduction band is 2 nm. At this distance tunnelling is expected to occur fairly frequently so that an appreciable electronic current can flow across the film. Also if the band-gap is small, electron tunnelling from states in solution into the conduction band of the oxide can occur.

(b) Even if the band-gap is large {greater than 3 eV (289.4 kJ mol^{-1})} electrons can tunnel through the entire film if it is sufficiently thin.

Tantalum[72] provides an example of an electronically insulating oxide film across which electron transfer by any of the above mechanisms cannot occur. As a result the film can reach a thickness of several hundred nanometers and maintain a potential difference of several hundred volts.

The large overpotential associated with oxygen evolution has been observed by many workers and for various metals. Furthermore, in most cases, there is a slow time-variation.[73,74] As with other electrode reactions, the magnitude depends greatly on the electrode material. Ruetschi and Delahay[75] have shown that a negative correlation exists between the oxygen evolution overpotential and the energy of the metal-hydroxyl (M-OH) bond.

In the formulation of a mechanism for oxygen evolution it is important to know whether the oxygen comes directly from the electrolyte or whether it is formed via metal oxides. This point has been investigated by Rosenthal and Veselovskiy[76] in the case of platinized platinum. A surface oxide was first formed

anodically in an electrolyte which contained water enriched with O^{18}. The surface oxide of the platinum was thus also enriched with O^{18}. The electrolyte was then replaced by an unenriched sample and the first amounts of oxygen evolved were investigated for O^{18} content. A substantial increase above the normal O^{18} content was found. Direct chemical participation of the surface oxides can be inferred from these results.

The oxygen evolution overpotential decreases with increasing temperature. In the case of platinum Bowden[77] has reported that the dependence of current (i) on temperature (T) at a constant potential of 1.95V corresponds to a linear relationship between log i and 1/T. The slope yields an activation energy of 42.3 kJ $mole^{-1}$.

In concentrated acids discontinuities in the current-voltage curve have been observed. Gerovich et al[78] have investigated platinum in $HClO_4$ containing the oxygen isotope O^{18}. They have shown that at potentials more anodic than that at which the discontinuity occurs, part of the evolved oxygen comes from the ClO_4^- ion suggesting that the discontinuity represents the onset of direct anion participation in the oxygen evolution reaction.

1.13. The Mechanism of Oxygen Evolution

In an analysis of the oxygen electrode reaction Milner[79] has pointed out that an enormous number of reaction paths are possible if all intermediates are considered. Even if drastic assumptions are made, more than ten mechanisms are still possible. The values of kinetic parameters for many of these paths

are identical and therefore evidence other than that obtained from Tafel slopes is required to unambiguously identify the complete mechanism. To date no mechanism has been rigorously proved in this way.

The possibility of hydroxyl radicals participating in the oxygen evolution reaction was pointed out in an early review by Hickling.[80] The correlation between oxygen overpotential and the energy of the M-OH bond[75] described in Section 1.12, affords further support for this idea. Thermodynamic calculation by Hickling and Hill[81] has shown that the interpretation of oxygen overpotential on platinum in terms of oxygen atoms as the potential-determining species is not feasible. The hydroxyl radical is a reasonable alternative since, at a theoretical pressure of 1 atm, it was estimated[81] to have a potential of 2.82V against a hydrogen electrode in the same solution. On this basis the hydroxyl radical activity on platinum is about 10^{-22} atm at the commencement of appreciable oxygen evolution.[82]

Formation of adsorbed hydroxyl radicals probably occurs via the transfer of an electron from a water molecule to the electrode

$$H_2O \longrightarrow OH_{(ads)} + H^+ + \bar{e} \qquad 1.13.1.$$

The water molecule involved would presumably be situated in the inner region of the double layer. This would provide an explanation for the sharp increase in oxygen overpotential which occurs[78] as current density is increased in concentrated acid solutions (see Section 1.12). At high current densities the rate of discharge exceeds the rate at which water molecules can reach the surface and so the potential rises until a value is

reached where direct anion discharge can occur.

In the mechanism favoured by Hoare[83] in the case of platinum, equation 1.13.1 is the rate-determining step and is followed by a fast reaction

$$OH_{(ads)} + OH_{(ads)} \rightleftharpoons O_{(ads)} + H_2O$$

or

$$OH_{(ads)} \rightleftharpoons O_{(ads)} + H^+ + e^-$$

Oxygen is evolved by the reactions

$$O_{(ads)} + O_{(ads)} \rightleftharpoons (O_2)_{(ads)}$$

and

$$(O_2)_{(ads)} \rightleftharpoons O_{2(g)}$$

An alternative mechanism[82] regards the formation of adsorbed peroxyl radicals as the slow step, viz.

$$OH_{(ads)} + O_{(ads)} \xrightarrow{slow} O_2H_{(ads)} \xrightarrow{fast} O_{2(g)} + H^+ + \bar{e}$$

In view of the fact[84,85] that hydrogen peroxide is itself oxidized at potentials greater than 0.85V, the possibility of detecting peroxide as a product of the anodic oxidation of water is negligible.

1.14. Ruthenium and Iridium as Substrates for Oxygen Evolution

The large-scale production of hydrogen gas by the electrolysis of water is currently of considerable interest[86] and the development of suitable thin-film cells based on the use of sheets of sulphonated fluorocarbon polymers has been described recently by Titterington and Austin.[87] As they have pointed out, one of the major sources of energy loss in such a cell* is the overpotential associated with the anodic process, i.e. the oxygen evolution reaction. The correlation between the oxygen overpotential and the strength of the metal-hydroxyl bond, reported by Ruetschi and Delahay,[75] has been mentioned earlier (Section 1.12). Of the noble metals ruthenium and iridium have the highest numbers of unpaired electrons per atom.[88] This suggests[89] strong metal-hydroxyl interaction and, consequently, low oxygen evolution overpotential. Furthermore, they are among the very few metals whose oxides behave as metallic conductors.[90,91]

Appreciable oxygen evolution on ruthenium has been reported[92,93] at relatively low overpotentials with simultaneous corrosion of the metal. Thermally produced films of ruthenium dioxide (RuO_2) have, however, been reported[90,94] as being resistant to corrosion while possessing oxygen evolution overpotential values as low as those for the metal. It has further been observed[95] that the addition of ruthenium salts to the electrolyte enhances oxygen evolution at platinum anodes. Very little data is available[96] on the anodic behaviour of iridium but the results of Damjanovic and co-workers[97] seem to indicate a low oxygen evolution overpotential as expected from the large number[88] (1.7) of unpaired

*See Appendix 1, p.168.

electrons per atom. Furthermore, the metal has long been regarded as highly resistant to corrosion even when used as an anode.[98,99] Thin-film titanium-supported iridium and ruthenium oxide mixtures have found considerable application as a replacement for graphite, in the chlor-alkali industry.[100,101] This shows that there is not an insurmountable economic barrier to the commercial use of the rarer platinum metals.

The foregoing suggests that iridium and ruthenium based anode materials could possibly find use in thin-film cells for electrolytic hydrogen generation. Ruthenium metal appears to be unsuitable as an oxygen evolution substrate due to its ease of corrosion. However, the possibility of using ruthenium species on the electrode surface or in the electrolyte seems worthy of further study, as does the possible use of iridium metal. The object of the work on which this thesis is based was, therefore, to investigate the anodic behaviour of these elements, with particular emphasis on oxygen electrochemistry.

CHAPTER II

EXPERIMENTAL

A wide variety of experimental techniques is available to electrochemists. As well as the common techniques (titrimetric and spectrophotometric analysis, chromatography, mass spectrometry, etc.) which may be used in analysing the products of an electrochemical reaction, numerous electrometric methods present themselves. These include polarography (including alternating current polarography and pulse polarography), cyclic voltammetry, chronopotentiometry, conductivity measurements, coulometry, amperometry, potential step methods and many others. The majority of these involve investigation of the relationship between the current through a working electrode and its potential with respect to a reference; this category may be divided into two groups namely galvanostatic and potentiostatic methods. In the former the current is controlled and the potential monitored while in the latter the potential is controlled and the current monitored.

2.1 Galvanostatic Methods

These methods generally involve passing a constant current through the working electrode, first in one direction and then in the other direction. Usually the magnitudes of the cathodic and anodic currents are identical. The instrumental demands of such a technique are a constant current source, a current measuring device, a means of current reversal and a means of recording potential.

In the present investigation, two basic galvanostatic circuits have been used. The first, represented in Figure 2.1(a) utilized a stabilized power supply

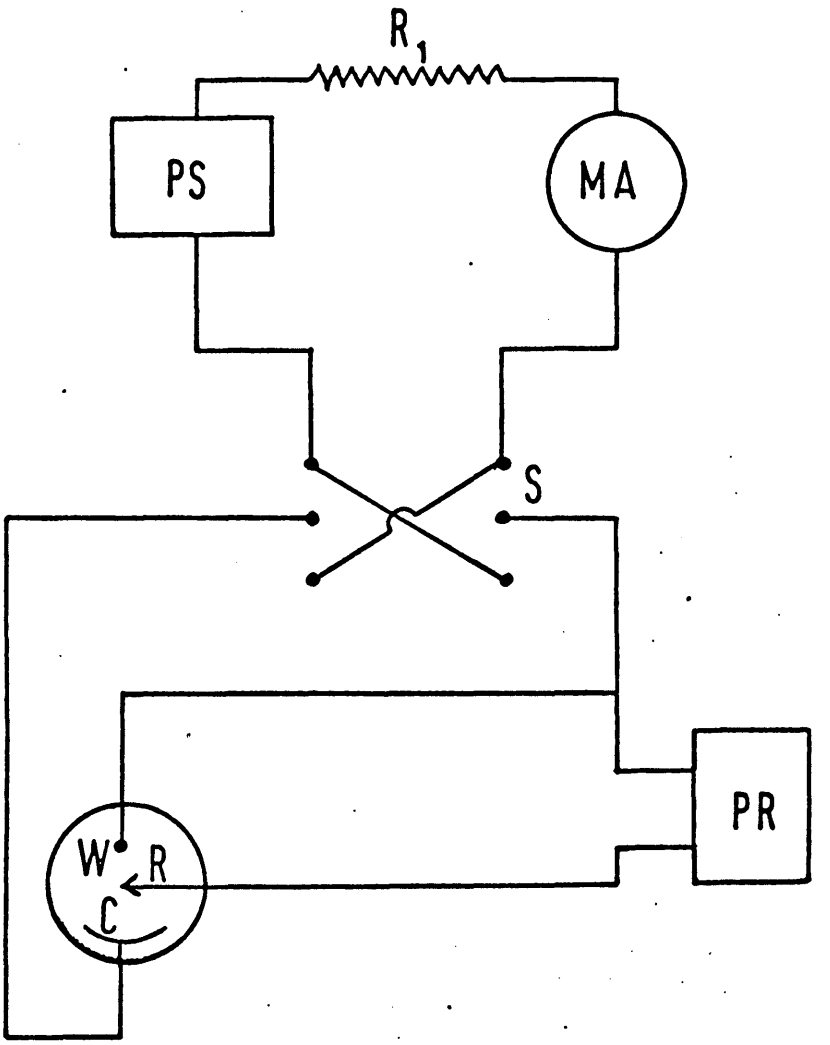

FIGURE 2.1(a) : Simple Galvanostatic Circuit.
PS is a stabilized power supply, MA is a milliammeter, S is a double-pole two-way switch and PR is a potentiometer recorder. C, R and W represent respectively the counter, reference and working electrodes of the cell.

(constant voltage, V) and a large resistance (R_1). R_1 and V were sufficiently large so that most of the voltage drop occurred across R_1 and variations in the potential across the cell had negligible effect on the current. The current could be measured by means of the milliammeter (MA); alternatively this could be replaced by a standard resistance and the current obtained by comparing the voltage across the resistance with a Weston standard cell by means of a potentiometer. The current could be reversed by means of the double-pole two-way switch, S. Typically, a supply voltage of 100V and a resistance $R_1 \sim 1M\Omega$ were used.

An alternative galvanostatic circuit utilizing negative feedback is illustrated in Figure 2.1(b) where A is an operational amplifier (i.e. a differential amplifier with high input impedance, very high gain and low output impedance). The reference voltage, V_1, is applied to the non-inverting terminal of the amplifier. The amplifier develops an output voltage which drives a current, I, through the cell and R_2 in series and the voltage V_2 across R_2 is fed back to the inverting terminal of the amplifier. The output voltage developed by the amplifier is

$$V_3 = K(V_1-V_2)$$

where K is the gain of the amplifier. Thus, if K is sufficiently large, the difference (V_1-V_2) is very small and to a good approximation

$$V_1 = V_2 = IR_2$$

Thus the circuit will maintain a constant current

$$I = V_1/R_2$$

through the cell. The direction of this current

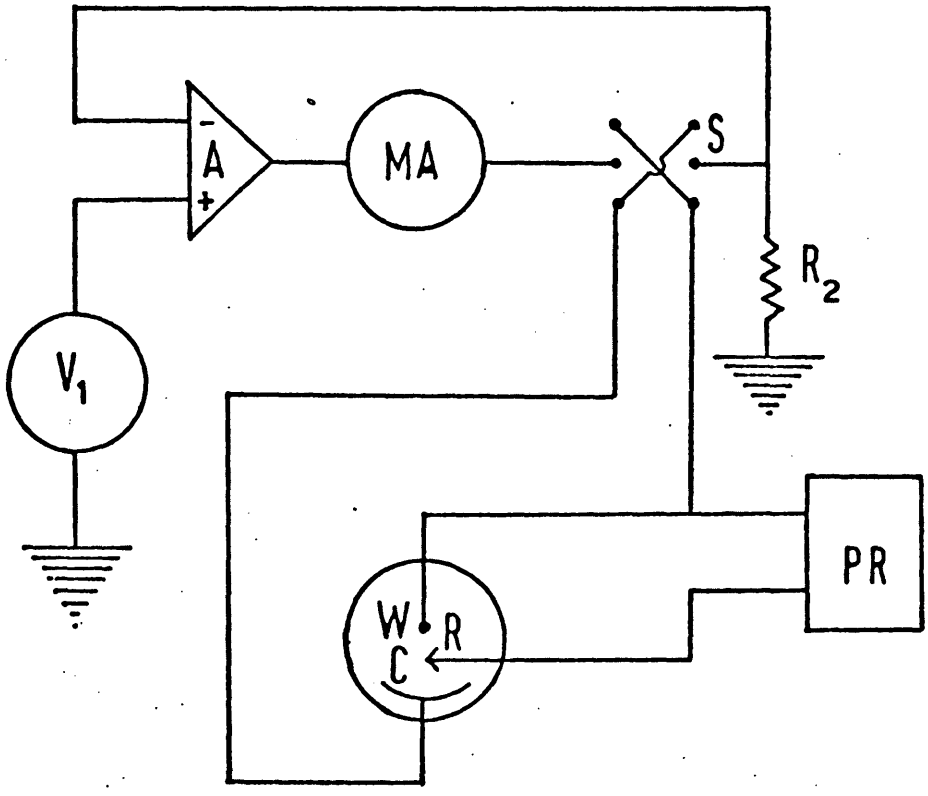

FIGURE 2.1(b) :- Galvanostatic Circuit Using Feedback.

MA, S, PR, C, R and W are as in Figure 2.1(a); A is operational amplifier and V_1 is a stabilized voltage source.

may be reversed by means of the double-pole two-way switch S. In the present work, this circuit has been occasionally employed using a Wenking potentiostat (Model 68FRO.5 or 68TS3) as operational amplifier.

Galvanostatic circuitry was used in obtaining charging curves in preliminary investigations of oxide films. A slight modification of the feedback circuit in Figure 2.1(b) was used in measuring solution resistance (see Section 2.3). However, in most experiments potentiostatic techniques were chosen and these will now be described in some detail.

2.2 The Basic Potentiostatic Method

In all potentiostatic methods, the potential of the working electrode with respect to a reference electrode is controlled and the current necessary to maintain this potential is measured. If the current is small and a convenient reference electrode is available, the potential of which will not change substantially when this current is passed through it, a two-electrode configuration may be used. The desired potential is applied across the electrodes and the resulting current is measured. Such a system is often used in polarography[102] where the desired potential is applied across a dropping mercury electrode (DME) and a mercury pool of substantial area in a chloride electrolyte. When the DME is cathodic with respect to the mercury pool, the latter behaves as a calomel electrode. Such an electrode is relatively non-polarizable and, since the electrode area is large compared with the DME, the current density is low and therefore the potential

across the mercury pool/electrolyte interface does not change substantially with variations in applied potential.

A two-electrode system has the advantage of simplicity but many situations arise where its application is not practical. If, for example, in the polarographic cell described, the DME is replaced by a platinum electrode which is then made anodic with respect to the mercury pool, the latter no longer behaves as a non-polarizable electrode and an alternative reference must be found. In many cases, particularly where the cell current is high, a convenient non-polarizable reference electrode is not available. A further error may occur in the presence of high cell current or poorly conducting electrolyte since there may be substantial current-dependent potential drop due to electrolyte resistance.[103,104] Both problems may be alleviated by use of the three-electrode configuration, described in Section 1.2. The reference electrode is contained in a separate cell compartment which terminates in a capillary known as a Luggin capillary. This is brought to within about 1 mm of the working electrode surface so that the error in potential due to solution resistance is small.

If a three-electrode cell is used in potentiostatic investigations, some form of feedback control is necessary. In its crudest form this might involve manual variation of the current through the cell so that the voltage reading between the working and reference electrodes remains constant. This is usually done automatically by means of a potentiostat. The first potentiostat was designed by Hickling[105] in 1942 and was a very crude instrument when compared with the more sophisticated solid-state devices

available today. A potentiostat is basically a high-power operational amplifier and the potentiostatic control circuit may be represented as in Figure 2.2. The working electrode is connected to circuit ground and the output potential of the amplifier is applied, through a standard resistance R_1, to the counter electrode so that the output current of the amplifier flows through the cell. The potential of the reference electrode, V_1 with respect to ground, is applied to the inverting input of the amplifier and a control potential V_2 is applied to the non-inverting input. The output potential, V_3, of the amplifier is given by

$$V_3 = K(V_2-V_1)$$

where K is the open-loop voltage gain of the amplifier. Since K is very large, the quantity (V_2-V_1) must be small (typically a few millivolts) for practical values of V_3, and so to a good approximation

$$V_1 = V_2$$

Thus the potential of the working electrode with respect to the reference electrode is automatically controlled at $-V_2$. The potential drop across R_1 may be used to monitor the current through the cell.

The potentiostats used in the present investigation were Wenking, model 68FRO.5 or model 68TS3. Potential step techniques and both fast and slow potential sweep techniques were used. Some a.c. impedance measurements were also made. The type of circuit employed is illustrated in Figure 2.3.

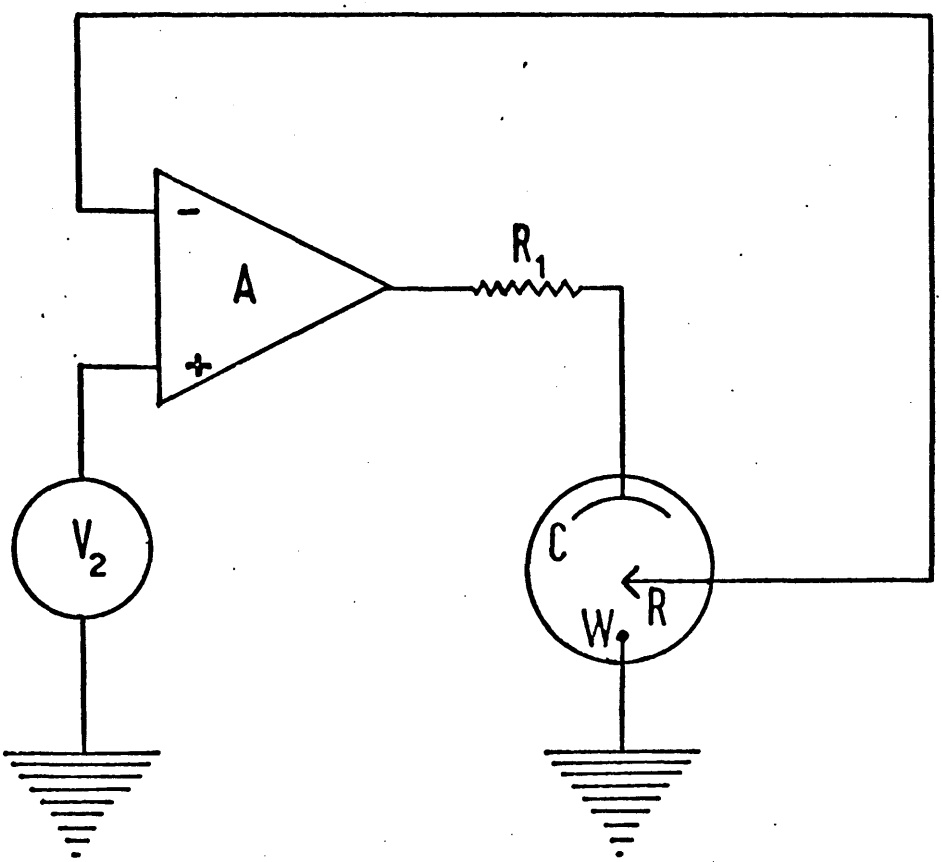

FIGURE 2.2 : Basic Circuit for Potentiostatic Control. C, R and W are as in Figure 2.1(a); A is an operational amplifier and V_2 is a voltage source.

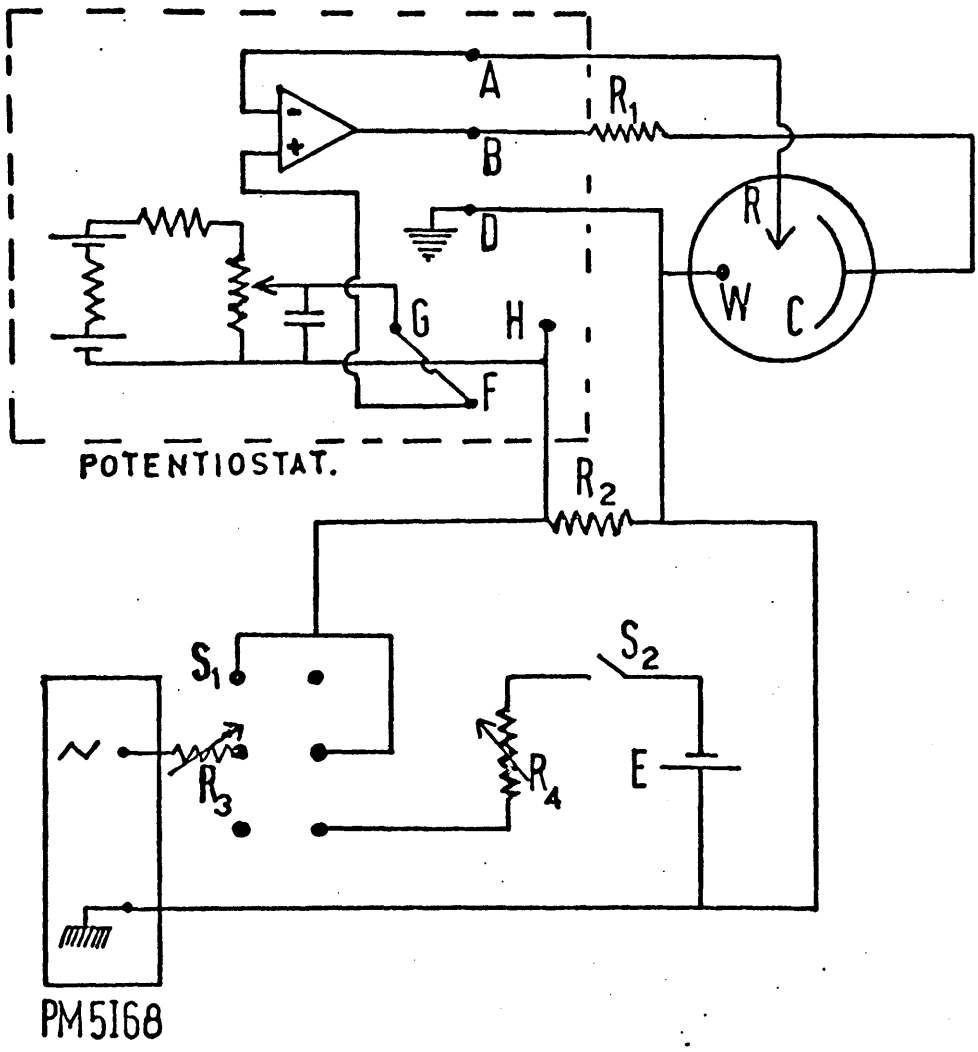

FIGURE 2.3 : Circuit used for Potential Step and Potential Sweep Techniques.

The potentiostat is a Wenking model 68FRO.5 or 68TS3; A, B, D and F are the terminals for the reference electrode, counter electrode, working electrode and control potential respectively; G and H are the output of a variable potential source available on the instrument. PM 5168 is a function generator (Philips) supplying a triangular waveform, S_1 is a double-pole two-way switch, S_2 is a simple switch and E is a 2V (lead-acid) cell; C, R and W are as in Figure 2.1(a); R_1 was chosen so that the potential drop across it was usually ca. 100 mV; R_2 = 1 kΩ, R_3 and R_4 variable, 100Ω - 10Ωkω.

The control potential for the Wenking potentiostat was obtained either from the triangular wave output of a Philips PM 5168 function generator or from a lead-acid cell (E), together with the internal variable potential source supplied with the potentiostat. By means of the double-pole two-way switch, S_1, either a potential step (using the lead-acid cell and switch S_2) or a potential sweep (using the triangular waveform of the PM 5168) could be obtained. The current through the cell was monitored by recording the voltage across the standard resistance, R_1, using a potentiometric recorder or oscilloscope. The circuit used for a.c. impedance measurements is illustrated in Figure 2.4. A sine-wave of suitable amplitude (~ 10 mV peak-to-peak) and frequency (e.g. 200 Hz), from a Philips PM 5100 low frequency generator is superimposed on the triangular sweep by means of the summing amplifier circuit. The a.c. voltage across the standard resistor, R_1, is separated from the d.c. by means of the capacitor C and the resulting signal is amplified, rectified and recorded on a potentiometric recorder. The d.c. current may be recorded simultaneously by monitoring the d.c. voltage across R_1.

2.3. Error associated with Solution Resistance

As already pointed out, error in the measured potential due to solution resistance (commonly referred to as "solution iR error") is considerably reduced by the use of a three-electrode system and a Luggin capillary. However, some error remains, due to the resistance of the solution between the working electrode and the tip of the capillary, and this may be significant at high current density

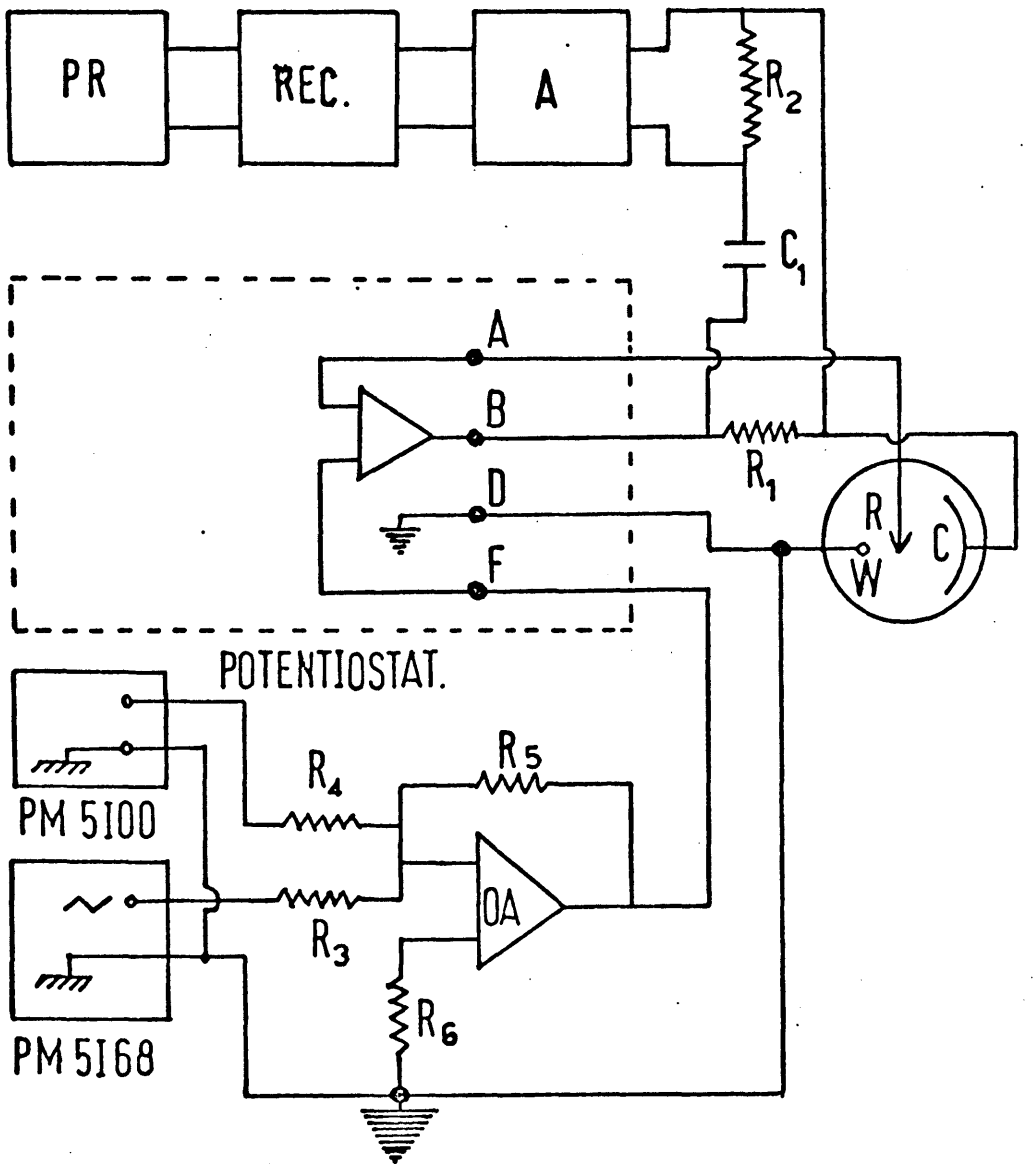

FIGURE 2.4 : Circuit for A.C. Impedance Measurements during Potential Sweep.

Potentiostat is Wenking model 68FRO.5; function generator and R_1 are as in Figure 2.3; C, R, W and PR are as in Figure 2.1(a); PM 5100 is a sine-wave generator (Philips), OA is an integrated circuit operational amplifier (LM741CN, National Semiconductor), A is an amplifier (gain ca. 100) and REC is a rectifier; R_2 = 1 kΩ, R_3 = R_4 = R_5 = 10 kΩ, R_6 = 3.3 kΩ, C_1 = 1 μF.

values. It is possible by means of the current interruption technique[103,105a] to make reasonably accurate measurements of this resistance. The technique involves halting the current flow through the cell momentarily while observing the potential of the working electrode relative to the reference electrode. Following the cessation of current flow, the working electrode potential relaxes because of discharge of the double layer through Faradaic processes. However, the time interval involved in this process has been estimated[105a,106] to be fairly long (ca. 0.3 to 0.5 msec for typical electrodes) and so the difference between working electrode potentials measured before a current interruption and within 5 to 20 μsec following an interruption is essentially the ohmic drop of the cell.[107]

The circuit used for such measurements in the course of the present investigation is illustrated in Figure 2.5. The potentiostat (Wenking, 68FRO.5) is used in a galvanostatic mode (cf. Section 2.1 and Figure 2.1(b)). The current step was applied using a signal from the square-wave output of the function generator (Philips PM 5168) via the potential divider R_2, R_3 and the resulting change in potential was measured by means of a storage oscilloscope (Philips PM 3251 or Advance 052200/2007Y/2006X). The results obtained in a typical series of such measurements are shown in Figure 2.6. The magnitude of the change in potential is found to vary linearly with that of the corresponding change in current in accordance with Ohm's Law. From the slope of the graph the resistance, R_e, of the solution between the Luggin capillary and the working electrode may be estimated. Values of R_c, the resistance of the solution between the working and counter electrodes, may, if required, be obtained

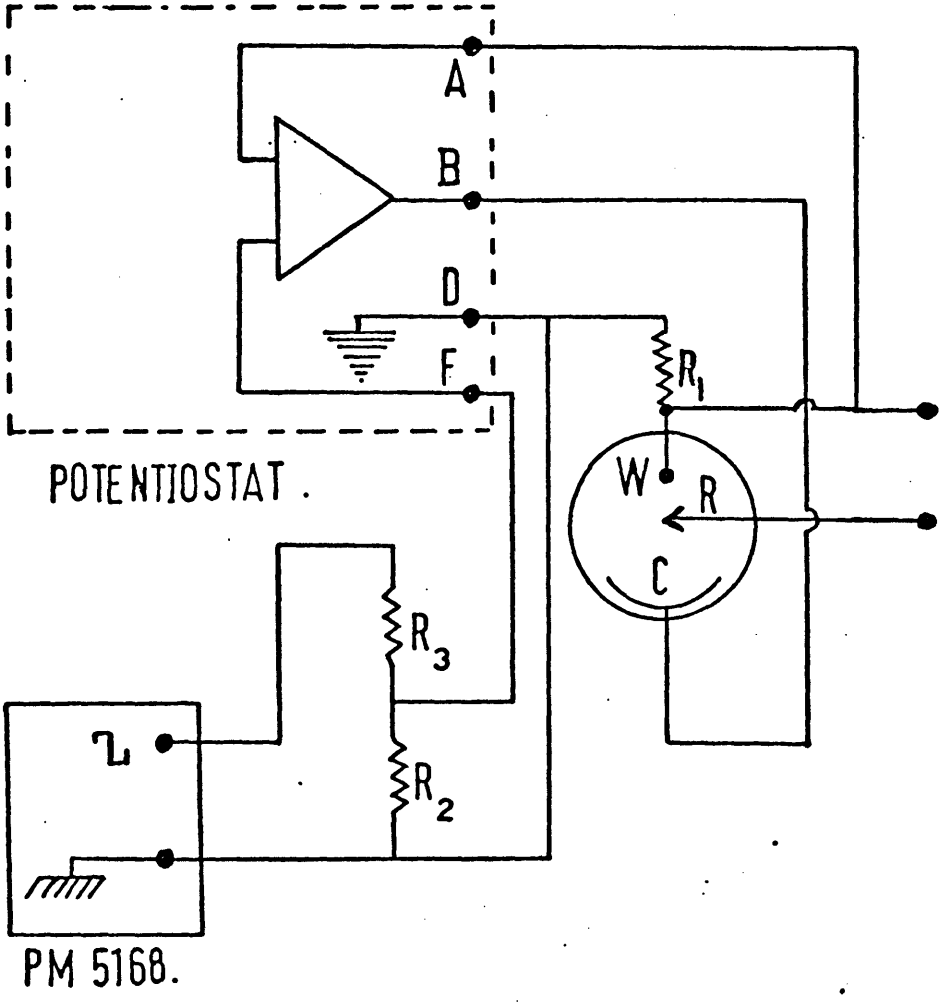

FIGURE 2.5 : Circuit used for Measurement of Solution Resistance

The potentiostat is as in Figure 2.4 and C, R and W are as in Figure 2.1(a). The square-wave output of the function generator (PM 5168) is used. R_1 = 10Ω and R_2, R_3 are variable 0 - 9.9 kΩ.

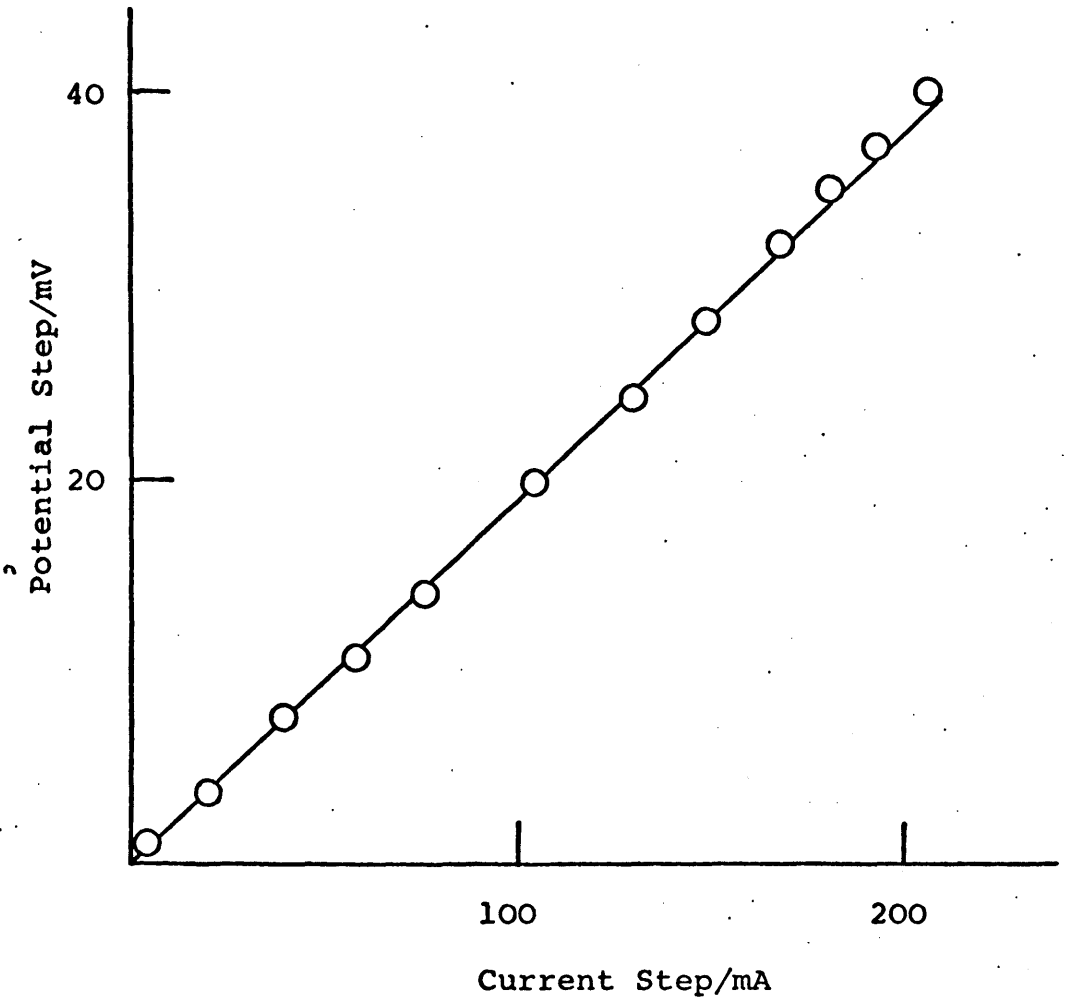

FIGURE 2.6 : Relationship between Current Step and Resulting Voltage Step for an Iridium Electrode in 1 mole dm^{-3} H_2SO_4 at $25^{o}C$.

in a similar manner. Typically, R_e = 0.2Ω, R_c = 2.0Ω.

2.4. Automatic Compensation of Solution iR Error

Error due to solution resistance may be eliminated, or at least substantially reduced, by the incorporation into the potentiostatic system of suitable correction circuitry.[108] When such compensation was required during the present investigation one of the circuits illustrated in Figures 2.7 and 2.8 was used.

The first of these (Figure 2.7) was used in experiments involving a step from a lower potential of 0.6V to a preselected upper potential. Currents at 0.6V were small so that there was no significant error due to solution resistance; however, at the higher values of upper potential, compensation of iR errors was required. A dummy cell consisting of the variable potential source (E_1, R_2 and R_3), the meter (MA), and the resistors (R_4 and R_5) was placed in parallel with the cell. The potential $R_2E_1/(R_2+R_3)$ simulated the potential across the working and counter electrodes. When the potential of the working electrode was at high anodic values current flow through the counter electrode was in the cathodic direction and since the latter consisted of a large area of platinum its potential was ca. 0 V. Therefore, R_2 and R_3 were chosen so that the potential across R_2 with S_2 open was equal to the pre-selected potential of the working electrode. R_5 was set to 1000 R_e and R_4 was then adjusted so that

$$R_5 + R_4 + R_{MA} + R_2R_3/(R_2+R_3) = 1000(R_c + R_1)$$

On closing the ganged switches S_1 and S_2, the control

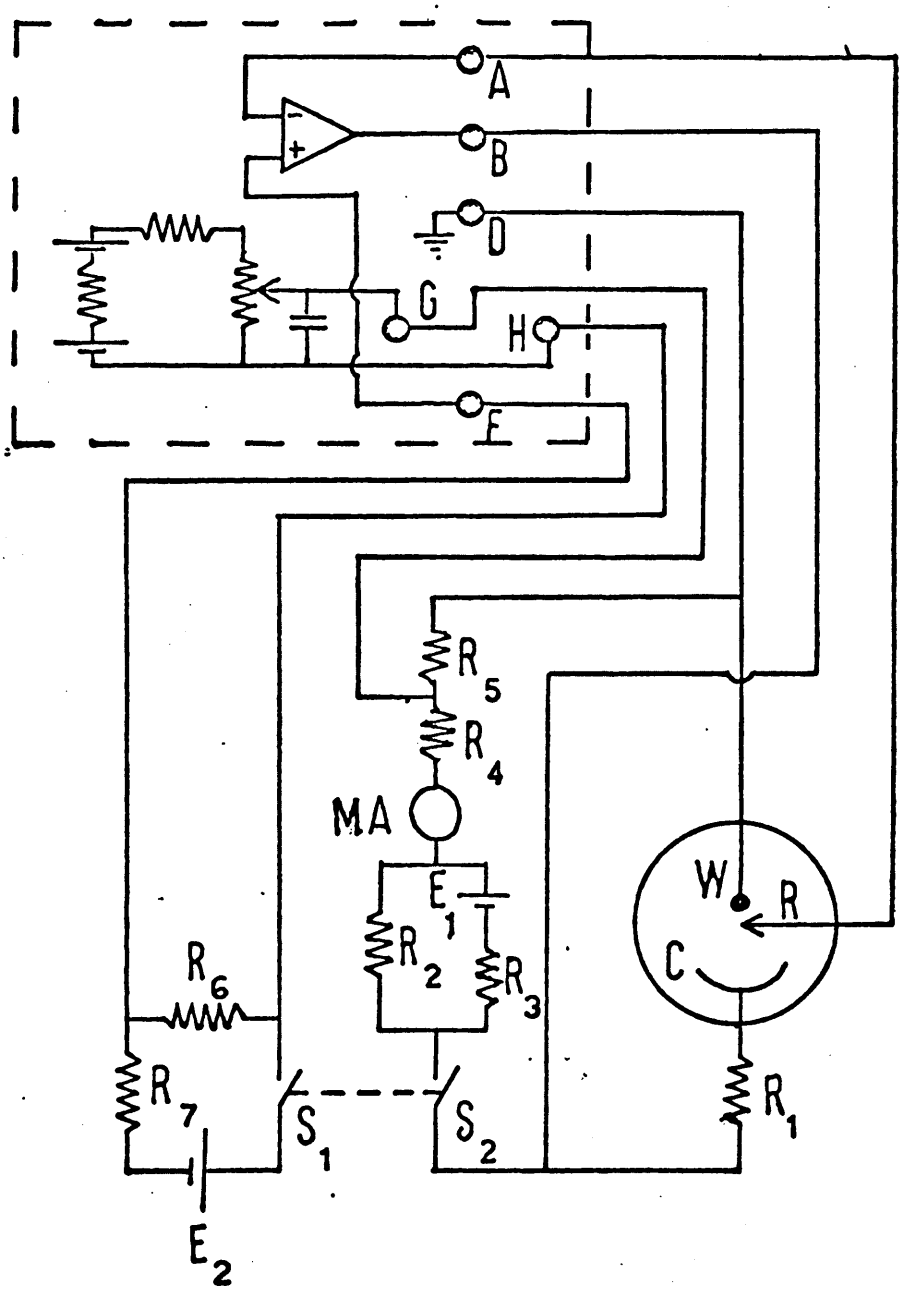

FIGURE 2.7 : Circuit for Automatic Correction of Solution iR Error.

The potentiostat is as in Figure 2.3; C, R and W are as in Figure 2.1(a); MA is a milliammeter, E_1 and E_2 are 2 V (lead-acid) cells and S_1, S_2 are gauged switches; R_6 = 1 kΩ and R_7 is variable 100Ω - 9.9 kΩ.

potential was increased from 0.6V to the pre-selected value and the dummy cell was simultaneously connected. Under these conditions

$$i_1 = 1000\ i_2$$

where i_1 was the current through the cell and i_2 was the current through the dummy.
Therefore

$$i_2 R_5 = i_1 R_e$$

was the potential across R_5 and, since this was included in the control loop, correction for potential drop across R_e was automatically effected.

The circuit in Figure 2.7 had the disadvantage of being suitable only for a fixed potential. Furthermore, changing to a different potential required adjustment of R_2, R_3 and R_4. To overcome these difficulties another circuit was designed (Figure 2.8). Here a correction resistance R_2 was inserted between the working electrode and the potentiostat. The potential across R_2 was amplified by an inverting amplifier of gain $-R_4/R_3 = -2$. The output of this was fed to one input of a summing inverting amplifier, the control potential E_1 being fed to another input of the same amplifier. This output potential, E_2, was applied to the control terminal of the potentiostat. Now

$$E_2 = -(E_1 + 2iR_2)$$

where i is the (anodic) cell current.

The potential of the reference electrode lead is

$$E_R = E_2$$

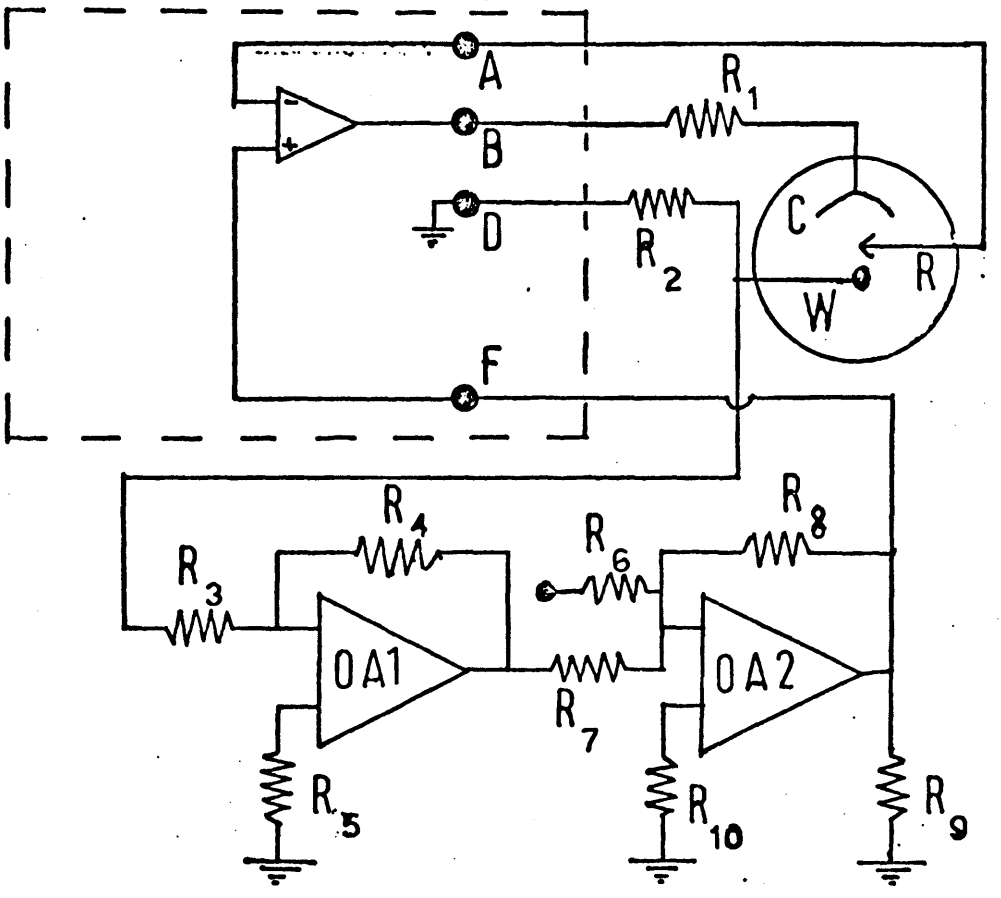

FIGURE 2.8 : Feedback Circuit for Automatic Correction of Solution iR Error.

The potentiostat and R_1 are as in Figure 2.3; C, R and W are as in Figure 2.1(a); OA1 and OA2 are as OA in Figure 2.4; $R_3 = R_6 = R_7 = R_8 = R_9 = 10\ k\Omega$, $R_5 = 5\ k\Omega$, $R_{10} = 3.3\ k\Omega$.

and the potential of the working electrode lead is

$$E_W = iR_2$$

Therefore the potential difference between these two is given by

$$E^1_{WR} = E_W - E_R = -iR_2 - E_2$$

$$= -iR_2 + (E_1+2iR_2)$$

$$= E_1 + iR_2$$

Thus the corrected potential of the working electrode is

$$E_{WR} = E^1_{WR} - iR_e = E_1 + iR_2 - iR_e = E_1 - i(R_e - R_2)$$

$$= E_1 \text{ if } R_2 = R_e$$

(All potentials except E_{WR} and E^1_{WR} are quoted with respect to ground).

It is often found in practice that it is not possible to make $R_2 = R_e$ as this degree of positive feedback would cause the circuit to oscillate. However, it is usually possible to use a value of R_2 which is about 90% of R_e. In potential sweep experiments on iridium, for example, a resistance $R_2 = 0.88\ R_e$ was used, thus correcting for 88% of the solution iR error.

2.5. Electrodes and Cells

In an experimental cell it is important that the current density and hence the potential should be uniform over the entire surface of the working

electrode.[104] This requirement is met if all points on the working electrode are equivalent with respect to distance from the counter electrode. The precise geometrical requirements are less stringent if solutions of high conductivity are employed. In the cells described below, the counter electrode was therefore arranged about the working electrode in as symmetrical a manner as practicable.

Two designs of cell were used. Cell No. 1 (Figure 2.9) consisted of a glass water-jacketed vessel supplied by Metrohm having a plastic lid with sockets for B14 ground-glass cones. The working electrode was constructed by soldering wire of the metal under investigation to a copper lead and sealing it through one end of a glass tube. About 10 mm of the wire was exposed and a ground-glass cone on the tube fitted into a socket in the cell lid. Surrounding the working electrode was a helical spiral of platinum wire which served as a counter electrode. This arrangement gave excellent current distribution in the high conductivity electrolytes (1 mole dm^{-3} $HClO_4$, H_2SO_4 or NaOH) used. The hydrogen reference electrode was constructed as shown in Figure 2.9 and the tip of the Luggin capillary was fixed about 1 mm from the surface of the working electrode. A nitrogen inlet and outlet and a thermometer (not shown) were fitted through further sockets in the cell lid. The cell was thermostatted at (25 ± 0.1)°C by circulating water from a constant temperature bath through the water-jacket. This cell was normally used except in the investigation of iridium corrosion.

Cell No. 2 is illustrated in Figure 2.10. The Luggin capillary is rigidly fixed to the stem of the working electrode which also incorporates a gas outlet.

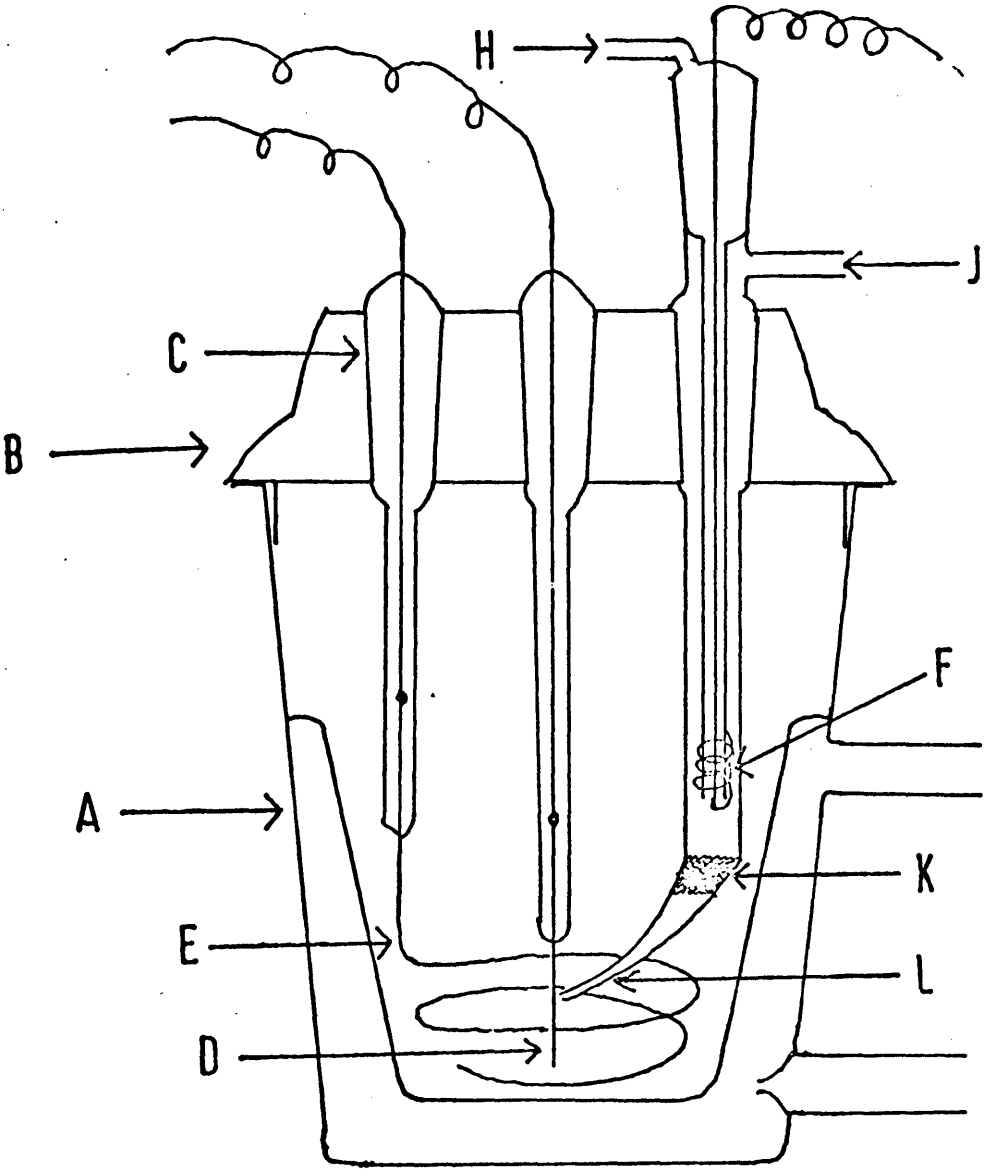

FIGURE 2.9 : Cell no. 1.

A = water jacket; B = cell lid; C = B14 joint;
D = working electrode; E = counter electrode;
F = hydrogen electrode consisting of a piece of platinum wire entering through the hydrogen inlet tube; the end of the wire is platinized;
H = hydrogen inlet; J = hydrogen outlet;
K = glass wool plug; L = Luggin capilliary.

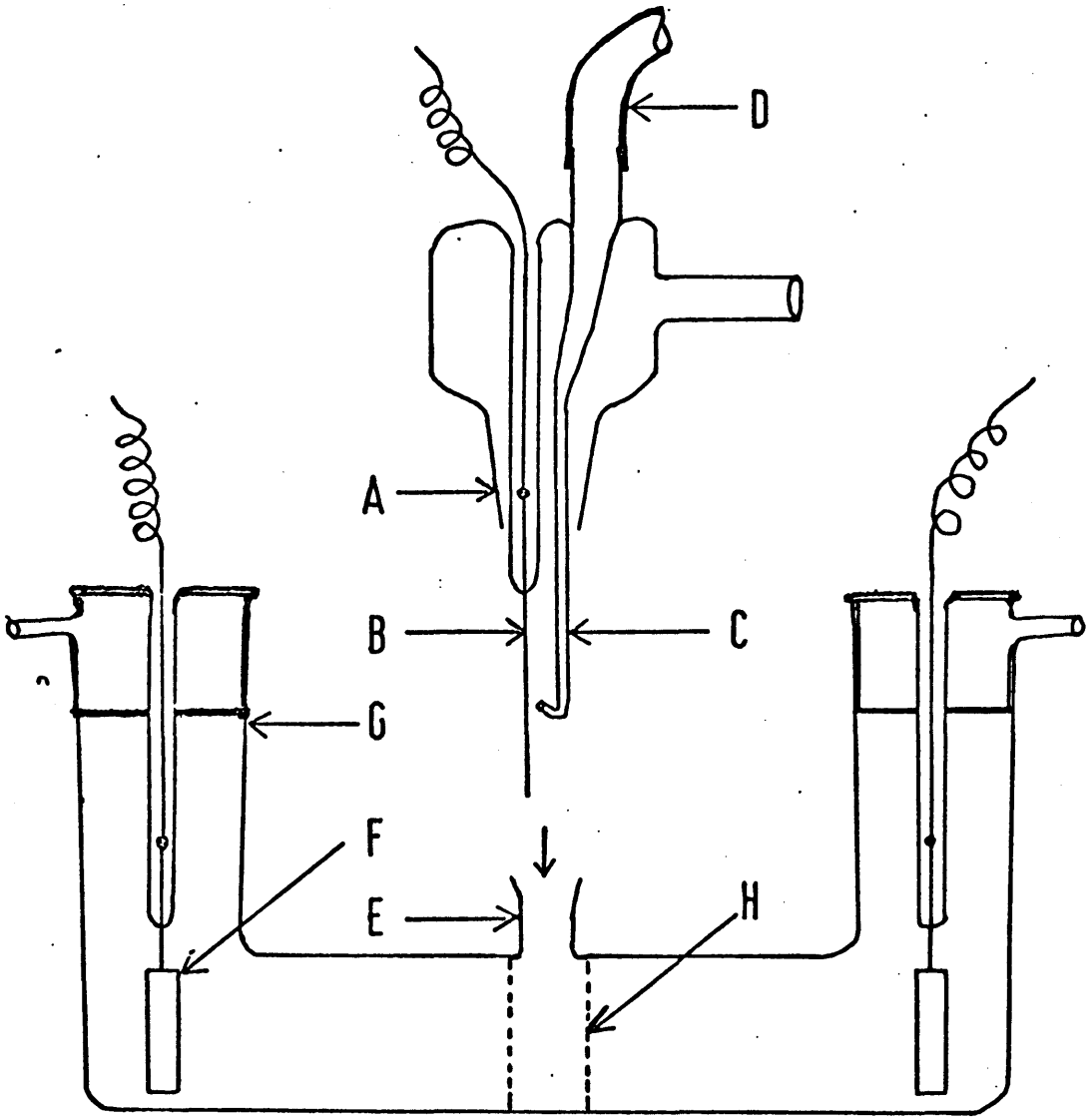

FIGURE 2.10 : Cell no. 2.

A = ground glass cone to fit E; B = iridium wire working electrode; C = Luggin capillary; D = polythene tube to hydrogen electrode compartment; E = ground glass socket to take A; F = platinum gauze counter electrode; G = ground glass joint; H = sintered glass frit (porosity 3).

A piece of polythene tubing connects the Luggin to the reference electrode compartment, Figure 2.10(a). The counter electrode consists of two pieces of platinum gauze, one on each side of the working electrode and separated from it by means of sintered glass discs. This cell was primarily used in studying the corrosion of an iridium working electrode and the sintered glass confined the corrosion product to the working electrode compartment. Both the main cell section and the hydrogen electrode compartment were immersed in a water bath at (25 ± 0.1)^{o}C.

The water used in electrolyte preparation was triply distilled, once from alkaline potassium permanganate and subsequently twice in a commercial quartz still. Analytical grade reagents were used. The wire for the construction of working electrodes was supplied by Koch-Light Laboratories Ltd. (platinum 99.999%, gold 99.999% and iridium 99.9%). Where oxygen would interfere, it was removed from solution by purging with white-spot nitrogen which had been further purified by passing it over a heated copper catalyst (BASF catalyst, 200^{o}C) and through a column of molecular sieve (Linde, Type 3A).

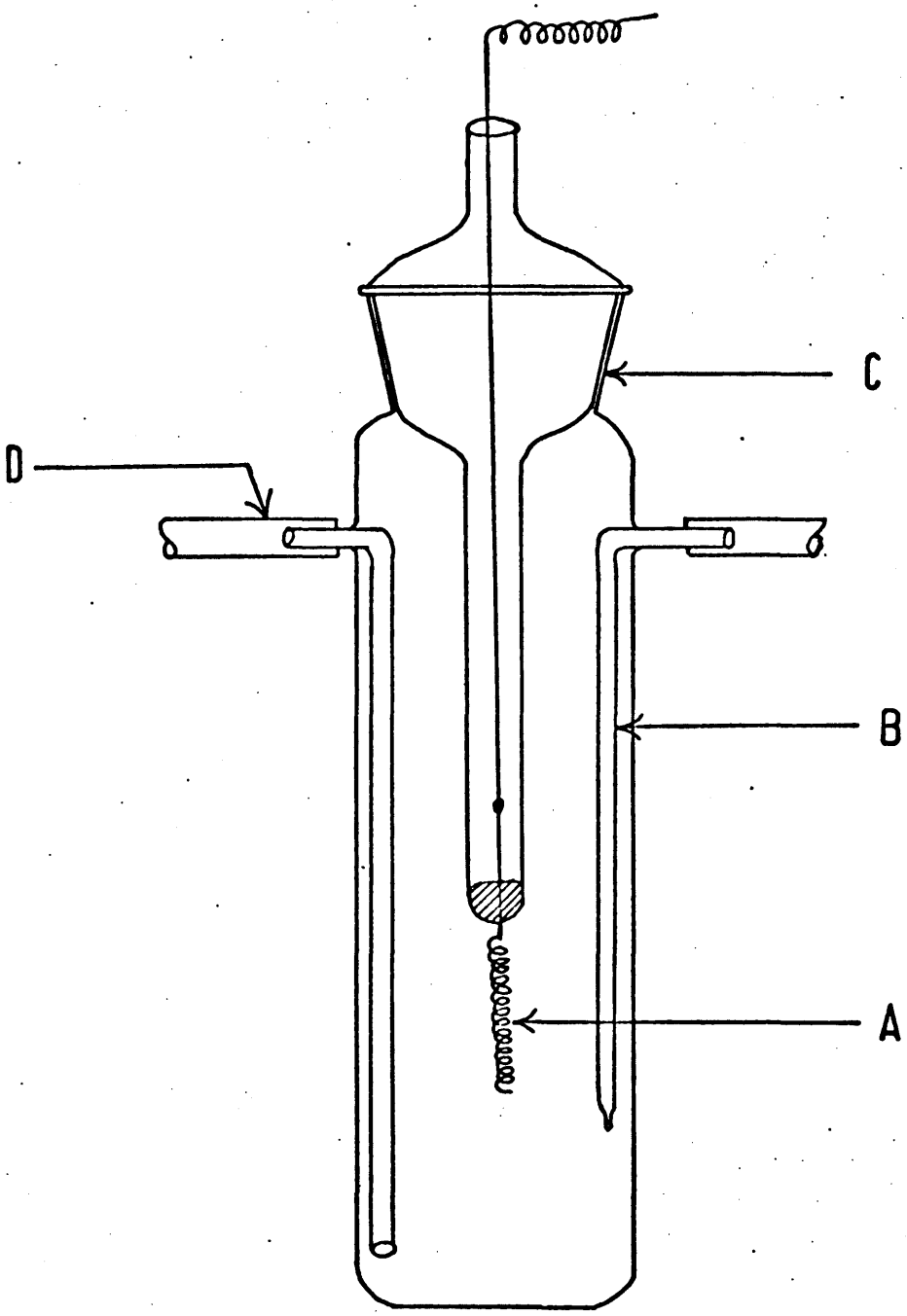

FIGURE 2.10(a) : Hydrogen Electrode Compartment of Cell No. 2.

A = platinized platinum wire; B = hydrogen inlet tube (outlet not shown); C = ground glass joint; D = polythene tube to working electrode compartment.

CHAPTER III

RUTHENIUM

Ruthenium was the last of the platinum metals to be discovered, being first reported by Osann[109] in 1827. A rare element, its abundance in the earth's crust is probably[110] near 0.0004 ppm. Like osmium it has a hexagonal close-packed crystal structure; the other noble metals have a face-centered cubic structure.[111] Ruthenium is very inert and is not attacked by acids.[112] When heated to 1000°C in oxygen the stable dioxide RuO_2 is formed.[113] The anodic electrochemistry of the metal has been investigated by Llopis and Vazquez[92] using ruthenium plate and by Burke and O'Meara[93] using ruthenized platinum.

3.1. Anodic Oxide Films on Ruthenium

Anodic charging curves obtained[92,93] in 1.0M $HClO_4$ starting from 0 V do not show a clear separation of three regions as found with platinum (cf. Section 1.10). The hydrogen film oxidation region extends up to rather positive potentials and the oxidation of ruthenium begins at low potentials so that the processes overlap. If the starting potential is slightly more negative than that of a hydrogen electrode in the same electrolyte, a first region corresponding to hydrogen film oxidation is distinguishable[92] but no region corresponding to double layer charging is evident.

Potential sweep experiments[93] confirm the above results. The curve obtained is in marked contrast to those reported for platinum[114,115] and most other noble metals[116,117] and there is strong overlap between the oxygen and hydrogen regions. However if the potential is allowed to go well into the cathodic region, to potential values at which vigorous

hydrogen evolution takes place, an inflection at about 0.25 V on the subsequent anodic sweep is reported.[93] It is suggested that this corresponds to the beginning of oxide film formation.

Llopis and Vazquez[92] reported two changes in slope giving three linear regions in the anodic charging curves. These are the hydrogen region already mentioned and two oxide regions and correspond to amounts of electricity Q_H, Q_{O1} and Q_{O2}, respectively. Region Q_{O1} begins at a potential of 0.55 V and this is regarded as the beginning of ruthenium oxidation. However, cyclic sweep experiments on ruthenized platinum[93] suggest that the oxidation of ruthenium begins at ca. 0.25 V. Region Q_{O2} begins at 1.05 V and it is suggested that RuO_2 formation begins at this potential. The value agrees quite well with the value given by Zoulov and Pourbaix[118] for RuO_2 formation.

The value of Q_H was found to increase as the starting potential was made more cathodic. Q_{O1} and Q_{O2} do not vary significantly with starting potential and values of 23 mC cm^{-2} and 25 mC cm^{-2} respectively, are reported. These quantities of electricity are much higher than those obtained in the case of rhodium. Assuming that Q_{O1} corresponds to formation of a monolayer of RuO and Q_{O2} to formation of a RuO_2 monolayer, the values found would imply a roughness factor in the order of 55 for the ruthenium plate electrode. This seems very high. In the absence of surface area measurements, a definite conclusion cannot be drawn as to the reason for the high oxide capacity but it seems likely that more than monolayer adsorption may be involved. However, Burke and O'Meara[93] have reported that the charge required to change the

potential of the ruthenized electrode from the hydrogen evolution region to that of oxygen evolution is about 110 mC cm^{-2}. This is appreciably less than the corresponding value (ca. 300 mC cm^{-2}) required for platinized platinum[119] but it is suggested[93] that the difference is due to the formation of a smoother, more adherent deposit in the case of ruthenium.

Cathodic charging curves in 1M $HClO_4$ from starting potentials ranging from 0.75 to 1.55 V have been examined.[92,93] Typically a linear curve without inflections is obtained tending in the end towards a steady value which corresponds to hydrogen formation. There is no initial drop in potential which could be related to charging of the double layer. Burke and O'Meara[93] have reported that the cathodic charging curve is longer than the anodic one and have suggested that an explanation may lie in the difficulty with which the oxide film on ruthenium is reduced. Thus, it is postulated that evolution of gaseous hydrogen commences before all oxide is removed from the surface. This may also explain why pretreatment at potentials of appreciable hydrogen evolution is required before the first inflection on either the potential sweep curve[93] or the anodic charging curve[92] is observed.

If a ruthenized electrode is potentiostatted initially at 0 V in oxygen-stirred solution and then put on open circuit the potential increases until a rest potential of ca. 0.9 V is eventually obtained[93] (after a period of at least 30 min). The oxide coverage of the surface at various times after putting the electrode on open circuit was estimated from anodic charging curves and a close inter-relationship between oxide coverage and potential

was found, both varying in a virtually identical manner with time. The current potential behaviour for the cathodic reduction of dissolved oxygen gas has also been investigated.[93] Compared with platinum, the reaction on ruthenium was found to require a considerably higher overpotential.

The results quoted above can be accounted for in terms of the strong affinity of ruthenium for oxygen. It has been pointed out by Llopis and Vazquez[92] that if the platinum metals are placed in order of increasing number of unpaired d-electrons per atom, the oxide coverage is also found to increase and the potential at which oxidation of the surface begins is found to decrease in the same order. These results indicate that it is reasonable, as suggested by Uhlig,[120,121] to suppose that the d-electrons participate directly in the bonding of oxygen atoms to the surface of platinum metals. Ruthenium and osmium which have the highest number of unpaired d-electrons per atom[88] also have the greatest affinity for oxygen. Rao and co-workers[88] quote a limiting value of 95% for the oxide coverage attained by a ruthenium electrode in oxygen-saturated solution compared with a value of 25% for platinum under similar conditions. It has been suggested that this strong affinity of the ruthenium surface for oxide species not only accounts for the low potential required to initiate oxide film formation and the consequent overlap of the hydrogen and oxygen regions but also explains the low oxygen rest potential at the heavily oxidized ruthenium surface. For a similar reason ruthenium is a very unfavourable substrate for oxygen reduction,[93] the adsorbed intermediate being highly stabilized and only reduced at large cathodic overpotential values.

3.2. The Anodic Properties of Thermally-Prepared Ruthenium Dioxide Films

Among the oxides of the transition metals, ruthenium dioxide (RuO_2) is rather unusual in that together with a few other oxides[90] (e.g. IrO_2, TiO), it exhibits a metallic conductivity of the order of 10^4 ohm^{-1} cm^{-1} in single crystals.[91,122] This is also found in films[123] prepared by the thermal decomposition of $RuCl_3$ although the values are some 1000 times less. As a consequence of the excellent results obtained in chlor-alkali cells,[124,125] considerable interest has arisen during the last few years in electrodes based on these materials. Their properties have been examined in some detail by Trasatti and co-workers.[126,127]

The electrochemical behaviour of thermally-prepared RuO_2 films[126,127] differs both from that of RuO_2 single crystals[126] and from anodically formed oxide.[93,127] The current/voltage curve for a single crystal is characteristic of a redox process whereas the thermally-prepared film of RuO_2 behaves as an electric capacitor exhibiting a charging and discharging process which does not effect the response of the electrode even after a very long working period. The curve for ruthenium is similar to that for the thermal ruthenium dioxide films except that current values are higher in the case of ruthenium. The similarity is expected since ruthenium has a surface oxide film at anodic potentials.[92,93] However, the properties of the anodically formed oxide differ from those of the thermally-prepared film in that the latter is not observed[126,127] to corrode at anodic potentials. The overpotential

for oxygen evolution on both thermal ruthenium dioxide[126,127] and on ruthenium[92,93,127] is much lower than on platinum.

Galvanostatic charging curves of thermal ruthenium dioxide films[126,127] show two linear regions, the change in slope occurring at about 0.3 V. If the charge (q) of the electrode is measured between the potential of oxygen evolution and 0.3 V, the values obtained from the anodic and cathodic curves are fairly similar. These values are reported to be independent of current density and, for a given electrode, are remarkably reproducible from one run to another; any variation indicates that the film has been damaged mechanically or chemically. Thus (q) represents a quantity by which the electrode may be characterized; the value depends on the temperature of preparation, the thickness of the film and the atmosphere in which it has been annealed. Trasatti and co-workers[126,127] concluded that in this potential region the ruthenium dioxide film is acting as a large capacitor and the current may be considered as a charging current.

The charge stored on the electrode measured by integration of the current potential curves is almost a linear function of potential as in the case of a capacitor. The slope of the graph gives an apparent capacity of about 100 mF cm^{-2} which is very large compared with the double layer capacity or the capacity due to surface films. As the rate of linear change in potential is increased, the integral capacity decreases although the slope of the line remains unaltered, i.e. the differential capacity is the same. This indicates that a relatively slow phenomenon which is not simple displacement of electrons must be involved in the charging process.

Further evidence for this is afforded by the fact that the electrode takes some time to reach zero current at any constant potential. It is suggested that the process is related to non-stoichiometry, the maximum charge storage capacity of the electrode corresponding to one electron for each ruthenium atom formally present as Ru^{3+}. In other words, in this range of potential the formal reaction

$$Ru^{4+} + e^{-} = Ru^{3+}$$

is responsible for the charge storage properties and is restricted to a number of atoms equal to the magnitude of the non-stoichiometry, whereas the remaining atoms in the lattice are unreactive. This formal solid-state redox reaction is accompanied by penetration of protons into the lattice during the cathodic charging, and expulsion of protons from the bulk of the solid phase during anodic charging.

The total charge required to change the potential of the electrode from the oxygen evolution region to the hydrogen evolution region depends on current density. It is also found that if the electrode is held at 0.1 V the charge capacity of the electrode obtained from the subsequent anodic charging curve increases with increasing time at 0.1 V. This suggests that modifications much slower than the process just described occur in the electrode at potentials more cathodic than 0.3 V. As further evidence of this the behaviour of an electrode after prolonged hydrogen evolution may be cited. An electrode kept at -0.05 V for 15 hr showed, 1 hr after release, an open circuit potential of about 0.5 V increasing very slowly. Likewise if the electrode was maintained under oxygen

evolution at 1.6 V for 15 hr the open-circuit potential decreased rather rapidly to 1.35 V after release. The normal rest potential (0.95 V) was easily established in this case, however, after a very short excursion of the electrode potential to values just above the hydrogen discharge region. In the case of the electrode which was cathodized for 15 hr, a rapid passage through the anodic region before the oxygen evolution region did not yield a similar result. Furthermore, persistent hydrogen evolution led to some collapse of the film with the deposition of a black powder, presumably ruthenium at the bottom of the cell. Trasatti and co-workers suggested[127] that below 0.3 V the entire lattice becomes unstable with respect to reduction. They concluded that penetration of hydrogen atoms is the most probable mechanism, reduction now involving all atoms in the lattice.

A reported difference[127] between a "dry" electrode (just prepared and dipped in the electrolyte) and a "wet" electrode (after some immersion and potential cycling) is worth noting. Although the current/potential curves for the two cases were similar, some quantitative differences were observed. It was suggested that the bulk of the electrode must undergo some rearrangement which might be associated with hydration or protonation of the lattice, before the current/potential curve could assume its usual shape.

3.3. Oxygen Evolution and Corrosion

A sharp increase in current was observed[93] on the current/potential curve of ruthenium in acid solution at about 1.4 V. In going from 1.4 V to

1.5 V, the anodic current increased from 1 mA cm^{-2} to 100 mA cm^{-2}. A similar increase, though of much smaller magnitude, was observed in alkaline solution though under these conditions no evolution of oxygen occurred. The increase in current density was accompanied by the development of a greenish-yellow colour in the solution, obviously due to ruthenium corrosion.[92,93] Evidence that the species obtained in acid was, in fact, the tetroxide is afforded by the report[93] that during the corrosion reaction in 1M $HClO_4$, a black solid was formed along the gas outlet line from the cell. This solid probably was hydrated ruthenium dioxide arising from the decomposition of the volatile and unstable tetroxide,[128] RuO_4.

The variation of current density with time at fixed anodic potentials was also investigated.[93] At 1.30 V the current density values were small and decreased in an exponential manner with time. At 1.40 V the initial values were also quite small but, rather than decreasing in the normal way, the current density in this case increased with time. A further unusual feature of the process was the fact that the increase did not occur in a regular manner but showed somewhat irregular jumps while continuing to rise for a period of at least 4 hr. At 1.45 V the current density was initially quite large and continued to increase regularly over the first 10 min after which time the process was complicated by the depletion of the ruthenium deposit on the underlying smooth platinum surface.

These results may be explained in terms of the anodic dissolution of ruthenium and the evolution of oxygen gas. The irregular rate of increase of current

density with time at 1.40 V has been attributed[93] to stress corrosion cracking.[129] At this potential value the corrosion reaction is slow and it has been suggested that stress, developing at the heavily oxidized surface, gives rise to cracking and partial dissolution of the oxide film at irregular intervals. Associated changes in corrosion and oxygen evolution rates were assumed to account for the irregular current increases.

The observed negative correlation[75] between experimental oxygen overpotential values and the estimated strength of the metal hydroxyl (M-OH) bond is mentioned earlier (Section 1.12). Thus, ruthenium, which is a strongly chemisorbing metal, evolves oxygen at a relatively low overpotential (0.17 V). However, the use of ruthenium as an oxygen evolution substrate is rendered impractical by the ease with which the metal corrodes at anodic potentials. Thermally-prepared ruthenium dioxide films[127] also evolve oxygen at low overpotentials and are reported not to corrode at the potentials involved. This type of electrode would, therefore, appear to be a useful substrate for oxygen evolution.

3.4. Investigation of Oxygen Evolution at Noble Metal Electrodes in the Presence of Ruthenium Salts

It has been reported[95] that the overpotential of oxygen evolution at a platinum anode in aqueous 1M $HClO_4$ is considerably reduced if ruthenium trichloride is added to the electrolyte. A suggested explanation of the lower overpotential was in terms of a catalytic mechanism occurring in solution due to the presence of

ruthenium ions. The results of further investigation of the effect are now presented. Experiments were carried out using cell no. 1. Ruthenium trichloride solutions were prepared by dissolving 0.1 g of the salt ($RuCl_3$. x H_2O, Johnson Matthey Chemicals Ltd.) in 100 ml of electrolyte solution. In most cases the addition of a 1 ml sample of this solution to the electrolyte in the working compartment of the cell (ca. 50 ml capacity) was sufficient to have a pronounced effect on the oxygen overvoltage.

Reproducibility of experimental results is generally a problem with solid electrodes, especially in the anodic region where oxide films produced on the electrode surface are not readily reduced.[49] It was found that in order to avoid effects associated with the previous history of the specimen, it was necessary to adopt a standard pretreatment. This involved cycling the electrode potential from 0 to 1.7 V at 2.5×10^{-2} Hz for 3 min, then 4 min at 0 V to remove oxide, and finally 3 min at 0.6 V to oxidize hydrogen or any other reduced species on the metal surface. This pretreatment, which caused considerable roughening of the electrode surface (as indicated in the case of platinum by the increased anodic oxide capacity) was found to be essential in the case of potential-stepping experiments.

RESULTS

3.5. Charging Curve Experiments

The lowering of the oxygen overvoltage in the presence of ruthenium trichloride is demonstrated in Figure 3.1 where charging curves are shown for platinum both in the absence and in the presence of

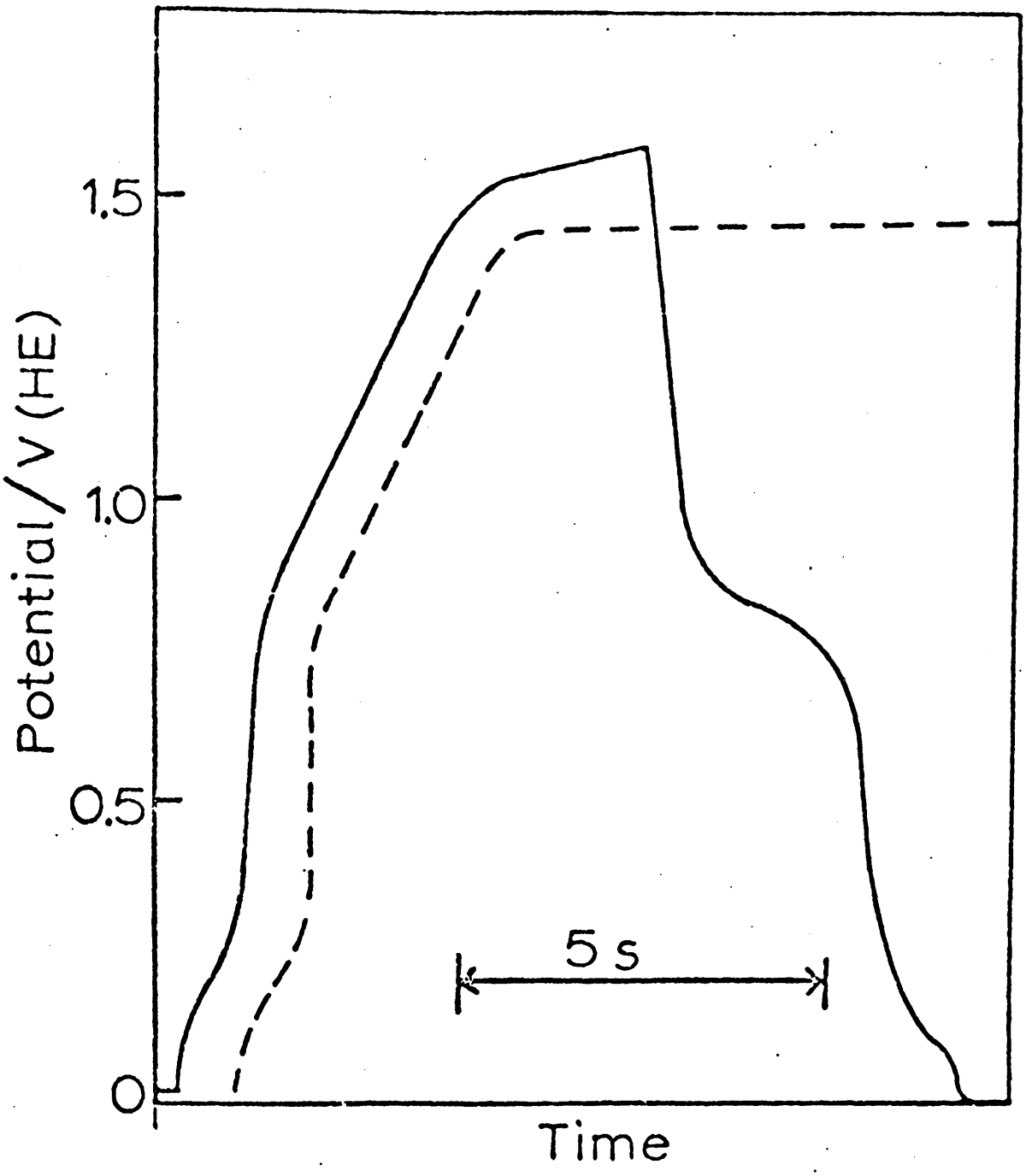

FIGURE 3.1 : Charging curve for a platinum electrode in 1 mol dm^{-3} $HClO_4$. T = 25°C, both in the absence (——) and in the presence (----) of ruthenium chloride in the solution. $RuCl_3$ concentration = 0.15 mmol dm^{-3}.

the ruthenium salt. As is well known from previous investigations of the anodic behaviour of platinum,[49] oxygen evolution in the absence of ruthenium does not commence until the end of the oxide film region, i.e. ca. 1.5 V. Even then the anodic potential increases gradually under constant current conditions as the oxide coverage or thickness on the substrate increases. In the presence of the ruthenium salt oxygen evolution commences at ca. 1.4 V and although the potential again tends to drift to more anodic values with time, the rate of increase is considerably less under these conditions, i.e. potentials were always lower in the presence of ruthenium trichloride for the passage of equivalent amounts of electricity. The addition of ruthenium trichloride to the acid solution when the electrode potential had already reached 1.55 V caused only a very slight reduction (ca. 20 mV) in the oxygen evolution potential.

3.6. Potential-step Experiments

Previous potential-step measurements with platinum in acid solutions[74] have clearly shown two stages, an initial oxide film formation process followed by the main oxygen evolution reaction. The complexity of the latter process is clearly shown by the recent work of Schultze[74] who reported a marked continuous variation of the current, i.e. rate of oxygen evolution, with time under potentiostatic conditions. The results shown in Figures 3.2, 3.3 and 3.4 refer largely to the second (oxygen evolution) stage of the reaction since preliminary experiments showed that at 1.6 V oxide film formation was virtually completed within a period of one second.

Figure 3.2, curve A illustrates the typical behaviour of a platinum electrode in ruthenium-free acid solution when the potential was stepped from the oxide-free region (0.6 V) to an oxygen evolution potential (1.6 V). This curve also demonstrates the fact that after the surface had been oxidized for a considerable period (325 s) at the higher potential, the addition of ruthenium trichloride caused only a slight increase in the oxygen evolution current. Subsequent pretreatment of the electrode in the presence of the ruthenium salt caused a considerable increase in the oxygen evolution current at 1.6 V (Figure 3.2, curve B), the rate for instance being ca. 15 times that for the same reaction in the absence of ruthenium after a period of 5 min at the oxygen evolution potential. An unexpected feature of the results was the fact that transferring an electrode which had been pretreated and anodized for 30 s at 1.6 V in an acid solution containing ruthenium to a similar solution containing no ruthenium resulted in continued enhancement of the oxygen evolution process (Figure 3.2, curve C). Obviously the lowering of the oxygen evolution potential in the presence of ruthenium must be due to some species deposited on the electrode surface, and apart from this initial discharge process, the lowering of the oxygen overvoltage does not require any further participation of dissolved ruthenium species. Whatever the nature of the species on the surface, its catalytic effect on the oxygen evolution process is lost once the electrode in the ruthenium-free solution is allowed to go cathodic. Subsequent anodic stepping experiments in the ruthenium-free solution give the results shown in Figure 3.2, curve D, i.e. typical of untreated platinum.

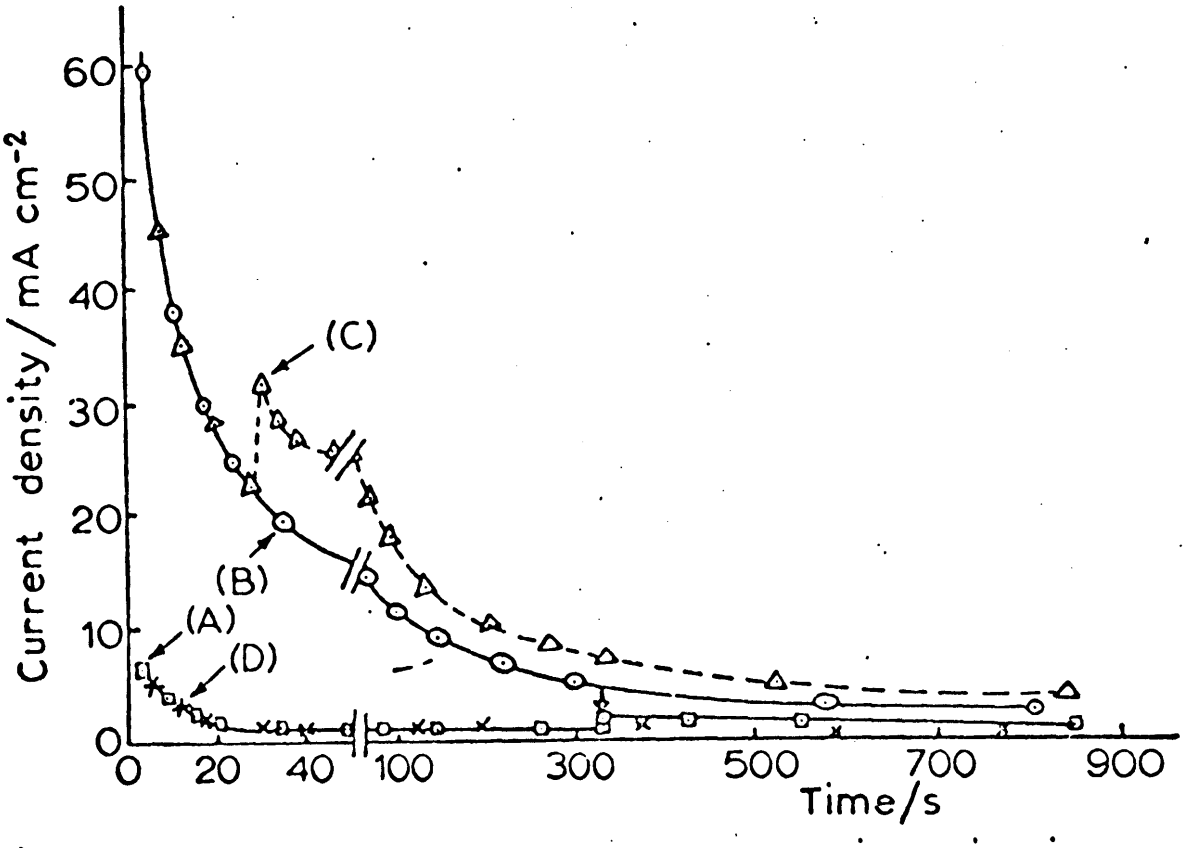

FIGURE 3.2 : Current decay curves for a platinum electrode whose potential was stepped at zero time from 0.6 to 1.6 V in 1 mol dm^{-3} $HClO_4$ at 25°C. (□) In the initial absence of $RuCl_3$ which was then added after the electrode had been anodized for 325 sec (see arrow); (○) electrode pretreated and the potential stepped in the presence of $RuCl_3$; (△) repeat of the previous run except that after 30 sec the electrode was transferred to ruthenium-free 1 mol dm^{-3} $HClO_4$ solution; (x) the same electrode activated in Ru solution whose potential after transfer to the pure acid was allowed to go to 0 V prior to applying the potential step. The $RuCl_3$ concentration in these experiments was 0.15 mmol dm^{-3}.

An attempt was made to investigate in more detail the potential range over which the species on the surface responsible for the lowering of the oxygen overvoltage was stable. A platinum electrode which had been pretreated and preanodized for a short time in the presence of ruthenium trichloride was transferred to a ruthenium-free solution and subjected to the potential variations shown in the inset in Figure 3.3. For example, after 50 s at 1.6 V the current density was 0.32 mA cm^{-2}; the potential was then lowered to 1.4 V for 1 min, returned to 1.6 V and after 50 s the current density was found to be slightly higher (presumably due to some loss of oxide) at 0.35 mA cm^{-2}. Next the potential was dropped to 1.2 for 1 min, returned to 1.6 V and the current again recorded after 50 s. This procedure was repeated a number of times on each occasion subjecting the surface film to a low potential for 1 min, reapplying the higher (1.6 V) potential and measuring the current density after a period of 50 s. The results shown in Figure 3.3 clearly show that an active surface tends to lose its catalytic properties when held at potentials less than ca. 1.0 V. It is evident from these results that after holding the electrode for 1 min at 0.7 V, the activity of the electrode surface for the oxygen evolution reaction is quite close to that of an electrode which had never been exposed to ruthenium (Figure 3.3, lower curve).

Further potential-step experiments, shown in Figure 3.4 demonstrate that the extent to which the platinum electrode is pretreated in the ruthenium solution has a marked influence on the subsequent rate of oxygen evolution at 1.6 V. Also demonstrated in Figure 3.4 is the fact that transferring the electrode from an acid to an alkaline solution

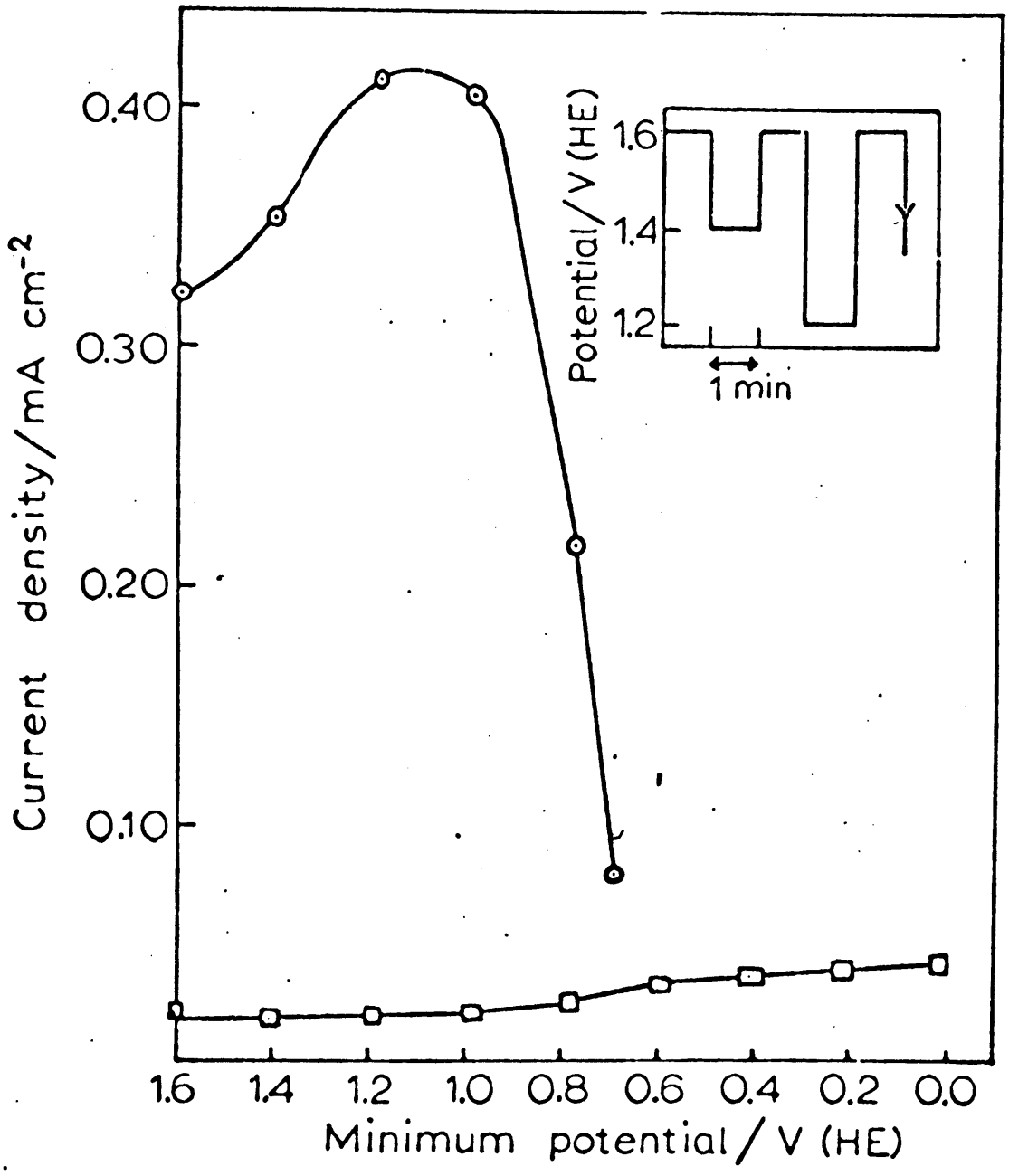

FIGURE 3.3 : Current values for a smooth platinum electrode at 1.6 V in ruthenium-free 1 mol dm^{-3} $HClO_4$ as a function of the progressively less anodic potentials to which the preanodized electrode has been subjected. The potential changes impressed on the electrode are given in the inset. (O) Anode preanodized in solution containing $RuCl_3$-catalytic activity maintained unless potential drops below 0.8 V; (□) electrode preanodized in $RuCl_3$-free solution.

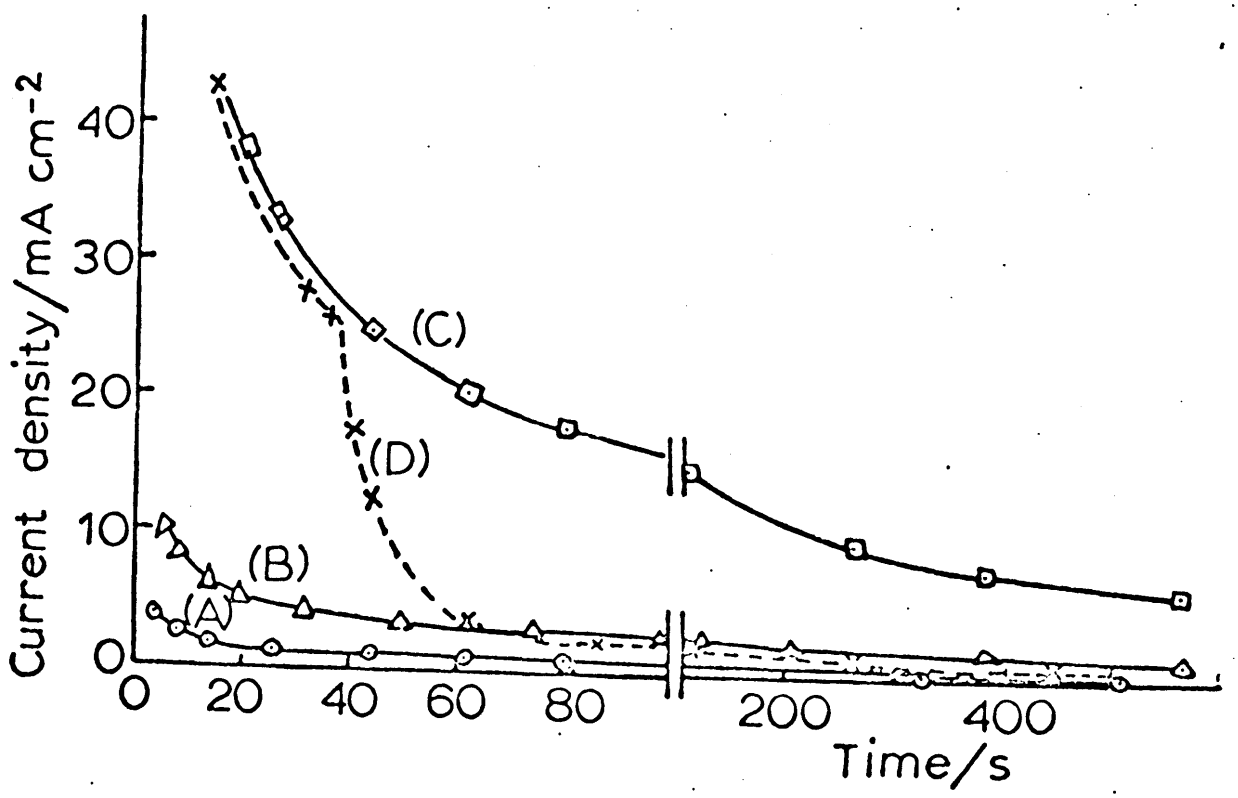

FIGURE 3.4 : Current decay curves for a platinum electrode whose potential was stepped at zero time from 0.6 V to 1.6 V in 1.0 mol dm^{-3} $HClO_4$ at 25°C. (O) Absence of $RuCl_3$; (Δ) $RuCl_3$ added just prior to the step; (□) electrode pretreated and stepped in solution containing $RuCl_3$; (x) effect of transferring an active (Ru-doped) electrode to an alkaline (1 mol dm^{-3} NaOH) solution. $RuCl_3$ concentration = 0.15 mmol dm^{-3}.

(curve D) virtually eliminates the ruthenium enhancement of the oxygen evolution process.

3.7. A.c. Polarography and Potential Sweep Measurements

The response of the platinum-solution interface to the applied a.c. voltage in the absence of the ruthenium salt is shown (dashed line) in Figure 3.5. In some respects this curve bears a similarity to the d.c. cyclic voltammogram for this system.[44] For example, on going in the anodic direction there is an increase in current at ca. 0.85 V corresponding to initial oxide film formation followed by a larger increase above 1.6 V corresponding to oxygen evolution, while on going cathodic from this region there is a sharp drop at ca. 0.75 V corresponding to loss of the oxide film. Addition of ruthenium trichloride to the solution caused two a.c. peaks to appear on the anodic scan (Figure 3.5), one at 0.79 to 0.8 V and the other at 1.38 to 1.39 V. A slight shoulder occurred on the subsequent cathodic sweep at ca. 0.4 V. An unusual feature of these peaks is that after adding the ruthenium salt with the potential held at ca. 0.37 V they do not appear in the first anodic scan. Those a.c. peaks for the solution containing ruthenium as illustrated in Figure 3.4 were only observed on the second and subsequent runs.

The conventional d.c. behaviour which was recorded at the same time as the a.c. results described above is illustrated in Figure 3.6. In this case, a lowering of the oxygen evolution potential and an increase in the oxygen evolution

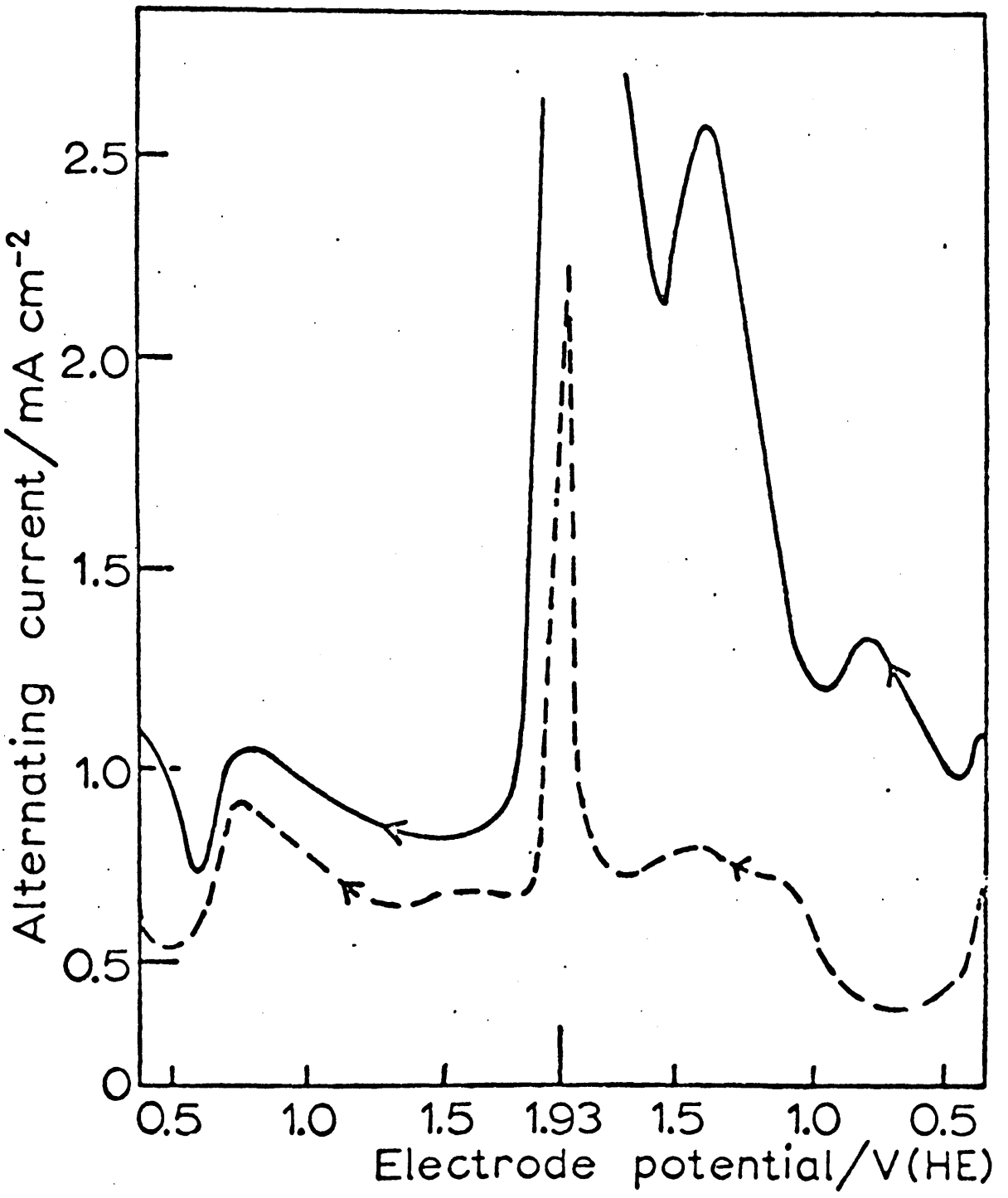

FIGURE 3.5 : Variation of the impedance (as measured by the a.c. response to a low voltage signal) of a platinum-solution interface as a function of electrode potential in both the absence (----) and presence (——) of $RuCl_3$ (1.5 mmol dm^{-3}) in 1 mol dm^{-3} $HClO_4$ solution at 25°C.

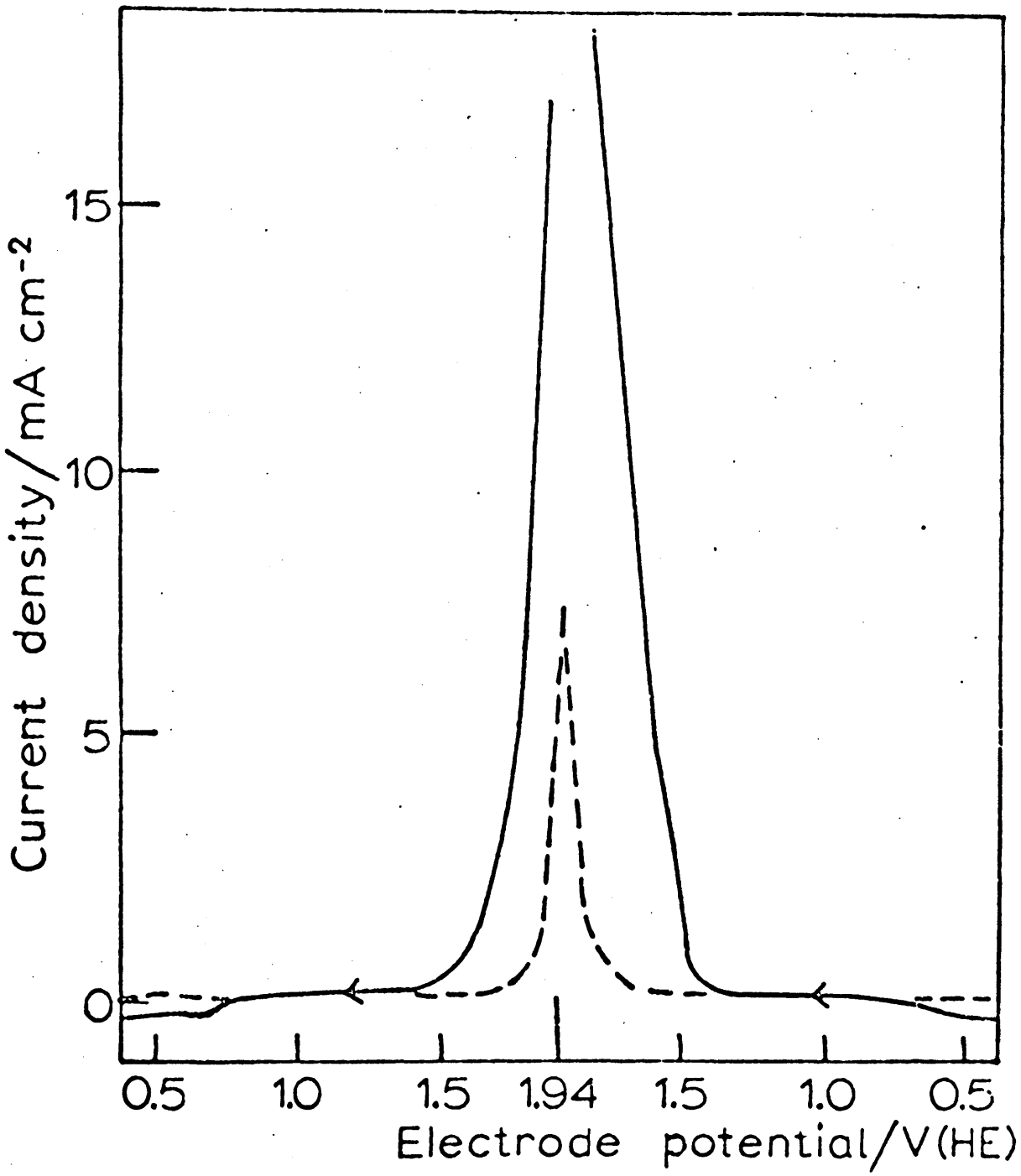

FIGURE 3.6 : D.c. potential sweep measurements with smooth platinum in 1 mol dm^{-3} $HClO_4$ at 25°C both in the absence (----) and presence (——) of $RuCl_3$ (1.5 mmol dm^{-3}) in the solution.

current at the higher potential values was observed even during the first run after the addition of the ruthenium salt. In subsequent runs the oxygen evolution current appeared to increase considerably; for instance in one particular case the current at the maximum point of the anodic sweep (1.94 V) increased on adding the ruthenium salt by a factor of ca. 3 (relative to the blank, i.e. no ruthenium present) on the first scan and by a factor of ca. 4.5 (again relative to the blank) on the second scan. In subsequent anodic scans it was noted that as the point at which the d.c. current showed a marked increase was lowered slightly, to ca. 1.40 V and the rate of current increase with voltage was unusually large and a definite shoulder began to appear on the anodic curve. It is possible that this shoulder was due to corrosion of metallic ruthenium deposited at the lower region of the potential scan.

3.8. Effect of pH

In order to test the effect of pH on the lowering of the oxygen overvoltage a series of phosphate buffer solutions were made up ranging in pH from 1.8 to 12.3. Addition of ruthenium trichloride to these buffer systems gave solutions which appeared to hydrolyse gradually with time giving a range of green to black suspensions. Most of these had little effect on the oxygen overvoltage and it was noted that at pH 7.0 freshly prepared solutions, which were active initially, soon became inactive. Even solutions of ruthenium trichloride in pure water developed a brown colloidal appearance. Total stability and marked catalysis was best observed with strongly acidic solutions, e.g. 1 M $HClO_4$.

3.9. Effect of Electrode Material

The influence of ruthenium trichloride in the solution on the anodic evolution of oxygen on a bright gold anode was investigated by means of slow sweep cyclic voltammetry. Typical results for an acid solution are shown in Figure 3.7 where in the case of the blank, curve (a), there was the usual high overvoltage for hydrogen evolution on gold and an increase in anodic current at 1.2 V corresponding to the onset of oxide film formation.[130] Addition of the ruthenium salt at ca. 0.9 V during the course of an anodic sweep gave a small peak just above 1.4 V and a considerable increase in the oxygen evolution current. The effects of the ruthenium salt were more marked in subsequent cycles and included the following: (a) a marked increase in the hydrogen evolution current; (b) a more pronounced peak just above 1.4 V; and (c) a further increase in the oxygen evolution rate right up to the sweep maximum at 1.73 V. The increased rate of hydrogen evolution is most likely associated with the plating out of ruthenium metal at the gold surface at low potentials with consequent sharp reduction of the hydrogen overvoltage. This deposit of ruthenium seemed to corrode vigorously at 1.4 V and the area under this anodic stripping peak was found to increase linearly (Figure 3.8) with the length of time that the potential was held at zero volts. The fact that the straight line in Figure 3.8 does not pass through the origin may be due to two factors: (i) oxidation of Ru(III) species in solution to a higher oxidation state at this potential value (1.4 V) and (ii) the experiments were carried out by a potential sweep technique so that even when the potential was not

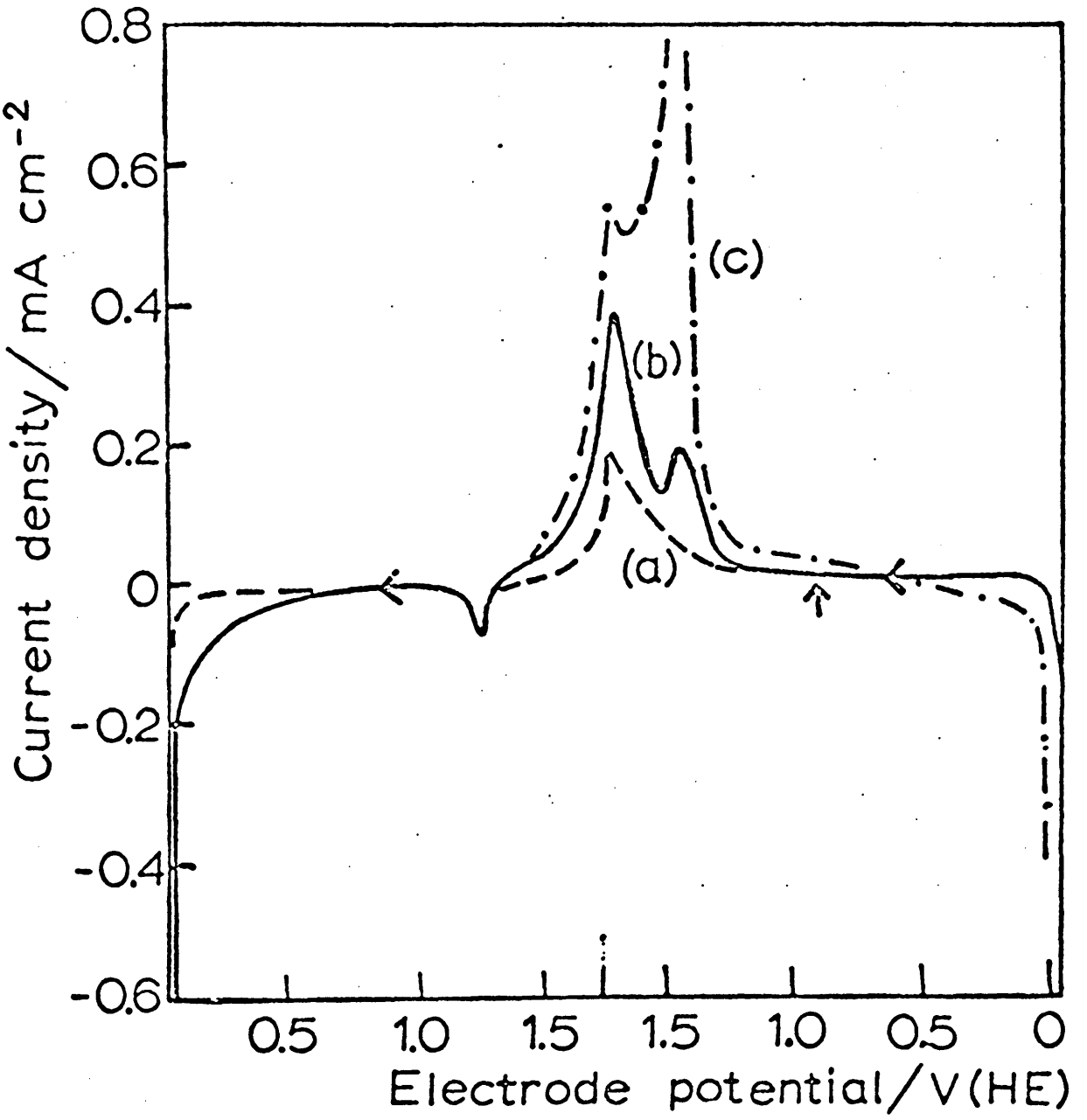

FIGURE 3.7 : Potential sweep measurements (d.c.) with a smooth gold electrode in 1.0 mol dm^{-3} $HClO_4$ at 25°C. (a) No $RuCl_3$ added, (b) first sweep after adding $RuCl_3$ (0.15 mmoldm^{-3}) at 0.9 V, (c) subsequent runs where $RuCl_3$ was present in the solution at all stages of the sweep.

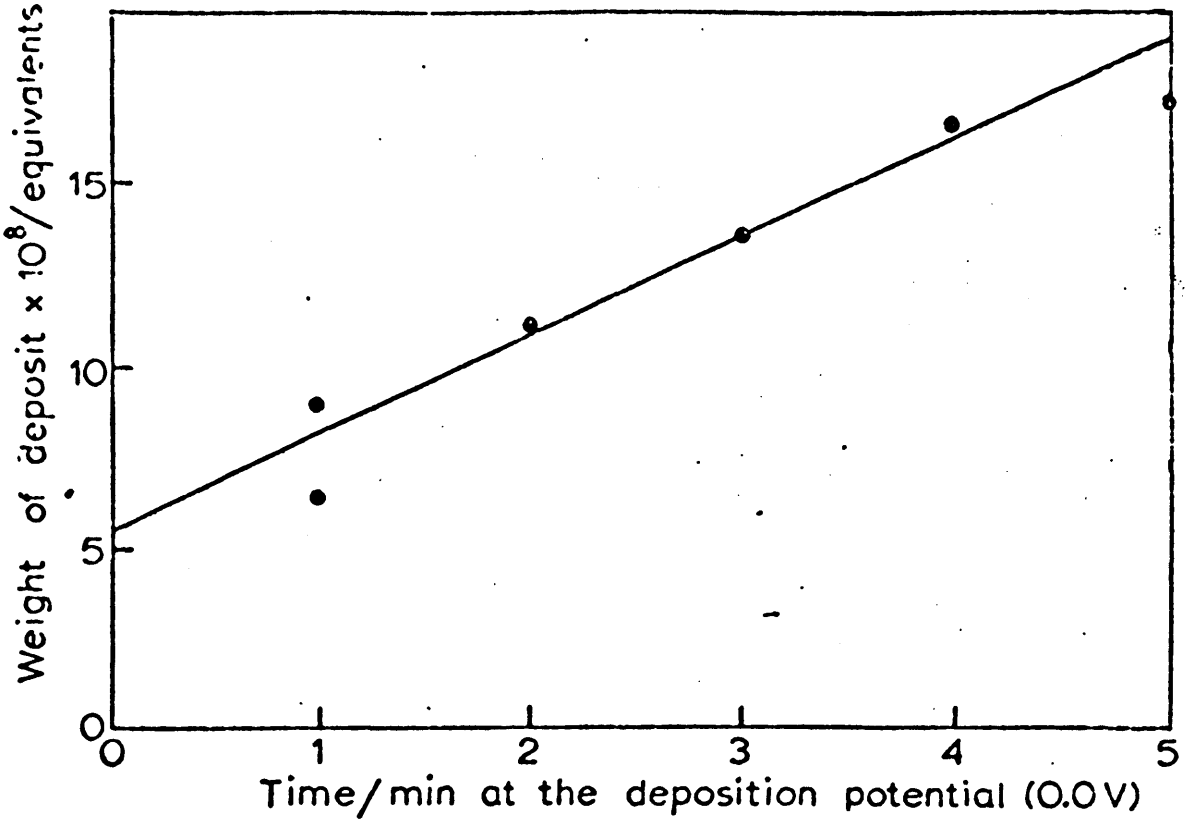

FIGURE 3.8 : Estimate amount of ruthenium deposited at a gold electrode as a function of the time that the potential was held at 0 V mol dm^{-3} as determined by the area under the anodic stripping peak at ca. 1.4 V (Figure 3.7).

held for any given time at O V there was still ruthenium metal deposited at the lower region of the sweep.

Similar potential sweep experiments were carried out with carbon electrodes; however, no detectable influence of the ruthenium salt on the anodic behaviour was detected in the case of this electrode material.

3.10. Discussion

It was suggested by earlier workers that the lowering of the oxygen overvoltage in the presence of ruthenium trichloride was due to the oxidation of the ruthenium ions to a higher valence state which then reacted with water resulting in oxygen evolution.[95] This type of catalysis is well known in electrochemistry, generally in the case of processes requiring considerable overvoltage, e.g. hydrogen peroxide reduction on mercury in the presence of ferric ions.[131] However, since the catalysis in the present case can occur in a solution which is virtually free of ruthenium ions, the only requirement being that the platinum be pretreated in the presence of the ruthenium salt (Figure 3.2, curve C), it appears that the lowering of the oxygen overvoltage is primarily a heterogeneous phenomenon, most likely involving the incorporation of ruthenium into some type of surface layer.

There is clear evidence in the case of gold, and also indications in the case of platinum, that ruthenium metal was plating out at the surface at low potentials. Although it could therefore be argued that the lowering of the oxygen overvoltage was due to the conversion of the platinum

or gold to a ruthenium surface, this appears to be unlikely for a number of reasons. First of all, ruthenium metal is unstable and corrodes vigorously under anodic conditions[92,93]; secondly, the potential values observed during the charging curve for platinum in the presence of ruthenium trichloride (Figure 3.1) are typical of those for a clean platinum electrode - at least up to the onset of oxygen evolution; finally, despite the fact that the corrosion of the ruthenium layer shows up as a sharp, quite distinct peak in the case of gold (Figure 3.7) the oxygen evolution process is considerably enhanced at higher potential values. It appears from the latter evidence that the corrosion and evolution are separate processes which may have in common the fact that they occur at a potential corresponding to a change in the oxidation state of the ruthenium. Apparently the ruthenium species responsible for the catalysis are incorporated, doped, or trapped in the platinum or gold oxide film on the surface, and the deposition and corrosion processes may have a considerable influence on the concentration of these catalytic sites in the film.

The lowering of the oxygen overvoltage due to the incorporation of ruthenium species in the oxide film can be explained in a number of ways. If one assumes that this overvoltage is associated with slow electron transfer through the oxide film,[70] then doping with ruthenium oxide, which is a metallic conductor,[91] would be expected to lower the voltage drop across the oxide film. If, however, the rate-determining step is a chemical process at the electrode surface, ruthenium species could enhance the oxygen evolution process by stabilizing the hydroxyl radical, a commonly accepted intermediate

in the oxygen evolution process,[49,75,81] with the result that the concentration of such radicals and the probability of their reacting to yield oxygen[82] will be increased. In chemical terms an increase in the oxidation state of ruthenium species at ca. 1.4 V may result in two hydroxyl radicals, or a hydroxyl radical and an oxygen atom, being held as adjacent ligands to the same central atom, thus favouring their combination to yield oxygen gas. Such a mechanism is generally accepted in the case of homogeneous catalysis involving transition metal ions.[132] It may be seen that the interpretation of oxygen overvoltage in terms of either intermediate radicals[82] or the formation of unstable valence states[133,134] are virtually identical since both involve an increase in the oxidation state of the surface atoms followed by loss of oxygen.

The a.c. response of the platinum electrode in the presence of ruthenium trichloride is not easily explained. The virtual absence of the a.c. peaks at 0.8 V and 1.4 V during the first anodic scan after adding the salt (despite the fact that there was an increase in the rate of oxygen evolution during this first run) suggests that these peaks, which were quite marked in later scans, were associated not with ruthenium species in solution but with changes in some species on the electrode surface. From thermodynamic data[118] ruthenium metal should be stable in 1 M $HClO_4$ below 0.6 V; above this a wide variety of oxides and hydroxides, some quite stable and others not, may be produced. It does not seem possible at this stage to assign either of the two a.c. peaks to a definite electron-transfer process. The loss of catalytic activity on transfer of an active

electrode into alkaline solution (Figure 3.4, curve D) can also be accounted for in terms of thermodynamic data[118] as at high pH the ruthenium oxide is probably leached out of the film in the form of the ruthenate or perruthenate ion.

One of the most unusual properties of ruthenium, which it shares with only a few other transition elements, is the ability to form oxide bridges with two three-centre molecular orbital bonds.[135] This can account not only for the metallic conductivity of RuO_2 but may also be involved in the incorporation of ruthenium in the oxide film on platinum. Reduction of these oxide bridges would lead to loss of ruthenium and a diminution of catalytic activity (Figure 3.3). The absence of catalytic effects in the case of the carbon electrode may be partly due to the inability of this smaller, non-transition, element to participate in oxide bridging.

Platinum is the most common anode material used in experimental cells. Furthermore, most of the fundamental research into anodic processes has been carried out using platinum. It is now apparent, however, that other anode materials may be superior to platinum, at least in some respects. Ruthenium is a more effective catalyst for anodic oxygen evolution but its limited resistance to corrosion renders its use impractical. Thermal ruthenium dioxide films are also better electrocatalysts for various anodic processes and these also have a high resistance to corrosion.

Some improvement in the catalytic properties of platinum has been obtained by pretreatment in the presence of ruthenium salts. It has been shown that,

contrary to the initial suggestions,[95] this effect is probably due to the incorporation into the platinum surface film of ruthenium species. The improvement is of a rather transient nature, however, the ruthenium species being easily removed from the surface. Efforts to find a better oxygen evolution substrate led to consideration of iridium, a platinum metal with d-electron properties similar to those of ruthenium. This metal is, apparently, highly resistant to corrosion and its electrochemical properties do not appear to have been exhaustively investigated.

CHAPTER IV

IRIDIUM

Part 1: The Oxide Film Region

Iridium was isolated by Smithson Tennant[136] in 1803. Its density is very close to that of osmium but values based on x-ray determinations of the lattice parameters suggest that iridium has the highest density of all the elements.[112,137] It is attacked by oxygen at red heat to give the dioxide which forms a surface film and protects the metal from further oxidation until much higher temperatures are reached.[112] Iridium is extremely resistant to chemical corrosion, being unaffected by all acids.[112] It has been reported to corrode both at anodic potentials[96,138] and under the influence of alternating currents[99,138] in chloride media. Its anodic behaviour, particularly in chloride-free media, has, however, been studied[98] much less than, for example, that of platinum. In the present work both the anodic oxide formation (discussed in this chapter) and anodic oxygen evolution and associated corrosion (Chapter V) have been investigated.

4.1. Oxide Films on Iridium

The metal forms a stable dioxide, IrO_2, which may be isolated both in anhydrous[139] and in hydrated[140] forms. Both the anhydrous and hydrated forms of the sesquioxide, Ir_2O_3, may also be isolated but are chemically not as stable as the dioxide.[140] The trioxide,[139,140,141] dioxide[140,141] and monoxide[140] (but not the sesquioxide) have been detected in the gas phase and, while there is no evidence for the existence of the solid monoxide, there are reports in the early literature of a compound[142] approximating IrO_3.

Hoare[33] investigated the Ir/O_2 electrode and observed the effect of pH and oxygen partial pressure on the rest potential. He concluded that a layer of adsorbed oxygen atoms is formed on an iridium surface in contact with oxygen-saturated acid solutions. Charging curves[54,143] and cyclic voltammetry[55,56,144,145] have shown that oxide films are formed on iridium electrodes at anodic potentials. Estimates of the degree of coverage at the beginning of oxygen evolution vary, however, from a single monolayer to 20 monolayers.

Bold and Breiter[56] have inferred from potential sweep data that a monolayer of oxygen is adsorbed prior to oxygen evolution but that a further small amount of oxygen is adsorbed even after evolution begins. They have suggested that the additional oxygen is dissolved in the surface layers of the metal lattice. Kurnikov and co-workers[145] have also used potential sweep techniques to investigate the anodic oxidation of iridium and have reported that, in contrast to other metals of the platinum group, the adsorption of oxygen on the metal proceeds with the formation of comparatively thick (phase oxide) layers. Monolayer coverage was achieved by these authors at a potential of 0.6 V - 0.65 V in 0.5 mole dm^{-3} H_2SO_4 and the adsorption increased rapidly with increasing potential, reaching more than 20 monolayers before evolution of oxygen commenced. Results have also been reported[145] for experiments carried out in alkali and it appears that, while adsorption of oxygen begins at a lower potential, the total amount of oxygen adsorbed is only half as great as in acid.

4.2. The Reversibility of the Oxide Formation and Reduction Reactions

Charging curves for the platinum metals[41,143,146] (especially platinum itself) usually show that the oxide films are reduced only at potentials considerably more cathodic than those at which they are formed. This effect, frequently referred to as hysteresis, is also evident in the cyclic voltammograms of platinum[44,50] and most of the platinum metals.[55] The cyclic voltammogram of iridium[55,56,144] in acid solution, however, shows peaks corresponding to the formation and reduction of the oxide film at approximately the same potential. This suggests that the electrochemical oxide formation and reduction reactions on iridium are reversible processes. Peaks on the voltammogram obtained in alkaline solution[145] occur at potentials different from those in acid; but here again there is little hysteresis between the oxide formation and reduction processes. There appears to be some discrepancy, however, between this recent work of Kurnikov and co-workers[145] and the earlier work of Bold and Breiter.[56] The latter reported that in alkaline solution the reduction peaks occur at potentials slightly more cathodic than the corresponding oxide formation peaks. The reported hysteresis (ca. 150 mV) is, however, much less than that generally observed in the case of the other platinum metals.[44,55]

Stonehart and co-workers[147] have investigated the behaviour of the oxide reduction peaks on platinum, palladium, rhodium and iridium. Electrodes were anodized at various potentials and for various times and the oxide was then reduced in a cathodic potential sweep. It was reported in the case of all

the metals investigated, except iridium, that as the pretreatment potential was made more anodic, the potential of the oxide reduction peak shifted to more cathodic values. A similar cathodic shift of the reduction peak was observed if the anodization time at a given potential was increased. This effect was notably absent in the case of iridium. Kurnikov and co-workers[145] have also observed this effect and have furthermore reported that the maxima on the cathodic potential sweep curve of iridium lie at the same potentials regardless of the potential at which the oxide layer was formed. The increasingly cathodic potential values required for oxide reduction in the case of platinum, palladium and rhodium were attributed by them to an increase in strength of the bond of oxygen to the metal and the result with iridium was regarded as evidence for the absence of such bond-strengthening in this case. Stonehart and co-workers[147] investigated the effect in some detail in the case of platinum. They postulated that the progressive change in the potential for reduction of the film was due to rearrangement of the platinum and oxygen species from an ad-layer type of arrangement to a two-dimensional Pt-O-Pt surface phase. From the results obtained on iridium they concluded that no such rearrangement occurred on that metal. This would be expected in the case of iridium if the anodic film was formed as a phase oxide, a situation which seems plausible in view of the reported[145] growth of multilayer films.

4.3. The Present Investigation

In the course of cyclic voltammetry experiments on iridium, Capon and Parsons[144] recently observed that if the electrode potential was cycled continuously

in the region 0.05 V - 1.4 V over a period of ca. 1 hr, currents in the oxide region progressively increased. No explanation was put forward and the effect was not further investigated.

During preliminary experiments in the present study of the anodic behaviour of iridium, similar results were obtained. Since these showed that the oxide capacity of an iridium electrode was dependent on its pretreatment and in view also of the remarkable discrepancy between the values reported by Kurnikov and co-workers[145] and those reported by Bold and Breiter,[56] it was decided to investigate the effect in detail.

The iridium electrode used had an exposed area of 0.22 cm^2 and was constructed as described in Section 2.5. Experiments were carried out using 1.0 mole dm^{-3} H_2SO_4 as electrolyte in cell no. 1 (Figure 2.10). The electrochemical techniques used were charging curves, cyclic voltammetry and a.c. impedance measurements.

RESULTS

4.4. Charging Curves

Conventional charging curves obtained with iridium anodes in nitrogen-stirred acid or alkaline solutions suggest that only a monolayer of oxygen is adsorbed on the metal surface prior to oxygen gas evolution.[54,143,148] The absence of any arrest in the potential against time curves over the oxide layer region is taken as

evidence for the absence of any type of stoichiometric oxide (e.g. IrO_2) formation. In the present investigation it was found that although this type of conventional charging curve was obtained following a preliminary anodization at 1.935 V, markedly different results were obtained if, after this initial oxidation, the electrode potential was cycled in a triangular manner at 10 Hz in the range 0.01 to 1.5 V for a short period, e.g. 1 min. The resulting charging curve (Figure 4.1) showed an unusually large oxide charge capacity, and marked potential arrests were noted at about 0.75 and 0.94 V in the anodic direction and at 1.40 and 0.96 V on the subsequent cathodic curve. This change in behaviour of the iridium surface persisted almost indefinitely provided that the potential of the electrode did not rise above ca. 1.6 V for any length of time. However, if an "activated" electrode with its enhanced oxide charge capacity was anodized at 1.935 V, then subsequent charging curves showed the conventional lower capacity, rather featureless, oxide layer region.

In what follows the phrase "activated at 10 Hz" will be used to indicate that the potential of the electrode was varied in a triangular manner between 0.01 and 1.5 V at a frequency of 10 Hz.

4.5. Cyclic Voltammetry

In Figure 4.2, the full line illustrates the type of cyclic voltammogram obtained with an iridium electrode which had been anodized at 1.935 V for 1 min and then activated at 10 Hz for a further 1 min. The dashed line shows the results obtained

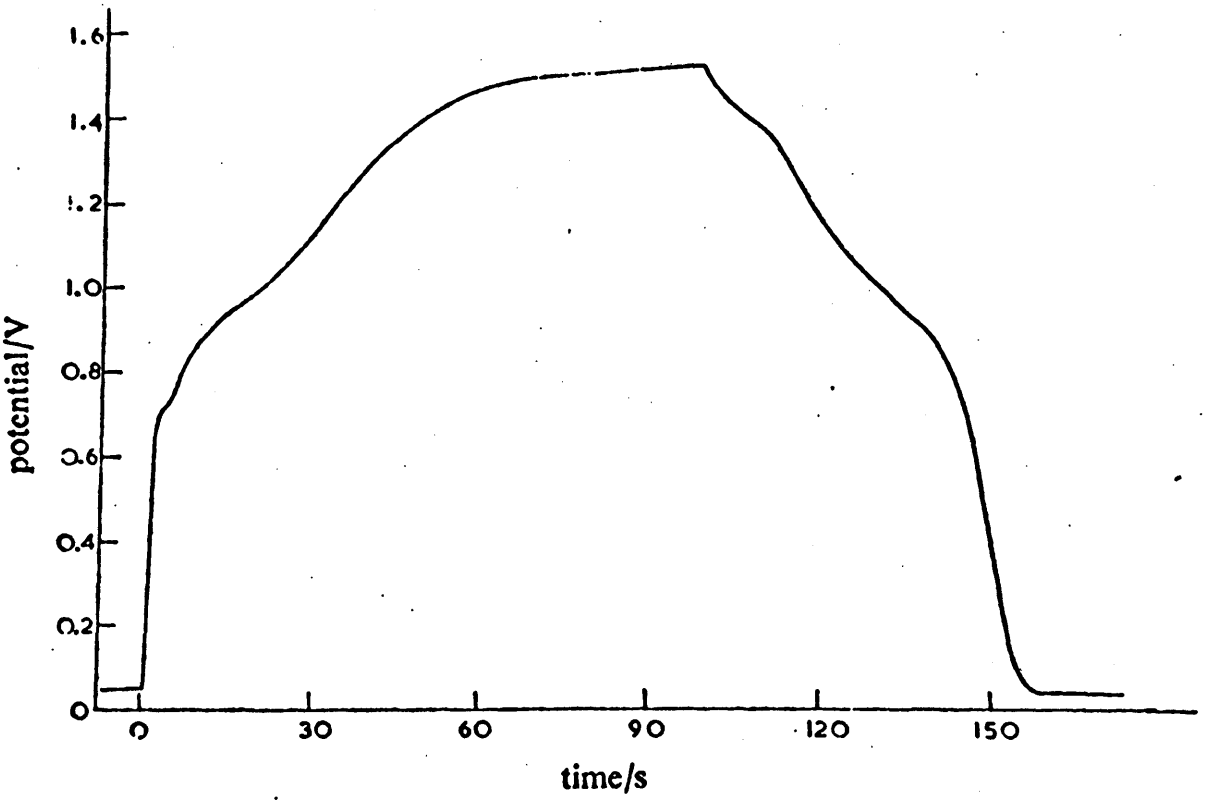

FIGURE 4.1 : Anodic and cathodic charging curves for a smooth iridium electrode activated at 10 Hz for 1 min (see text); 1.0 mol dm^{-3} H_2SO_4 at 25°C, c.d. = 182 μA cm^{-2}.

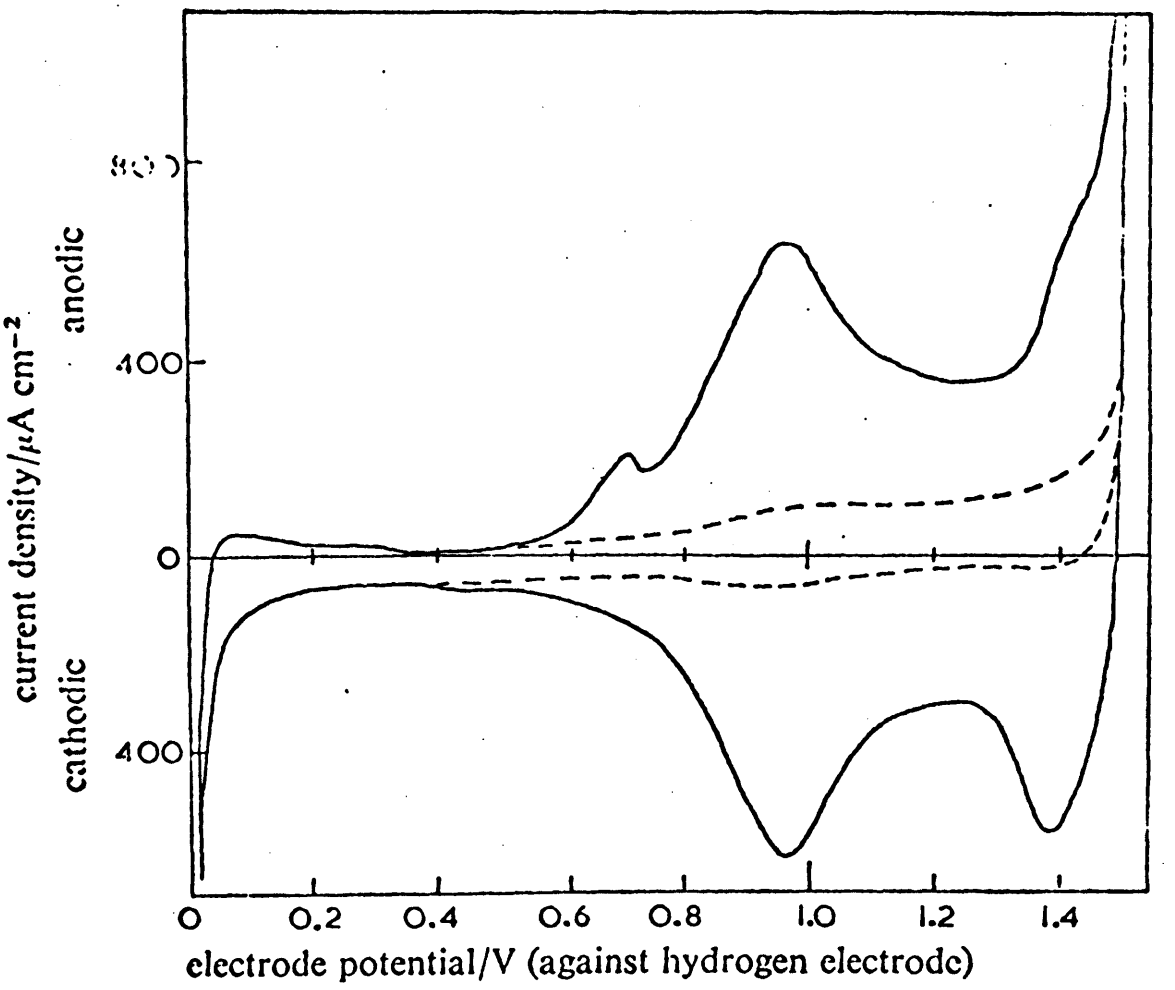

FIGURE 4.2 : Cyclic voltammogram (30 mV s^{-1}, 0.01 Hz) for a smooth iridium electrode in 1.0 mol dm^{-3} H_2SO_4 at 25°C. The full line is typical of an activated electrode whereas the dashed curve represents the behaviour of a deactivated electrode as discussed in the text.

when the activation at 10 Hz was omitted. The oxide charge capacity is obviously much greater in the first case. On the basis of these results one can distinguish two types of iridium surface: the first is an activated surface with a high oxide charge capacity and the second a deactivated surface with low oxide charge capacity. Transformation of one type to the other is readily achieved: an activated surface may be deactivated by strong anodization (above ca. 1.6 V; see Section 4.7) while a deactivated surface may be activated as described earlier by cycling its potential.

A detailed examination of the cyclic voltammograms shown in Figure 4.2 is quite interesting. On both types of surface the main oxidation and reduction processes occur at about 0.97 V with, as noted previously,[55,56,147] remarkably little hysteresis. Activating the iridium surface at 10 Hz had the effect not only of increasing the overall oxide charge capacity but also of demonstrating clearly the existence of a minor peak on the anodic curve at about 0.7 V, and a shoulder on the same curve at about 1.4 V. A surprising feature illustrated in the results given in Figure 4.2 is that despite the effect of cycling on the oxide charge capacity of the iridium surface, the effect on the hydrogen capacity or hydrogen region of the curve was negligible. This important point is illustrated in Figure 4.3 where a plot of peak heights as a function of the degree of activation shows a continuous steady increase for all the oxide peaks while the hydrogen peak at 0.10 V remains constant. This lack of dependence of the hydrogen peak currents is a feature which may be noted also on some of the subsequent diagrams. The absence of the small peak at about 0.7 V on the

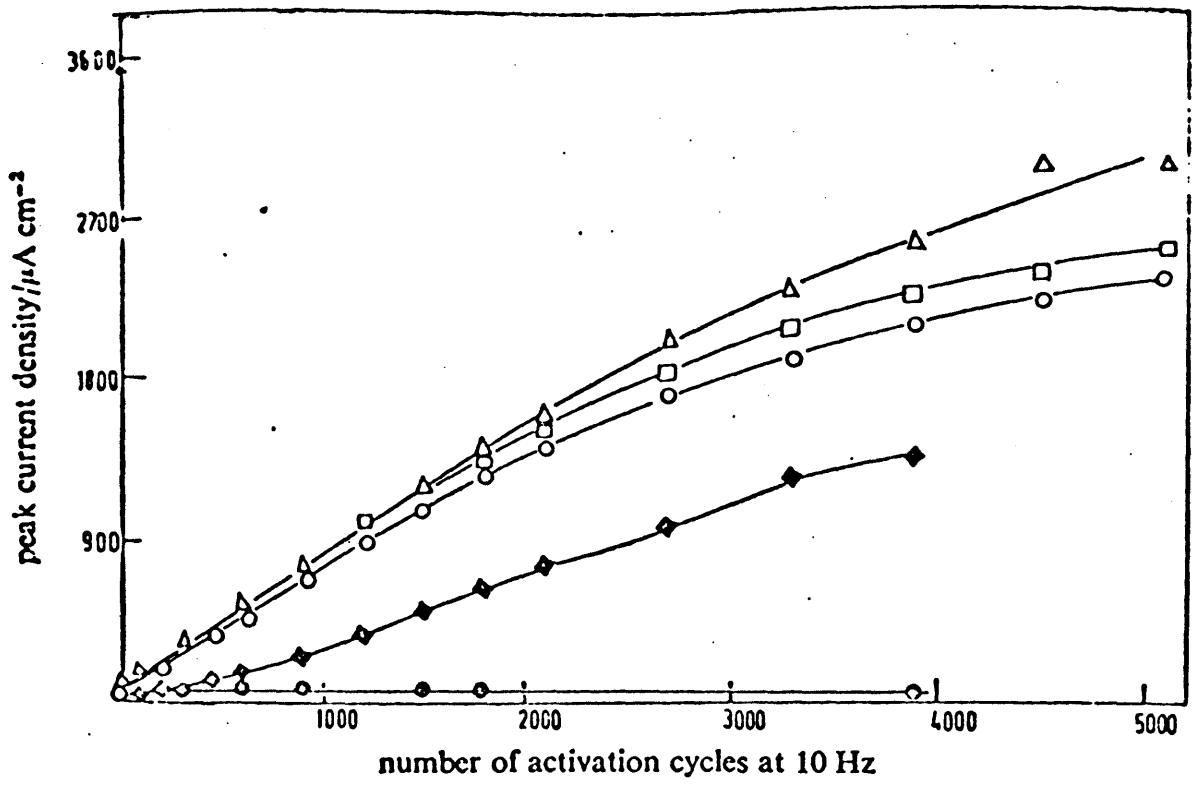

FIGURE 4.3 : Effect of activation at 10 Hz (see text) on the peak heights of the cyclic voltammogram. Δ, ◆ and ● refer to the anodic peaks at 0.98, 0.74 and 0.10 V respectively: O and □ refer to the oxide reduction peaks at 1.37 and 0.97 V, respectively.

cathodic side of the voltammogram of an activated surface and the fact that the cathodic currents in the double layer region are larger than the corresponding anodic currents for both activated and deactivated surfaces suggests incomplete reduction of the oxide prior to entering the hydrogen region.

Estimation of the oxide charge on the iridium surface involved measuring the area under the cathodic curve from the maximum anodic potential (usually 1.50 V) down to an arbitrary value of 0.40 V. The area thus obtained was compared with the area under the curve for the prior anodic sweep. Generally it was found that the area under the cathodic curve was about 90% of the area under the anodic curve in the case of an activated electrode. However, for a deactivated electrode the ratio of anodic to cathodic charge is of the order of 2:1 indicating incomplete reduction of the oxide in this case.

The effect of added chloride on the voltammograms was investigated for both activated and deactivated electrodes. In either case both the anodic and cathodic oxide peaks were unaffected on making the electrolyte 0.04 mol dm^{-3} with respect to HCl. Current levels at potentials close to the maximum (1.5 V) were slightly increased but this may be ascribed to some chlorine evolution at these potentials.

4.6. The Activation Process

The increase in the oxide charge capacity of the iridium surface was investigated by taking an initially inactive electrode and activating it at 10 Hz. At

regular intervals during the activation process the 10 Hz cycling was stopped and one or two cyclic voltammograms (0.01 - 1.5V at 0.01 Hz) run to observe any changes in surface behaviour. The oxide charge capacity of the surface was estimated in each case from the area under the oxide reduction portion of the curve as described earlier. From the results (Figure 4.4) it is clear that the oxide charge capacity of the iridium surface increases markedly with increasing number of activating cycles. For instance, the initial oxide charge capacity after anodizing at 1.935 V was 2.11 mC cm^{-2} but cycling the potential 5000 times (at 10 Hz) increased this capacity to 46 mC cm^{-2}. The simplest explanation for this increase in oxide charge capacity is roughening of the electrode surface as is known[149] to occur when the potential of platinum metals is cycled in the presence of dissolved hydrogen gas. That this is not the case is clearly shown by the fact that activating the electrode for oxygen uptake has virtually no effect on the hydrogen capacity of the surface which should also vary with surface area.

A feature of the activation process worth mentioning is the fact that for a particular degree of activation, successive scans at 0.01 Hz gave identical curves over the whole potential range. Furthermore, stopping the activation to record these scans had no apparent effect on the rate of increase of oxide charge capacity as a function of the number of cycles (Figure 4.4). Clearly whatever change was responsible for increasing oxide charge capacity of the surface was of a permanent character (provided that the potential was not allowed to rise above ca. 1.55 V).

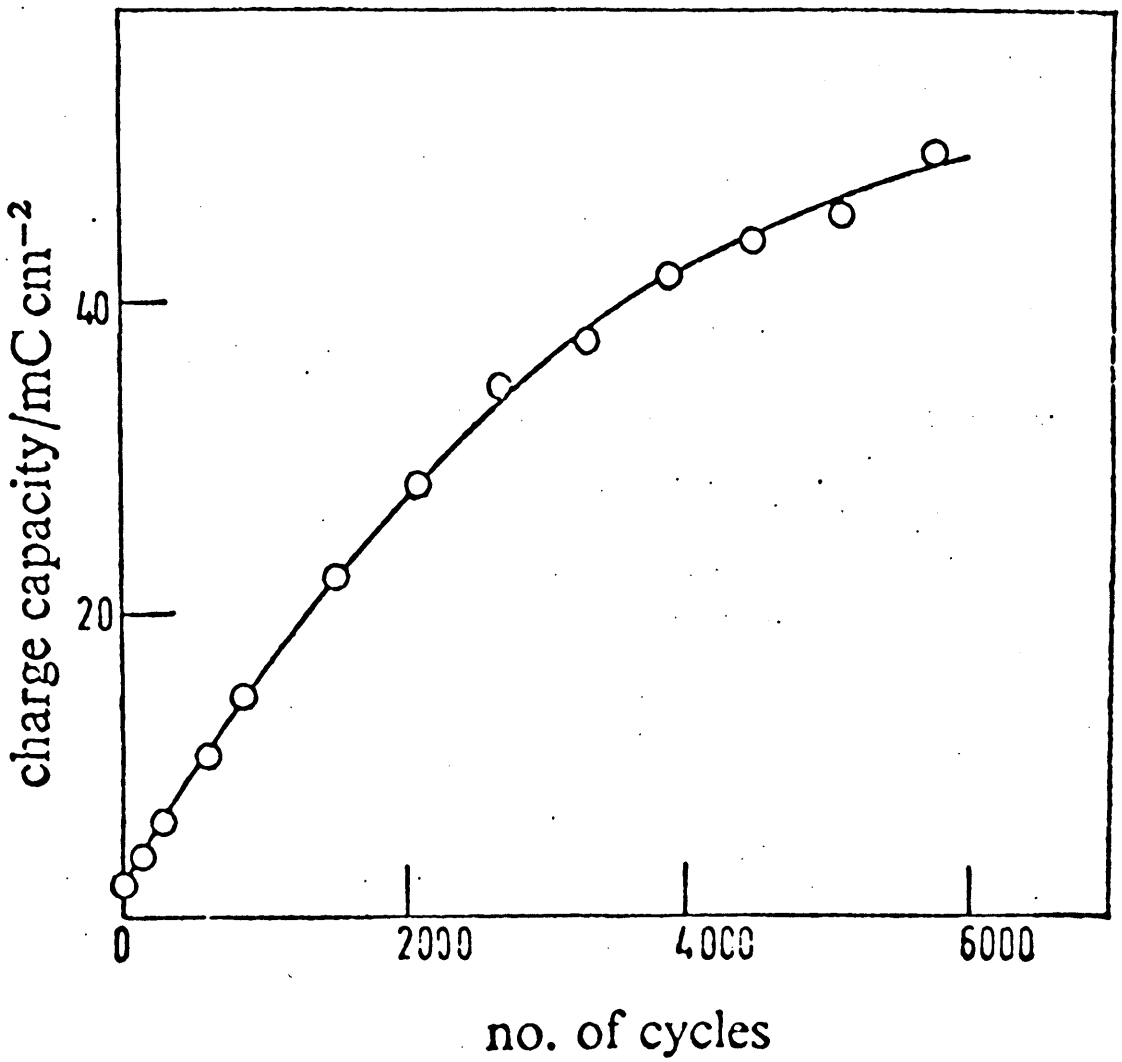

FIGURE 4.4 : Effect of activating at 10 Hz on the capacity of a smooth iridium electrode in 1.0 mol dm^{-3} H_2SO_4 at 25^{o}C.

4.7. The Deactivation Process

As mentioned previously the oxide charge capacity of an active surface was markedly reduced by anodizing at 1.935 V. To investigate this effect the following experiment was carried out. A smooth iridium surface was first strongly deactivated by maintaining it at a high anodic potential (1.935 V) for 1 min; this ensured a uniformly low level of activity at the beginning of each run. The electrode was next activated at 10 Hz for 1 min and then maintained at a selected anodic potential in the range 1.50 to 1.75 V for 1 min. Cyclic sweeps (0.02 - 1.5 V) at 0.01 Hz were then carried out. As shown in Figure 4.5 the height of all oxide peaks in the resulting voltammograms showed a marked decrease for pretreatment potentials above about 1.63 V. In contrast to this the height of both anodic hydrogen peaks and the cathodic current at 0.025 V were virtually independent of the anodic pretreatment.

The transition from high to low oxide charge capacity was also investigated as a function of the period of anodization at the high potential value in the following manner. The electrode was deactivated initially by keeping at 1.935 V for a preselected period of time. The effect of the latter pretreatment times on the oxide charge capacity of the surface was determined from peak height measurements on subsequent cyclic voltammograms (0.01 - 1.5V at 0.01 Hz). From the results shown in Figure 4.6 it is evident that the enhanced oxide charge capacity of the iridium surface decreases rapidly with time as a result of anodization at 1.65 V, whereas the two hydrogen peaks are, as usual, unaffected.

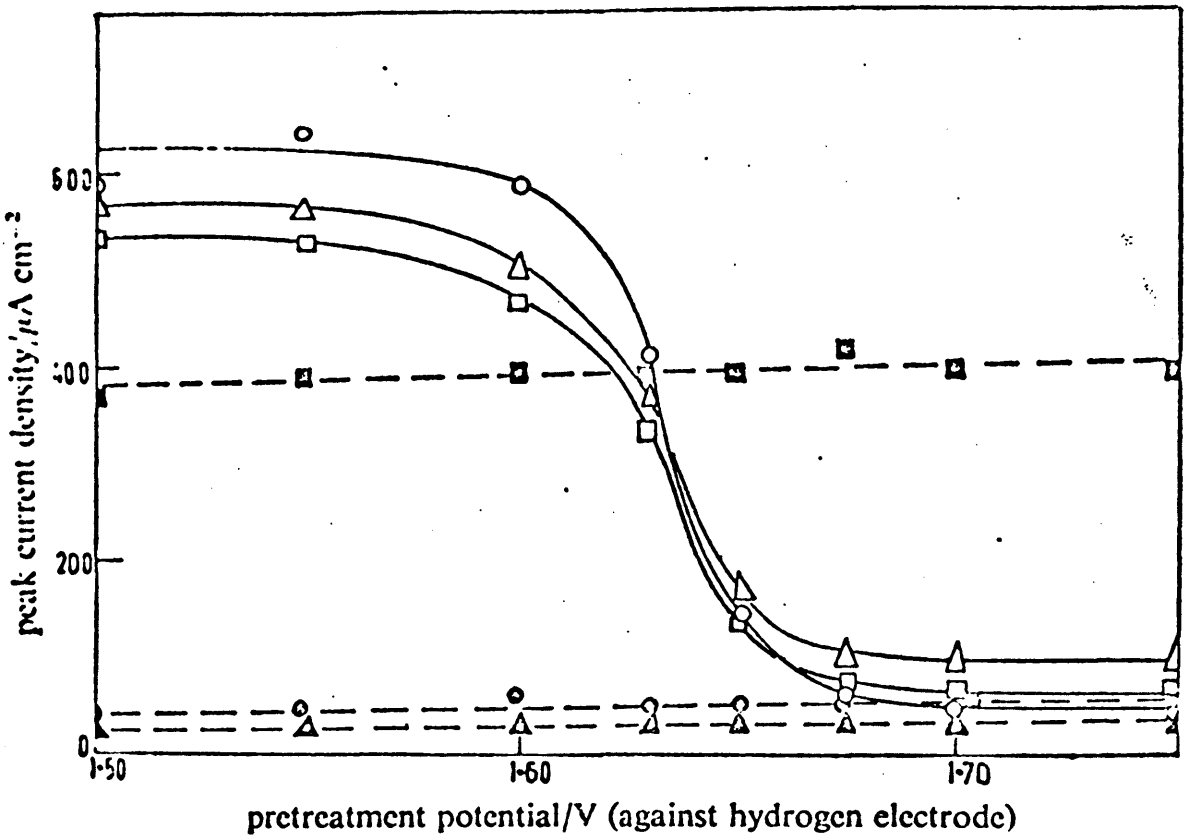

FIGURE 4.5 : Effect of anodic pretreatment potential on the peak heights of the cyclic voltammogram (0.02 to 1.5 V) of an originally activated iridium electrode: Δ , ▲, and ● refer to the anodic peaks at 0.98, 0.25 and 0.10 V, respectively: O, □ and ■ refer to the cathodic peaks at 1.37 and 0.97 V and the cathodic currents at 0.025 V, respectively.

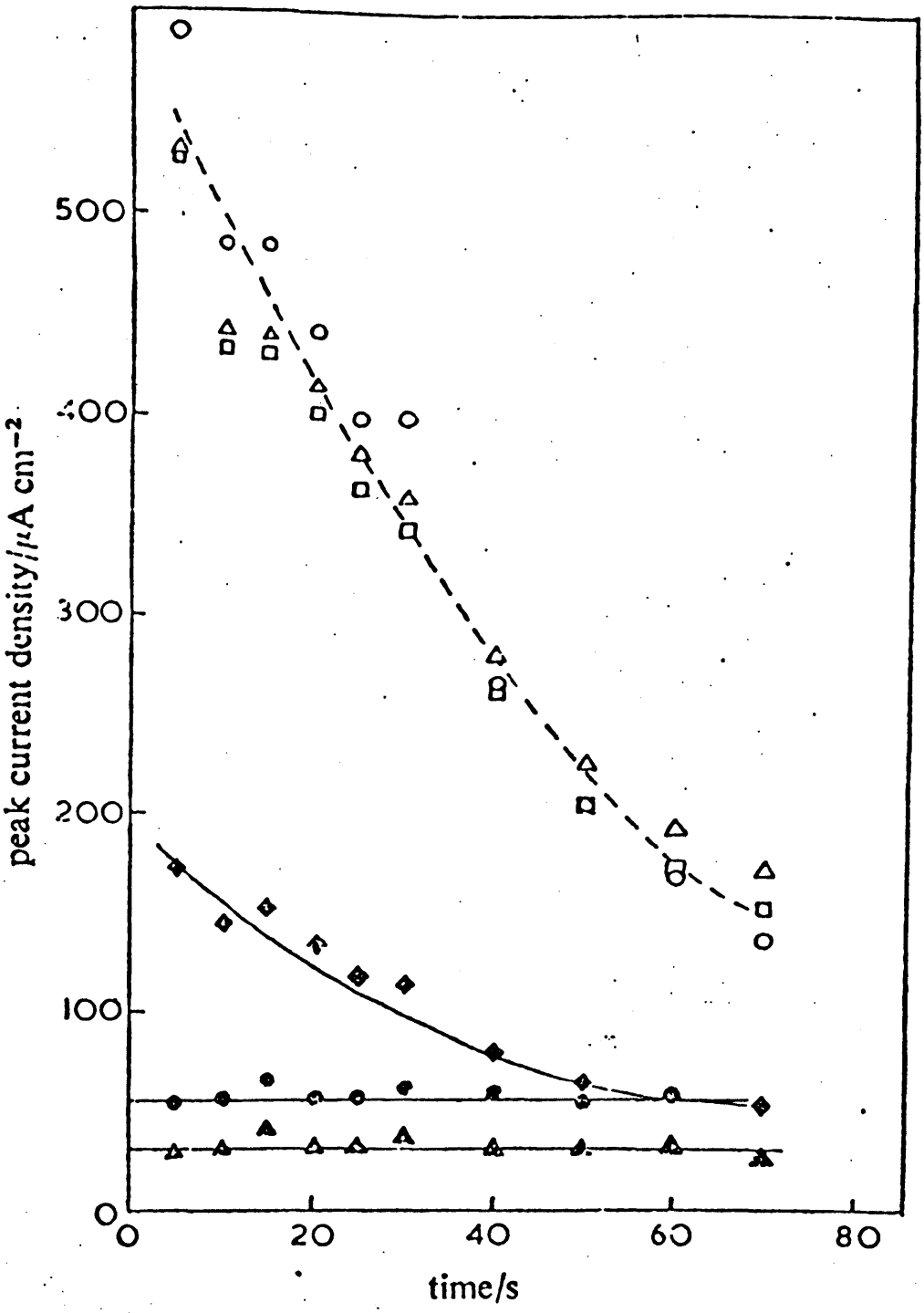

FIGURE 4.6 : Peak heights on the cyclic voltammogram as a function of the pretreatment time at 1.65 V. Δ, ◆, ▲ and ● refer to the anodic peaks at 0.98, 0.74, 0.25 and 0.10 V, respectively: O and □ refer to the oxide reduction peaks at 1.37 and 0.97 V, respectively.

4.8. Visual Observation of the Electrode

Measurements of the area under the hydrogen-film oxidation region of the cyclic voltammogram (e.g. Figure 4.2) showed that the hydrogen coverage was substantially unaltered by the activation process. The value obtained, 350 μC cm^{-2}, compares rather well with a recent literature report[150] of 310 μC cm^{-2}. If it is assumed that the 350 μC cm^{-2} corresponds to complete hydrogen coverage on a metal which according to d-band theory can chemisorb quite strongly,[52] then the charge for an oxide monolayer would be 700 μC cm^{-2}. Given a value of 46 mC cm^{-2} as the oxide charge capacity of a well-activated electrode (see Figure 4.4) then if the charge storage process were conversion of metal to metal oxide the amount of oxygen in the surface oxide would be ca. 66 times that for monolayer coverage. If however, as would appear to be the case (see Discussion), the charge storage is due to stoichiometry changes in the oxide, then the oxygen content of the surface could be greater than this by a factor of some small integer (possibly 4).

In fact visible changes were observed during the course of potential sweeps at 0.01 Hz for an iridium electrode which had been activated at 10 Hz for at least 1 min. The colour of the surface changed from a whitish metallic appearance at lower potentials to blue-black above about 1.0 V during the anodic sweep, and returned to the original white state at about 0.9 V during the subsequent cathodic sweep. Also of interest was the fact that if the potential sweep was extended to higher anodic values, the iridium surface changed colour from white to blue-black as

usual at ca. 1.0 V but changed back to white at ca. 1.7 V even though the potential was still increasing in the anodic direction. If the anodic scan was stopped for a short while at 1.65 V the electrode maintained a dark colour and oxygen bubbles could be seen evolving; however, if the scan was allowed above about 1.7 V, the colour rapidly changed to white. The transition from dark to white colour at these potentials was irreversible, i.e. on the subsequent cathodic scan the dark colour did not reappear.

4.9. Increase in Oxide Charge at Higher Potentials

The shoulder on the oxygen evolution current at about 1.4 V in the cyclic voltammogram (Figure 4.2) indicates further increase in the oxide charge content of the surface in this region. The effect of potential on the extent of this increase was investigated by deactivating the electrode for 1 min at 1.935 V, activating at 10 Hz for 1 min, and then running slow (0.01 Hz) potential sweeps from 0.01 V to some selected upper limit in the range 1.35 to 1.65 V. It was found (Figure 4.7) that although the two lower anodic oxide peaks and the lower oxide reduction peak remained essentially constant, the first oxide reduction peak at about 1.4 V increased markedly as the maximum potential of the sweep was increased over the region indicated. Obviously the degree of oxidation of the anodic film was increasing in this region which is close to the critical potential for deactivation. In fact the slight drop in some of the oxide peak values in Figure 4.7 for scans where the maximum exceeded

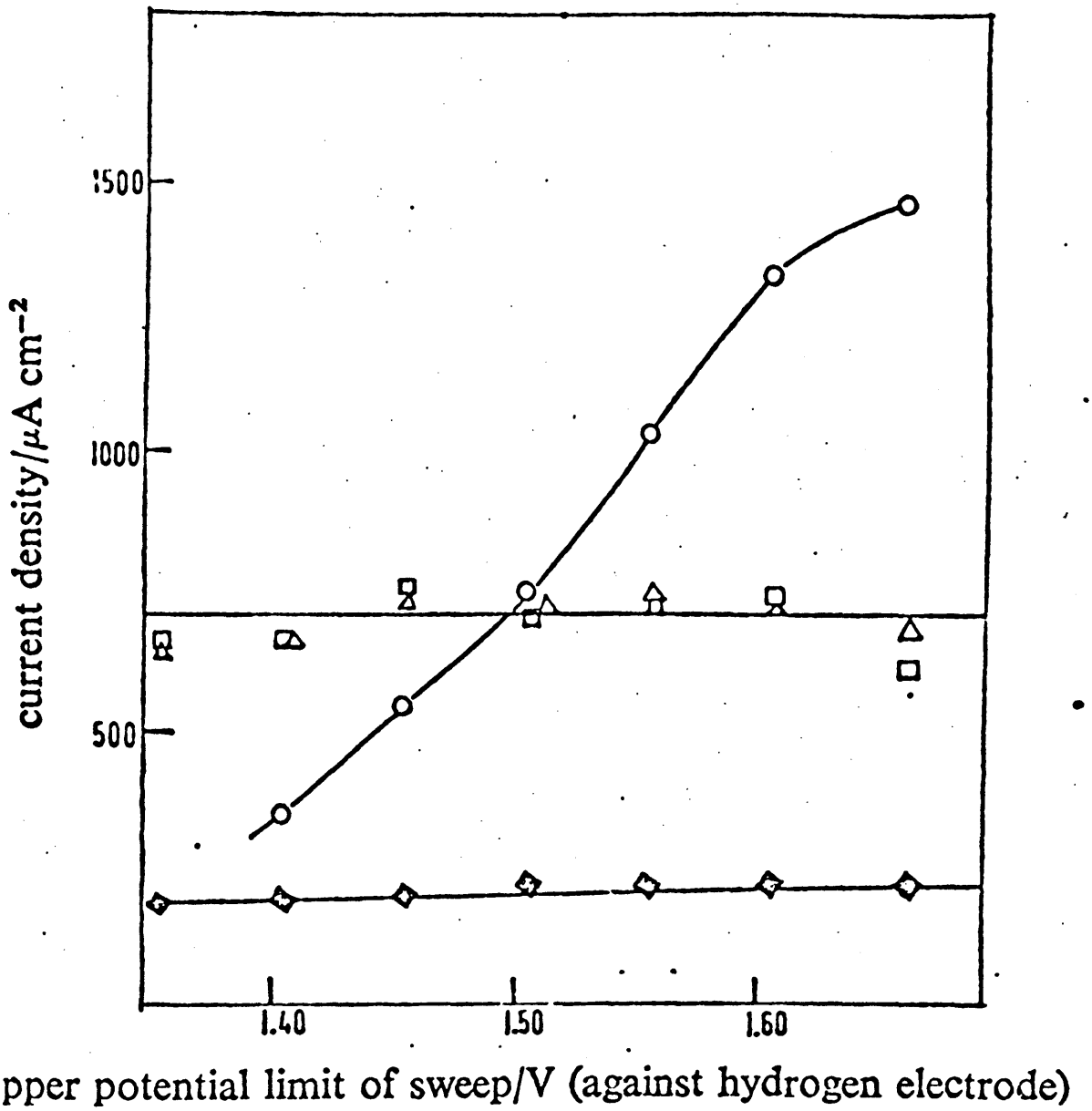

FIGURE 4.7 : Variation of peak heights with increasing maximum of the voltage scan. Δ and ◆ refer to the anodic peaks at 0.98 and 0.74 V, respectively: O and □ refer to the oxide reduction peaks at 1.37 and 0.97 V, respectively.

1.60 V is quite likely due to loss of oxide charge capacity as a result of the commencement of the deactivation process.

4.10. Impedance Measurements

The response of the iridium/solution interface to an a.c. signal is illustrated for the oxide layer region in Figure 4.8. Again there is a marked difference in response between activated and deactivated surfaces, the a.c. currents being much larger in the case of the former. From Figure 4.8(a) it can be seen that the a.c. current behaviour is highly reversible below 1.5 V, the a.c. peaks on the anodic scan being reproduced at approximately the same potential on subsequent cathodic scans. However, if the anodic scan was allowed to increase to higher potentials, for instance to 1.74 V, then the a.c. current values in the subsequent cathodic sweep were considerably lower {Figure 4.8(b)}. An interesting feature of the latter experiment was the appearance of a sharp a.c. current peak at ca. 1.56 V.

DISCUSSION

4.11. The Expanded Lattice and Irreversible Oxide Theories

Bold and Breiter[56] reported briefly on an observation that the oxide coverage of the surface increased with time during the course of potential

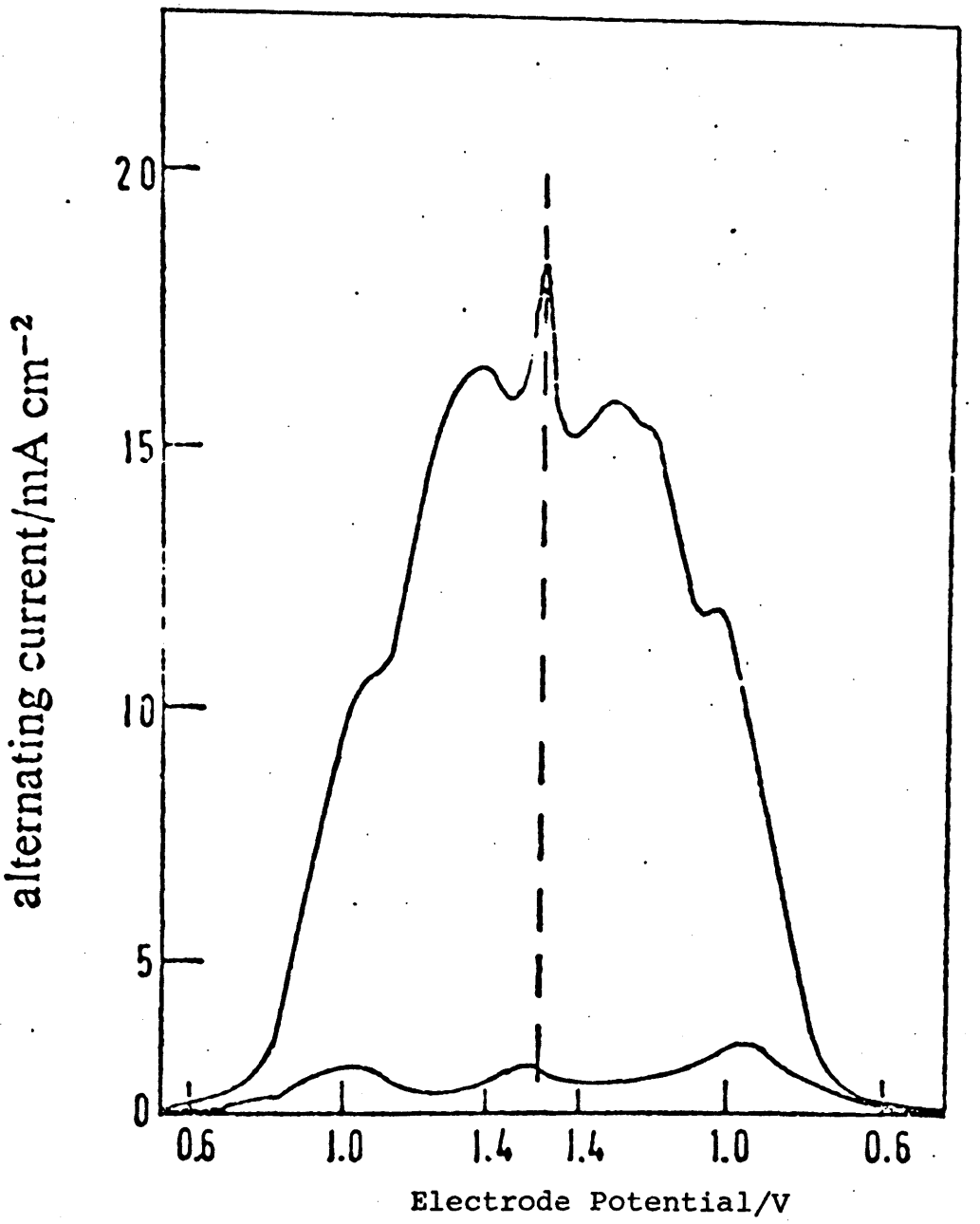

FIGURE 4.8(a) : A.c. response of the iridium/solution interface to a low amplitude signal (10 mV p-p) as a function of potential during sweeps up to 1.52 V in the anodic region. Lower curve refers to a deactivated electrode and upper curve to an electrode which was activated at 10 Hz for 1 min.

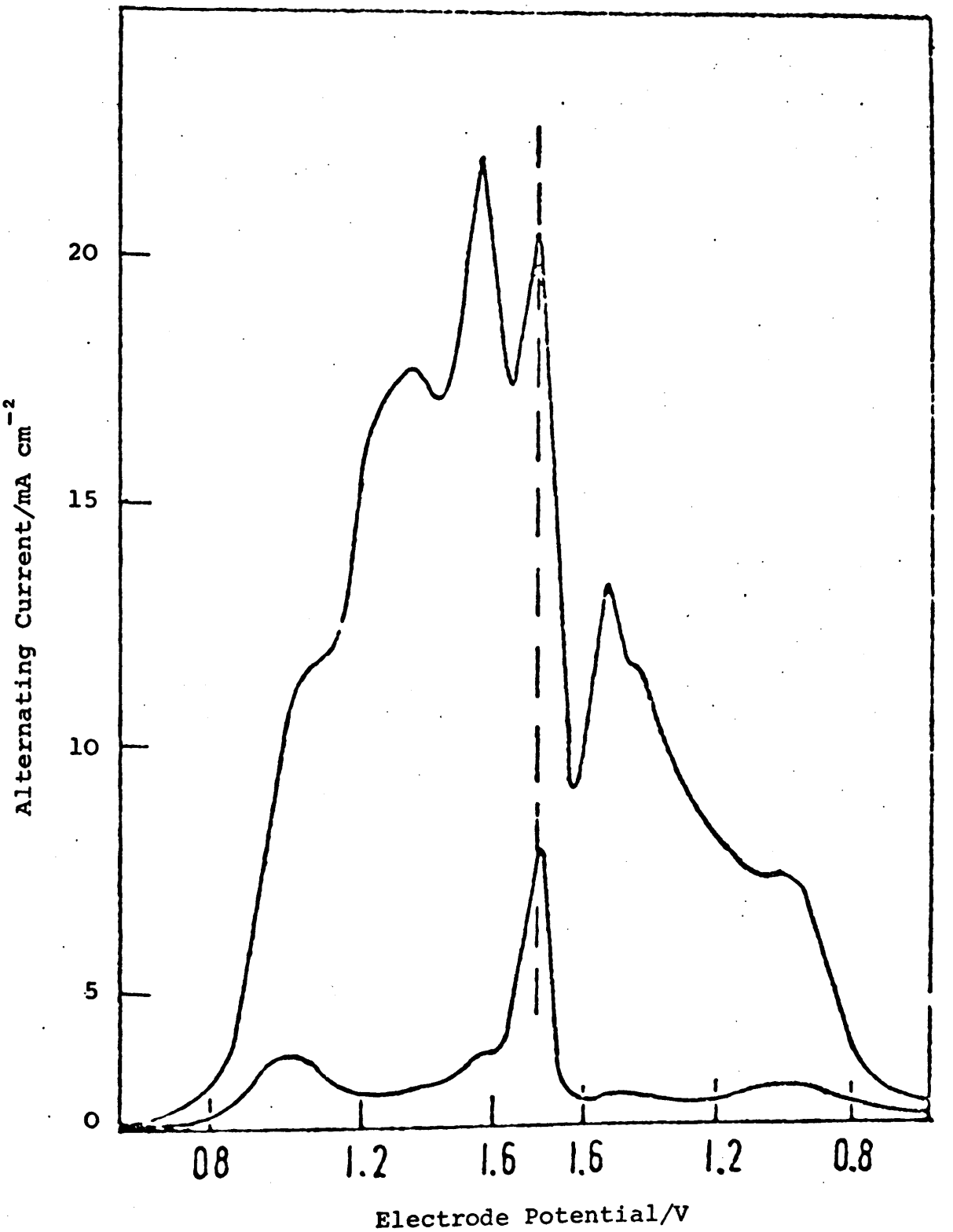

FIGURE 4.8(b) : A.c. response of the iridium/solution interface as in Figure 4.8(a) except that the sweep is allowed to reach a higher maximum of 1.74 V.

sweep experiments on iridium. Without investigating the phenomenon in detail, they attributed the increase to an expansion of the surface layer of the metal lattice. Thus the enhanced anodic charge capacity may be treated in terms of the conventional view of the oxidation of a noble metal surface (e.g. platinum) except that there is penetration of oxygen into the expanded metal lattice. In contrast to this is the view expressed by Woods[151] that the growth of the voltammetric peaks is due to the irreversible formation of an oxide species on cycling. According to this view, currents in the oxide region of the cyclic voltammogram are associated with changes in oxide stoichiometry. It is assumed that the oxide film formed anodically on iridium is retained under cathodic conditions so that, under all conditions, one is dealing with an oxide rather than with a metallic iridium electrode.

Iridium has a wide range of oxidation states ranging up to +8 and a variety of oxide species, e.g. Ir_2O_3, IrO_2, IrO_3, are reported. There are three different couples each with equilibrium potentials (E_o) in strong acid in the region of 0.9 V, viz.[152]

$$2Ir + 3H_2O \rightarrow Ir_2O_3 + 6H^+ + 6e^-, \quad E_o/V = 0.926 - 0.0591\ pH \qquad (1)$$

$$Ir + 2H_2O \rightarrow IrO_2 + 4H^+ + 4e^-, \quad E_o/V = 0.926 - 0.0591\ pH \qquad (2)$$

$$Ir_2O_3 + H_2O \rightarrow 2IrO_2 + 2H^+ + 2e^-, \quad E_o/V = 0.926 - 0.0591\ pH \qquad (3)$$

There is some discrepancy between these values and that of the main anodic peak on the voltammogram at 0.98 V; however, this is not too surprising as the exact potential

probably depends on the degree of hydration of the film. In terms of the expanded lattice theory where one is considering metal/metal oxide transitions the anodic processes involved may be (1) or (2), whereas in terms of the oxide retention theory the stoichiometry changes involved can be explained in terms of (3). According to the latter view processes (1) and (2) are irreversible whereas (3) is highly reversible. However, it is quite probable that other species, e.g. non-stoichiometric oxides, and hydroxides, are present in the anodic film. Since equilibrium potential values are not available for many of these species, and in any event evidence based on peaks on the cyclic voltammogram is an unreliable basis for phase identification, the nature of the activated anodic film on the iridium surface must await some type of spectroscopic investigation, e.g. X-ray photoelectron spectroscopy.[153]

4.12. Hysteresis

The lack of hysteresis between the main oxidation and reduction peaks at 0.98 V is highly unusual for a noble metal. The discrepancy can be explained if one accepts that with iridium the oxide merely changes oxidation state whereas with other noble metals the oxide is formed from, and reduced to, the metal. Such a change in oxidation state could occur by the further oxidation of an oxide of low valency during the anodic sweep. On the cathodic sweep the oxide would return to the original state with consequent loss of oxygen. While bonds in such oxides may have appreciable covalent character, the oxygen must bear a significant negative charge in view of its marked

electronegativity. Comparing some ionic radius values[154].(O, 0.73 Å; O^-, 1.76 Å; O^{2-}, 1.32 Å; Ir^{4+}, 0.68 Å; Ir, 1.36 Å) it is difficult to see how oxygen could be absorbed or desorbed through an oxide film of the order of 100 atoms in thickness sufficiently rapidly to give reversible behaviour. The changes in oxidation state could alternatively be explained in terms of the inter-conversion of an oxide and a hydroxide corresponding respectively to the higher and lower oxidation states. In accord with a mechanism suggested by Trasatti and co-workers[94] for ruthenium oxide films, such an interconversion might be brought about by the migration of protons into the oxide and out of the hydroxide. A process of this nature seems more likely to give reversible behaviour than one involving the intermigration of oxygen and iridium. Indeed the lack of a comparable mechanism makes the lack of hysteresis extremely difficult to explain in terms of the expanded lattice theory.

4.13. The Mechanism of the Activation Process

As indicated above, the activation process on cycling the potential may be explained in terms of growth of an irreversible oxide. The main anodic process during a voltage sweep involves the oxidation of the low-valence oxide to a higher state but some iridium metal is also oxidized. It is evident from the voltammogram that during the course of a potential sweep the stoichiometry of the oxide film varies and the corresponding changes in the ionic dimensions and oxide structure probably create stress variations across both the oxide itself and the oxide/

metal interface which favour oxidation of the metal. Such a process, involving intermigration of oxygen and iridium, would be expected to be kinetically slow. On the subsequent cathodic sweep the oxide is reduced to the lower valence state but not to iridium metal. Thus on each sweep there is a net increase in the amount of irreducible oxide on the surface with a consequent increase in the charge capacity. The rate of this charge capacity increase per activating cycle has been estimated from Figure 4.3 as 13.3 $\mu C\ cm^{-2}$, the value being taken after an activation period of 1 min at 10 Hz. This value represents only about 0.13% of the charge capacity of the oxide film, i.e. after 1 min of activation the major portion of the charge is involved in oxide stoichiometry changes.

4.14. The Ratio of Anodic to Cathodic Charge

According to Feldberg and co-workers[40] and also Vetter and Berndt[41] the ratio of anodic charge (Q_a) to cathodic charge (Q_c) for the oxide formation and dissolution processes on bright platinum is approximately 2:1 for the first measurements with a fresh platinum surface. This ratio decreases in subsequent measurements to values approaching 1:1. A similar effect has been noted here in the case of iridium where the ratio of anodic to cathodic charge $Q_a:Q_c$ is of the order of 2:1 for a deactivated electrode but changes to 1:1 on activation. Feldberg and co-workers[40] have explained their observations in terms of the formation of an oxide film on the platinum which is difficult to reduce beyond the

half-reduced state. The present results for iridium might be similarly explained if it is assumed that the oxide formed anodically is only partially reduced in the oxide region of the cathodic sweep. However, as discussed later, slow reduction of the outer layers of the remaining oxide may occur at potentials close to zero. In the case of an activated electrode the fraction of the total oxide film represented by this reduced outer region is small and so the anodic charge capacity Q_a is not significantly affected. However, for a deactivated electrode where the total amount of oxide on the surface is small, the fraction reduced at lower potentials may be appreciable with the result that the ratio $Q_a:Q_c$ may be closer to 2:1 than 1:1 for the initial cycles.

4.15. Deactivation at Anodic Potentials

Whatever the nature of the active layer produced on the iridium surface as a result of potential cycling, its properties are lost on anodization above about 1.60 V (Figures 4.5 and 4.6). It seems reasonable to assume that this deactivation arises due to loss by corrosion of the outer layer. As may be seen from Figure 4.7 the degree of oxidation of the iridium surface increases significantly in the oxygen evolution region. Evidently at about 1.60 V the outer layer is oxidized to a soluble iridium species, Although loss of this active layer is quite rapid (Figure 4.6) there is no indication of subsequent loss of iridium from the resulting deactivated surface until much higher potential values (> 1.80 V). Further indications of a marked change

in the behaviour of an iridium surface at the lower potential value are worth noting. First of all both the present investigation and the results of Damjanovic and co-workers[97,155] show that a sharp change in the Tafel slope for oxygen evolution occurs at about 1.57 V. Secondly, a peak occurs on the a.c. current against voltage curve at 1.56 V (Figure 4.8). According to the theory of a.c. polarography[156] such a peak is due to the coexistence of both components of a redox couple, a situation which would be expected to arise in the event of a corrosion process. The peak on the a.c. curve at 1.56 V corresponds to the potential where the oxidized and reduced forms of the couple are present at equal activities, and the fact that the corrosion/deactivation process becomes marked only at ca. 1.60 V (Figure 4.5) suggests that there is significant over-voltage associated with this reaction.

4.16. The Effect of Added Chloride Ion

A major advantage of the irreversible oxide theory is that it can account for the effect of chloride ions on the anodic behaviour of iridium. The presence of chloride ion in solution is known to inhibit the formation of an anodic oxide film on a clean platinum surface.[157] This effect can be explained in terms of specific adsorption of chloride ions onto the platinum in aqueous solution, and there is little reason for assuming that iridium should behave in a different manner. However, the oxide layer region of the cyclic voltammogram of iridium was unaffected by the addition of chloride. This suggests that the process involved here is not formation of an oxide film on a clean metal

surface but possibly hydroxide oxidation with proton transfer to the solution as described earlier. Thus, the oxidizable species (-OH) is already present in the oxide layer, and adsorption of chloride ion on an oxide surface is in any event probably not as strong as on a clean metal.

4.17. The Hydrogen Region

A major difficulty with the irreversible oxide theory arises in connection with the hydrogen region of the cyclic voltammogram. The anodic oxide film in question here is not the type of sintered oxide film prepared for application in the chlor-alkali industry by the thermal treatment of ruthenium or iridium trichloride on a titanium support.[94] Instead one is dealing with a freshly-deposited, unsintered, and probably hydrated iridium oxide film which can readily undergo a change in stoichiometry at ca. 0.975 V. Considering along with this the fact that the known oxides of iridium are thermodynamically unstable with respect to reduction below ca. 0.9 V under the conditions used, it seems unlikely that the surface would remain in the oxidized state at low potentials. Another point worth noting is the excellent agreement between the charge required for the anodic hydrogen region both in the present work and in the results of Bonnemay et al[150] for iridium (310 to 350 $\mu C\ cm^{-2}$) and that quoted by Gilman for platinum (300 $\mu C\ cm^{-2}$). These data would suggest an oxide-free metal surface and would in fact favour the expanded lattice theory unless one could visualise some type of hydroxide to oxide transition in the lower potential region

$$OH_{ads} \rightarrow O_{ads} + H^+ + e^-$$

The reverse of this process corresponds to hydrogen adsorption onto an oxide surface.

As noted earlier some slow reduction of the surface of the lower valency iridium oxide at low potentials would explain the discrepancy between the anodic and cathodic charges for a deactivated electrode. Further evidence for such a process is afforded by the fact that currents in the double-layer region are appreciably higher during the cathodic sweep than during the anodic sweep. This suggests that slow reduction of the lower oxide is occurring at these potentials on the cathodic sweep and it is reasonable to assume that this reduction continues in the hydrogen region. Furthermore, the magnitude of these cathodic double layer currents is not changed significantly after activation at 10 Hz. This suggests that the process involved is independent of the oxide thickness and is likely to be a surface effect. Thus, it is possible that the outer layers of the iridium oxide are reduced so that hydrogen can chemisorb on an array of iridium atoms supported on an oxide. Cyclic voltammetry is not a steady state technique and some oxygen may be diffusing slowly from the bulk to the surface and being reduced there over the lower region. Current flow across the oxide may well occur by an electronic mechanism since iridium oxide is known to exhibit electronic conductivity.[91] On continuing in the anodic direction above the hydrogen region the oxygen from the interior could reoxidize the surface thus preventing chloride ion inhibition of the anodic process.

4.18. Comparison with Related Work

Recent ellipsometric experiments by Otten and Vischer[158,159] are in agreement with the above results. The ellipsometric parameters, Δ and ψ for iridium measured at 0.2 V were found to change if the potential of the electrode was cycled. A corresponding increase in the anodic oxide capacity of the surface was observed. The results obtained in both cases indicated that relatively thick layers were formed; however, the values did not agree, those obtained by ellipsometry being considerably larger than those obtained by coulometry. This was interpreted as being due to local penetration, i.e. pitting, of the metal surface. Furthermore, a "disturbed metal layer" formed at the surface and extending towards the interior of the metal was assumed by these authors. This is equivalent to the expanded lattice theory. The lack of hysteresis was not discussed but it is difficult to understand how a process, such as oxidation of iridium metal, involving intermigration of oxygen and iridium could occur in a reversible manner. Similarly the lack of inhibition of the oxidation process by added chloride ion does not seem to be consistent with the theory. The possibility of proton migration[94] as the mechanism of oxidation and reduction was not mentioned in this work.

Rand and Woods[160] also observed an increase in the anodic oxide capacity of iridium electrodes during progressive slow potential cycling. They further reported that the electrode was deactivated if it was removed from the cell and soaked in hot chromic acid, and that a similar effect was observed if the electrolyte was replaced by 5 mole dm^{-3} H_2SO_4

and potential cycling was continued. In the latter case, however, it appears that the electrode retained some of its enhanced oxide charge capacity. The activation effect was interpreted in terms of the irreversible oxide theory and the deactivation in chromic acid or by cycling in relatively concentrated acid was regarded as occurring by dissolution of the oxide film. An observation[160] that a slow corrosion of iridium occurred during potential cycling is interesting in this connection and it was suggested that a balance existed between the formation and dissolution of the oxide layer in 5 mole dm^{-3} H_2SO_4. It was also reported that a black deposit, presumably an oxide, was sometimes formed by accidentally heating the iridium electrode during construction and that such an electrode showed similar behaviour to one which had been activated by potential cycling. This would appear to lend further support to the irreversible oxide theory.

While iridium appears to be an exception within the platinum metal group on account of the highly reversible valence change in its anodic film, this type of change is by no means uncommon in electrochemistry. Thus, the reaction of the nickel hydroxide electrode at anodic potentials in strong base involves the oxidation of $Ni(OH)_2$ to NiOOH; this has been widely investigated[161] and proton diffusion measurements in the anodic film were carried out recently by MacArthur[162] using potential sweep and pulse techniques. Similar work has been carried out in the case of the manganese dioxide[163] and vanadium oxide[164] electrode systems where the corresponding reactions are

$$MnO_2 + e^- + H^+ = MnOOH$$

and

$$V_2O_5 + e^- + H^+ = V_2O_5H$$

The first of these reactions is of considerable interest since it occurs at the cathode of the commercial zinc/manganese dioxide alkaline battery. It appears from a recent review[165] of proton conduction in solids that an investigation of proton migration in iridium oxide would be quite interesting.

It may be pointed out, in conclusion, that the present work seems to clarify the situation with regard to some rather unusual claims made in connection with an iridium electrode which was patented[166] as a pH-monitoring probe. According to Ives and Janz[167] this electrode is prepared by plating iridium onto a cleaned base metal and it should be operated in a solution in contact with air (but not pure oxygen). Measurements apparently show that this electrode has an E^o value of 0.97 V, it responds in a near theoretical manner to pH over the range 0 to 14 at temperatures from 0^oC to 70^oC. Furthermore, although it has a low impedance, it requires a high impedance measuring circuit as it cannot deal with more than 10^{-7} amp cm^{-2} without polarizing - a surprising disability for a supposedly reversible electrode as pointed out by Ives and Janz.

These facts suggest that the electrode in question here is the $IrO_2/IrOOH$ system, the pH response being due to the equilibrium

$$IrO_2 + H_3O^+ + e^- = IrOOH + H_2O$$

and the equilibrium potential of ca. 0.98 V according to the present work agreeing quite well with the quoted value of 0.97 V. Obviously this low impedance electrode will be easily polarized since only a small charge is required to saturate the oxide layer or denude it of protons.

CHAPTER V

IRIDIUM

Part 2: The Oxygen Evolution Region

Iridium is similar to ruthenium in many respects. Both form oxides which behave as metallic conductors:[126] their specific resistances are comparable with that of mercury and have positive temperature coefficients.[91] Of the platinum metals ruthenium and iridium have the highest number of unpaired d-electrons per atom;[88] this suggests strong metal-hydroxyl bonding[89] and, consequently, low oxygen evolution overpotential.[75] As discussed earlier (Chapter III), low overpotential for oxygen evolution is, in fact, observed in the case of ruthenium but a simultaneous corrosion reaction occurs.[93] However, iridium has long been regarded as extremely resistant to corrosion[98] and seems to be a much more interesting substrate for the investigation of the oxygen evolution reaction.

5.1. The Corrosion of Iridium

From a chemical point of view, iridium is an extremely stable metal.[112] It is unaffected by all acids (including aqua regia) and is only slightly attacked by non-oxidizing molten alkalis. For this reason it has sometimes been used instead of platinum for making crucibles and other apparatus.

Llopis and Jorge[96] have investigated the anodic corrosion of iridium in hydrochloric acid solutions. This was stated to proceed through the formation of $IrCl_6^{2-}$ and $IrCl_6^{3-}$, the formation of Ir(III) tending to be more important at less positive potentials. The metal was reported to be more resistant to corrosion than platinum under both d.c. and a.c. conditions.

A high overpotential was reported[96] for the anodic corrosion reaction; galvanostatic anodic and cathodic charging curves were used to study the effect. Passivity was reported to set in at potentials where the anodic formation of an oxide film occurs. For HCl concentrations higher than 4 mol dm^{-3} anodic charging curves could be divided into two sections, the first corresponding to corrosion of the metal and the second to evolution of chlorine and oxygen on the passivated metal. At lower acid concentrations no intermediate arrest was observed on the charging curves indicating passivation of the iridium even at the lower current densities. The values at which the electrode passivated were found to increase with increasing HCl concentration and temperature, but in any case they were much lower than those observed with platinum electrodes under similar conditions.

The anodic corrosion of iridium by direct current alone has also been studied[99] using radioactive tracer techniques. The isotope used was ^{192}Ir which has a half-life of 74.4 days. The results confirmed that the metal passivated very easily but some corrosion remained, its rate being very small and dependent on pH and chloride ion concentration. The nature of the complexes formed in this investigation was not discussed.

The activating effect of chloride ions on the anodic corrosion of the metal was explained[96] in terms of specific adsorption at the surface. This, it was claimed, leads to a weakening of the bonds between the surface atoms and the metal lattice. On the other hand, the formation of complexes leads to stabilization of metal ions on the solution side.

When the potential reaches a suitably positive value, metal ions pass to the solution side forming complexes with the chloride ions and it may be expected that specific adsorption will lead to a diminution of the free energy barrier that controls the rate of the anodic dissolution process.

Llopis[98] has further reported that the corrosion rate of iridium in chloride solution is markedly increased by superimposing an alternating current, this effect being less marked with iridium than with platinum. Results obtained in 6 mol dm^{-3} HCl showed that for a given direct current (i_c), the electrode remained passive until a certain value of alternating current (i_a) was superimposed. As i_a was further increased, the corrosion rate also increased. The effect of a.c. was stated to be more pronounced at low frequencies.

Valence states of dissolved iridium were determined and the formation of both Ir(III) and Ir(IV) was reported. The relative proportion of Ir(III) increased as the potential was made less positive, or as i_c was decreased, or as the ratio i_a/i_c was increased.

The corrosion of iridium in chloride solution under the influence of a.c. only was investigated[99] using mains frequency (50 Hz). It was found that, at constant alternating current density, the ratio of Ir(III) to Ir(IV) increased with acid concentration. Furthermore, the surface state of the electrode played a part so that the ratio obtained at a particular HCl concentration and a.c. current density was not always the same.

The nature of the ionic species existing in solution as a result of iridium corrosion by a.c. was studied[99] by UV and visible absorption spectroscopy. The spectrum obtained depended on the acid concentration used. It was possible to assign some of these to definite complexes. A slow time-variation of the spectrum was also reported in the case of the more dilute HCl solutions and this was attributed to the spontaneous reduction of Ir(IV) species to Ir(III).

The behaviour of iridium in sulphuric acid solutions during the passage of alternating currents of large amplitude was investigated by Boiko and Kadaner.[168] It was reported that corrosion of the iridium at 50 Hz a.c. in 7.5 mol dm^{-3} H_2SO_4 occurred at higher alternating current density values. The valency of iridium in the solution species depended on the current density. No corrosion was observed at 50 mA cm^{-2}, but at 100 mA cm^{-2} corrosion of iridium to the trivalent state occurred. At 250 mA cm^{-2} both trivalent and tetravalent iridium species were reported.

In summary then, corrosion of iridium under the influence of alternating current has been reported in both HCl and H_2SO_4 solutions. A slow corrosion reaction has also been observed for anodically polarized iridium in HCl solutions. There appear, however, to be no reports in the literature of iridium corrosion by d.c. in chloride-free media.

5.2. Oxygen Evolution on Iridium

Damjanovic, Dey and Bockris[97] have investigated platinum, rhodium, iridium and platinum-rhodium alloys as electrocatalysts for the oxygen electrode reaction. They reported that at potentials more anodic than 1.4 V, iridium was the most active of the substrates investigated. All the substrates showed two distinct linear regions with different slopes in the anodic overpotential region of the V-log i (Tafel) plot. Transition from one slope to the other was reported to be sharp. Except in the case of rhodium in acid solution, only one linear region was observed on the corresponding Tafel plot for oxygen reduction.

In the case of iridium, the line obtained at lower anodic overpotentials on the Tafel plot intersected the line for cathodic overpotentials at 1.23 V and it was concluded from this that the same mechanism accounts for both the oxygen evolution and reduction reactions. It was deduced from the Tafel slopes that the overall rate is controlled by an electrochemical step which occurs twice while the overall reaction occurs once. It was furthermore stated that two charge transfers precede the rate-controlling step in the case of the anodic reaction. Three reaction paths which satisfy this requirement were considered. Observation of the pH-dependence of the overpotential led to the conclusion that the following was the most likely mechanism.

$$S + H_2O \longrightarrow SOH + H^+ + e^-,$$

$$SOH + S + H_2O \longrightarrow SO + SH_2O + H^+ + e^-,$$

$$2SO \longrightarrow O_2 + 2S,$$

where S represents a site on the metal surface. This is termed the electrochemical oxide mechanism. More detailed consideration of the variation of overpotential with pH in both acid and alkaline solutions led Damjanovic and Wong[169] to support the electrochemical oxide mechanism at iridium electrodes.

The oxygen evolution reaction on iridium was also investigated by Hoare,[170] who reported a linear Tafel plot with a slope of 80 mV. It was concluded that the reaction takes place on a conducting layer of IrO_2 and that the mechanism is similar to that for platinum and rhodium. The observed Tafel slope (80 mV) compares poorly however with the value (40 mV) reported by Damjanovic and co-workers.[97] This casts some doubt on the latter group's mechanistic interpretation which was based almost solely on Tafel slope values. Indeed they themselves have noted that mechanism deductions can be made in this manner only when the change of the substrate with potential and time is negligible in the potential region of the kinetic analysis.

5.3. The Present Investigation

The poor agreement between published results and the lack of a generally-agreed mechanism indicated the need for further research on oxygen evolution at iridium. Since previous investigations tended to centre on low current densities, it was decided to study the behaviour of the metal over a wide range of anodic potentials and to investigate also whether any corrosion occurred.

Experiments were carried out using cell no. 2 (Figure 2.10). When cell currents were likely to exceed 2 mA automatic correction of solution iR was made, using the circuits in Figures 2.7 and 2.8. In potential step experiments, the electrode was pretreated by keeping its potential at 0.0 V for 1 min and subsequently at 0.6 V for a further 1 min.

All spectra were recorded on a Perkin-Elmer 402 ultraviolet-visible spectrophotometer using quartz cells.

RESULTS

5.4. The Time-Variation of Current

The variation of current density as a function of time was investigated for an iridium electrode at a number of different potentials. In each case the electrode was pretreated at 0 V and 0.6 V as described earlier. Results were plotted using logarithmic scales on both axes and are shown in Figure 5.1. Over the anodic range 1.50 V to 1.70V linear behaviour was observed, i.e. the logarithm of the current density decreased in a linear manner with the logarithm of time. Similar behaviour has been reported by Schultze[74] in the case of platinum for times greater than 1 sec and for potentials from 1.6 to 2.0 V. However, at potentials of 1.8 V and greater the anodic currents in the case of iridium decreased initially, then became steady for some time prior to undergoing a subsequent slow increase to approximately constant values. At a potential of 1.75 V the observed slope was intermediate to the two cases described above; evidently the transition from one type of behaviour to another occurred in this region.

5.5. Tafel Plots

The construction of a Tafel plot for the oxygen evolution process is generally complicated by the difficulty in attaining true steady-state values.[73,74] In the case of iridium the problem is alleviated

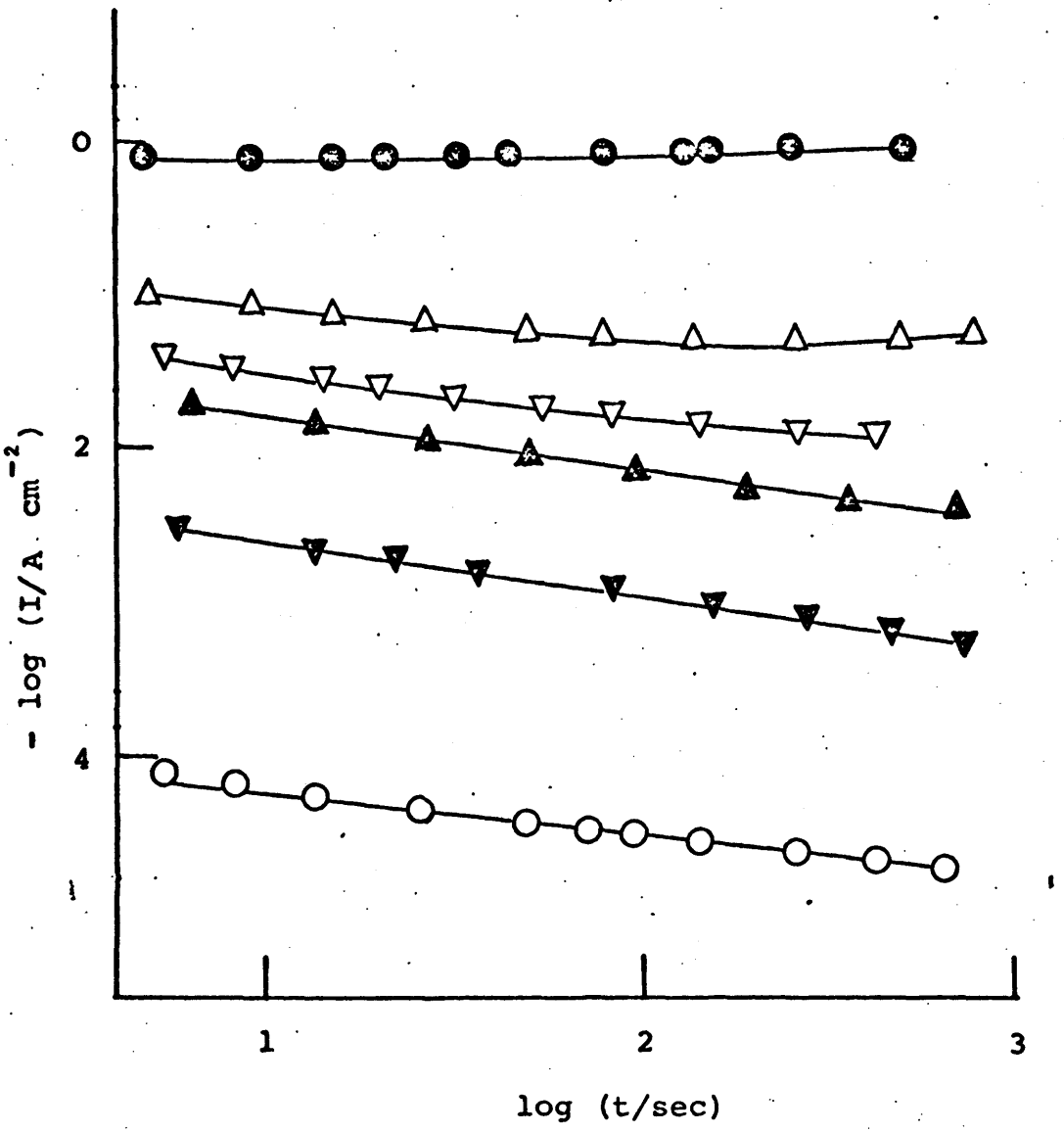

FIGURE 5.1 : Variation of current density with time at constant potential for an iridium electrode in 1.0 mol dm^{-3} H_2SO_4 at 25°C.following a potential step from 0.6 V.

●	1.90 V	▲	1.70 V
Δ	1.80 V	▼	1.60 V
▽	1.75 V	o	1.50 V

somewhat in the region above 1.8 V since here the currents reach a relatively constant value in a short time (typically 5 min). At lower potentials the current densities change; however, the rate of change becomes small at long times so that the variation of current density with potential may be examined by comparing the pseudo-steady-state current densities after a particular time at each potential. The resulting Tafel plot is shown in Figure 5.2. The current density values shown for potentials of 1.78 V and greater were the minima on the current decay curves. At potentials lower than 1.78 the values shown for iridium are the pseudo-steady-state current densities attained after a time of 60 min. The corresponding curve for platinum is also shown, the pseudo-steady-state values being measured in this case after 15 min.

It is apparent that over the range investigated (1.6 V to 1.95 V) the current density on iridium is much greater than on platinum (by a factor of 52 at 1.6 V and 1780 at 1.95 V). Three linear regions are evident on the plot for iridium: AB, BC and DE, with Tafel slopes of 53.5 mV, 112.0 mV, and 126.6 mV, respectively. Evidently the change in the anodic behaviour of iridium mentioned earlier in connection with the current decay curves must occur in the potential range CD. As will be described shortly this region also corresponds to the onset of corrosion. It may be worth noting that although the anodic current undergoes a marked increase over the short range CD, the regions on either side of this transition, i.e. BC and DE,have similar slopes.

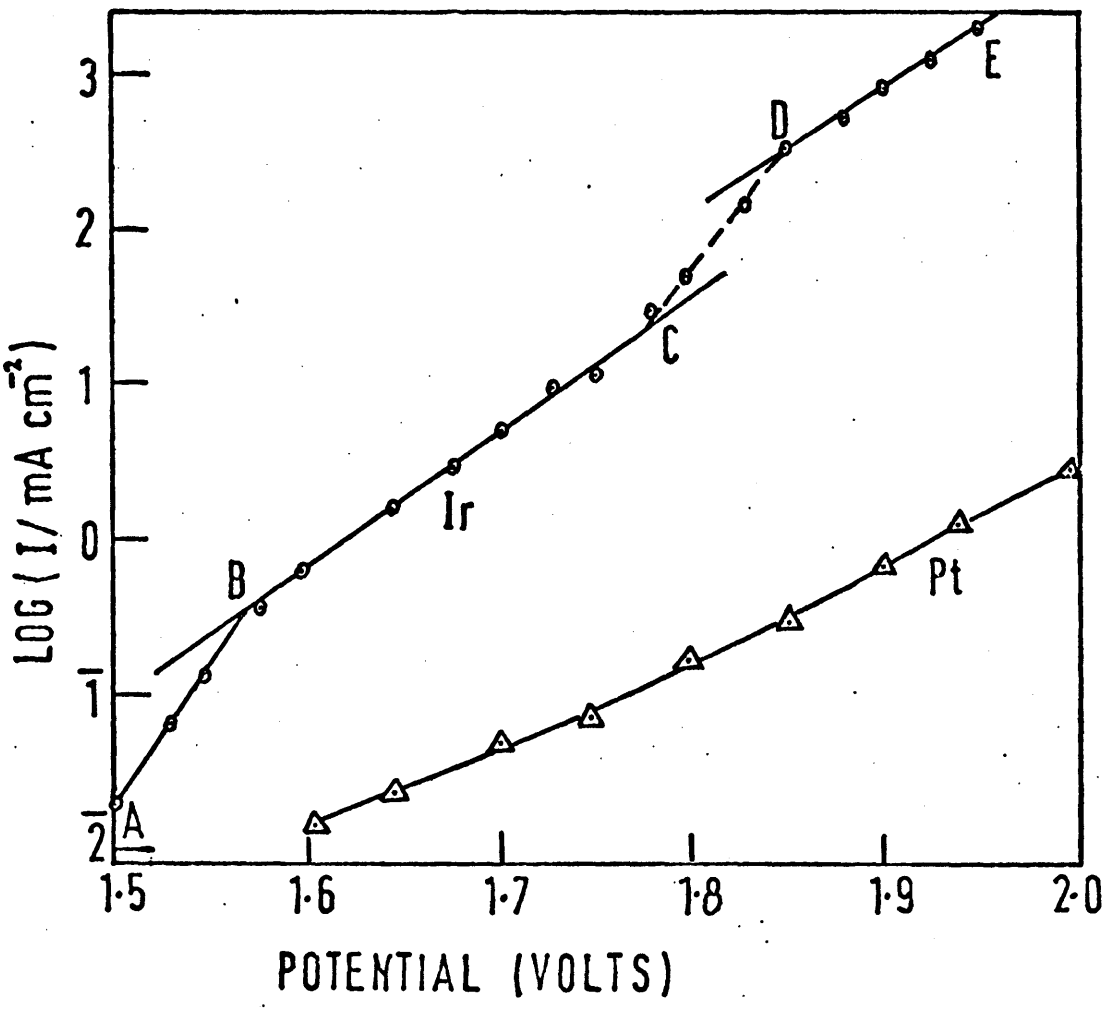

FIGURE 5.2 : Variation of log (current density) with potential in the case of iridium (O) and platinum (Δ) in 1.0 mol dm^{-3} H_2SO_4 at 25°C.

5.6. Effect of Electrolyte

The behaviour of platinum and iridium electrodes in acidic and alkaline electrolytes at high anodic potential was compared by measuring the current decay curve at a constant potential of 1.89 V. The results, which were again plotted using a logarithmic scale on both axes (Figure 5.3) clearly show that the highest current density was obtained with iridium anodes in acidic solution. In the case of platinum the current densities were of similar magnitude in 1.0 mol dm^{-3} as in 1.0 dm^{-3} NaOH but on iridium the current densities in acid were much greater (by a factor of ca. 51 after 1000 sec) than the corresponding values in base. However, even in base the current densities on iridium were much greater (by a factor of ca. 33) than the corresponding values on platinum. The current decay in the case of iridium in 1.0 mol dm^{-3} NaOH is similar to the behaviour of platinum under both acidic and basic conditions. The obvious exception is iridium in 1.0 mol dm^{-3} H_2SO_4, where an initial small decrease is followed by a slow subsequent increase in anodic current density. Evidently there must be an unusual mechanism for oxygen evolution at iridium anodes at high potential (> 1.75 V) in acidic media.

5.7. Corrosion

It was observed during the anodization of iridium at high potentials in acidic media that some corrosion of the metal occurred to give a brown species in solution. This side-reaction was investigated by pretreating the electrode at 0 V and 0.6 V as

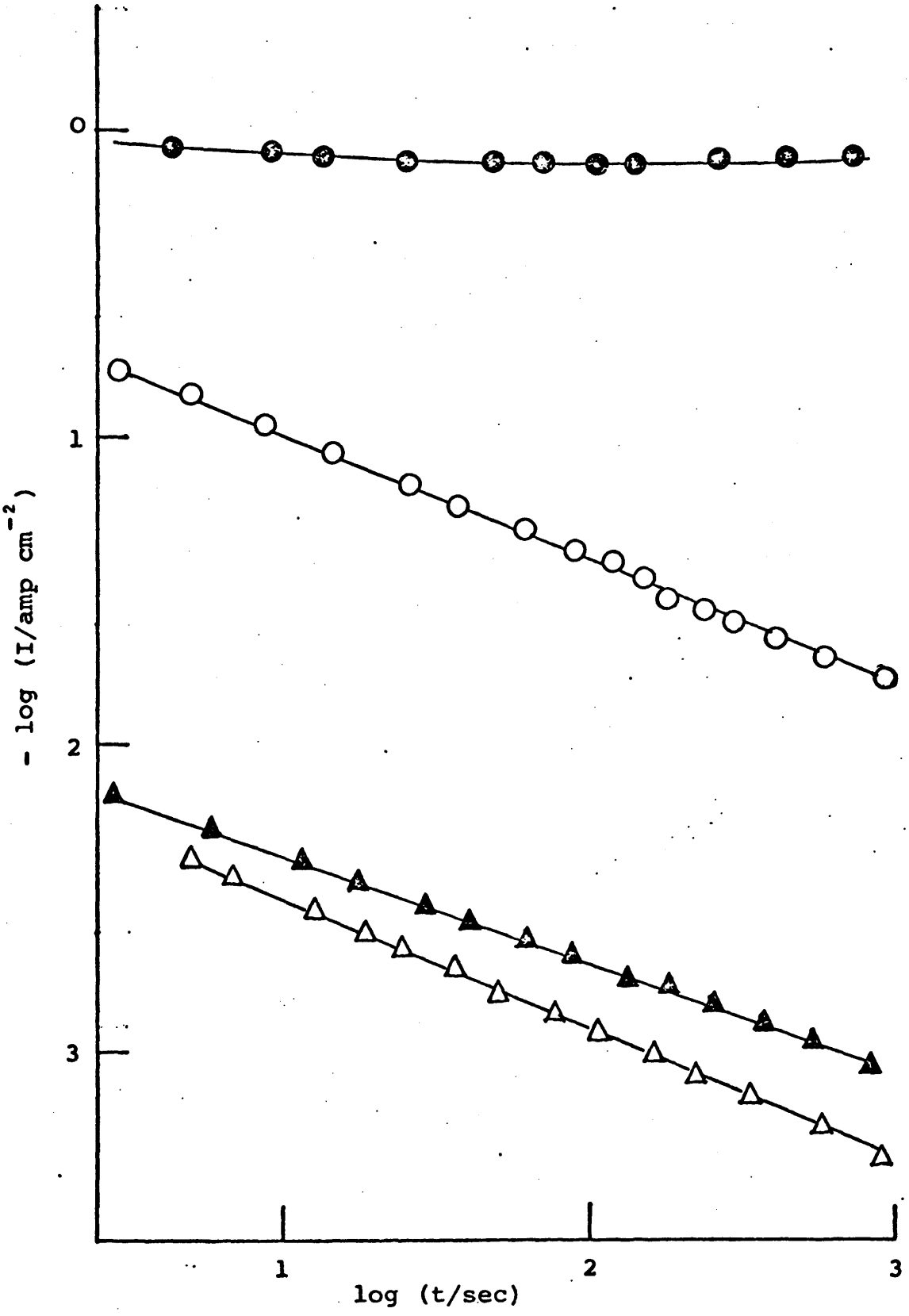

FIGURE 5.3 : Variation of current density with time following a potential step from 0.6 V to 1.90 V for iridium (●) and platinum (▲) in 1.0 mol dm^{-3} H_2SO_4 and likewise for iridium (O) and platinum (Δ) in 1.0 mol dm^{-3} NaOH. Temperature = 25°C.

mentioned previously and then stepping the potential to a preselected anodic value. After a given period of time the electrolysis was stopped and the electrolyte removed from the anode compartment of the cell. The iridium content of this solution was measured using the stannous iodide technique, and the UV-visible spectrum of the brown solution was also recorded. Fresh electrolyte was placed in the cell and the experiment was repeated at the same potential for different times. The quantity of iridium in solution, as estimated by the stannous iodide[174] analysis, was plotted against the anodization time. From these plots the rate of corrosion of iridium was determined at each potential in the range 1.85 V to 1.95 V. The optical density of the electrolyte at 455 nm (standardized to a volume of 15 ml) was also plotted against anodization time as shown in Figure 5.4. The linearity of the plots indicates that Beer's law was obeyed, and comparison with the iridium concentrations obtained by the analysis procedure yield a value of $\varepsilon = 1.2 \times 10^4$ litre $mole^{-1}$ cm^{-1} for the molar extinction coefficient.

The measured corrosion rates correspond to partial current densities for corrosion ranging from 18.6 μA cm^{-2} at 1.85 V to 633 μA cm^{-2} at 1.95 V, assuming an overall 6-electron process (e.g. Ir to IrO_2^{++}). Since the corresponding total current densities are 0.3 A cm^{-2} at 1.85 V and 1.85 A cm^{-2} at 1.95 V, the current density due to corrosion is a negligible fraction of the total in the potential range investigated. As shown in Figure 5.5, a linear Tafel-type plot of slope 59 mV was obtained by plotting the logarithm of the corrosion rate versus potential. Since the slope of the corresponding

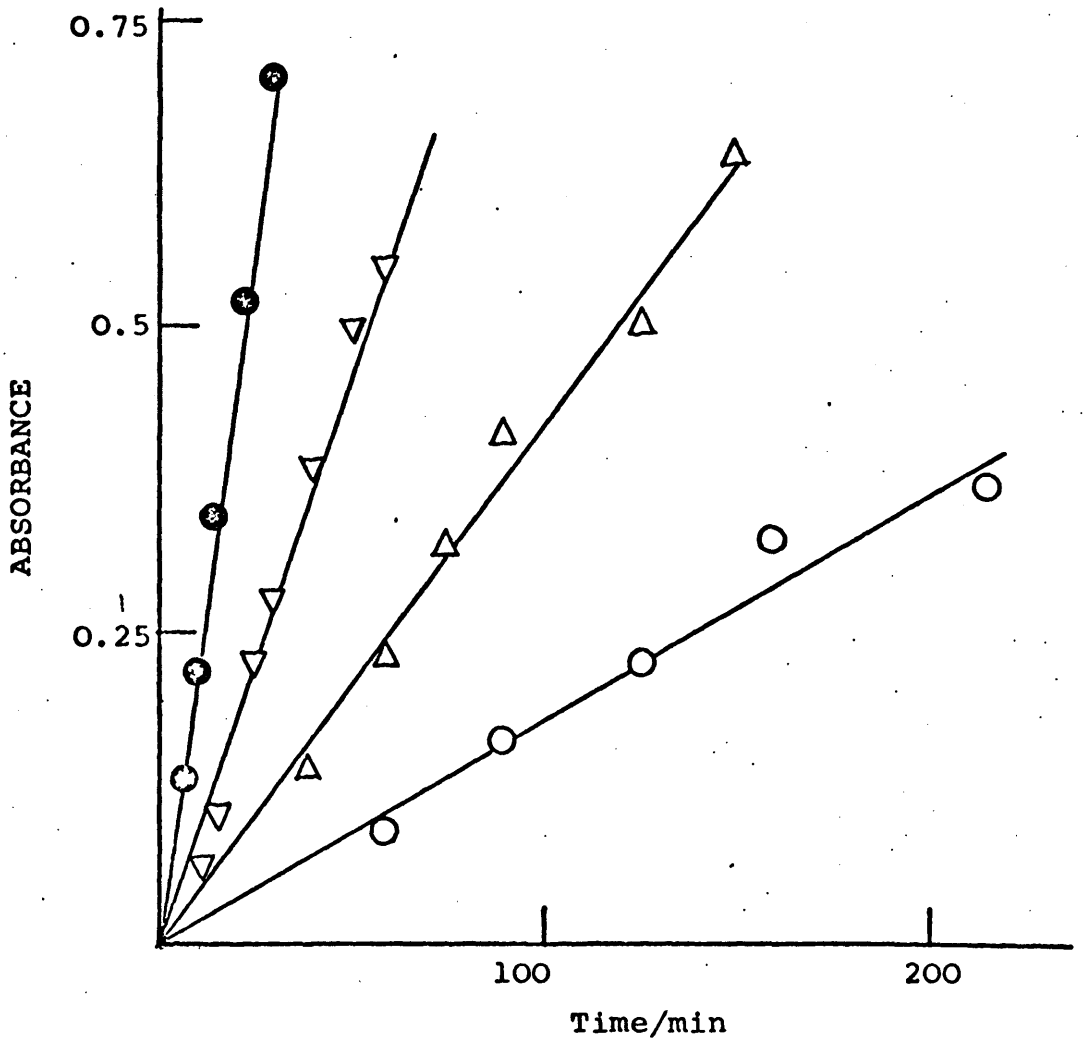

FIGURE 5.4 : Variation with time of the optical absorbance (at 455 nm) of the electrolyte (H_2SO_4, 1.0 mol dm^{-3}) during anodization of an iridium electrode at potentials of 1.95 V (●), 1.925 V (▽), 1.90 V (Δ) and 1.88 V (○). Temperature = 25°C.

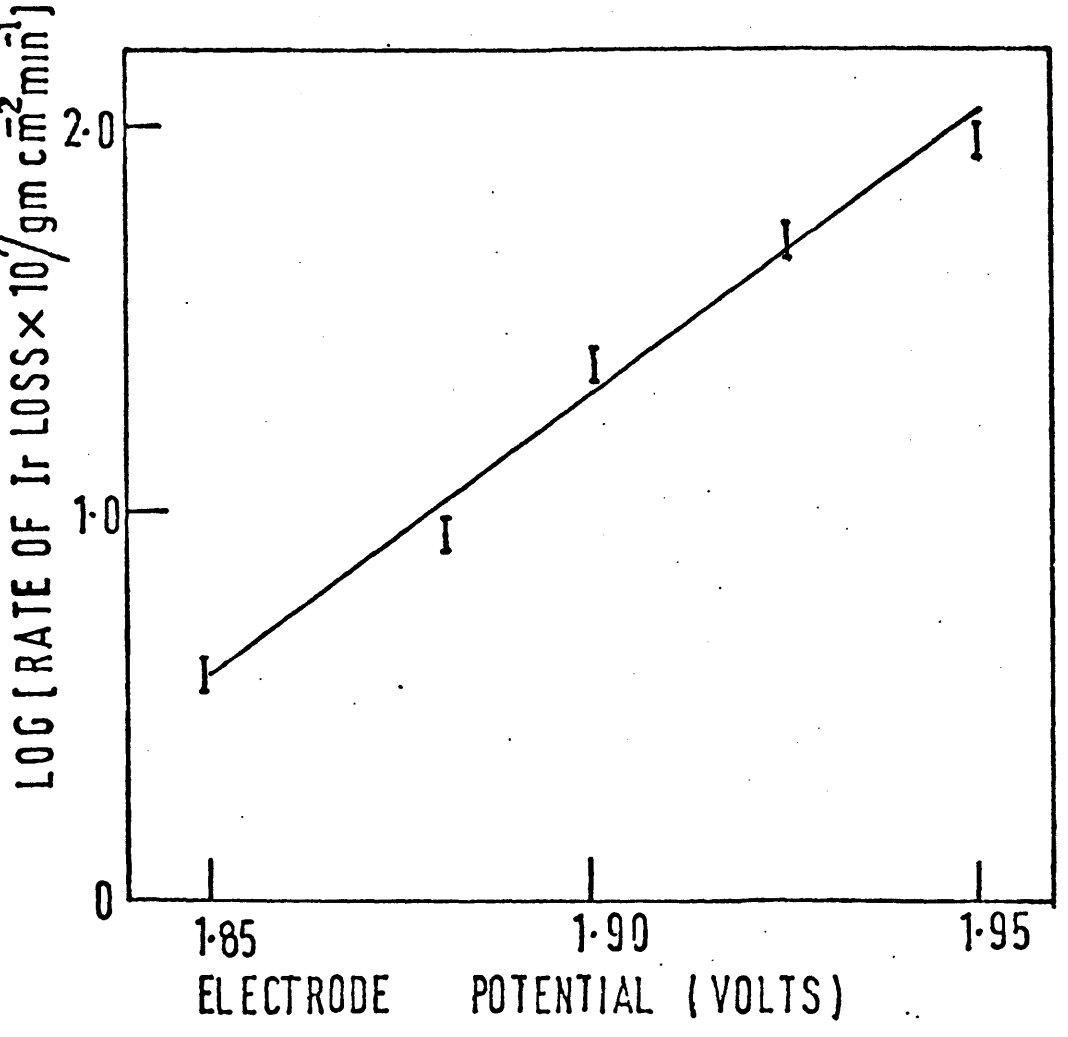

FIGURE 5.5 : Variations with potential of the rate of corrosion of an iridium electrode in 1.0 mol dm^{-3} H_2SO_4 at 25°C.

region of the Tafel plot for the total current (which is essentially the oxygen evolution current) as shown in Figure 5.2 is 126.6 mV, the rate of iridium corrosion is evidently increasing more rapidly than the rate of oxygen evolution.

5.8. The Solution Species

The UV-visible spectrum of the brown iridium species obtained from corrosion of iridium in 1.0 mol dm^{-3} H_2SO_4 (Figure 5.6) was found to have an absorbance maximum at 455 nm. A similar result was obtained if 1.0 mol dm^{-3} $HClO_4$ was used instead of H_2SO_4 showing that the iridium species obtained is not affected by the nature of the anion present. If the electrolyte containing the brown iridium species was allowed to stand for a few days its colour changed to purple and the spectrum was then shown to have an absorbance maximum at 535 nm (Figure 5.6). A similar colour change was obtained almost immediately if an oxidizable species (e.g. hydrogen or hydrogen peroxide) was added to the brown solution.

5.9. The Effect of Chloride Ion

The effect of added chloride ion on the oxygen evolution current was briefly investigated. Current-voltage curves for an iridium electrode in 1.0 mol dm^{-3} H_2SO_4 in the absence of chloride and in the presence of various concentrations of chloride ions are shown in Figure 5.7. Obviously at higher potentials the current densities are markedly

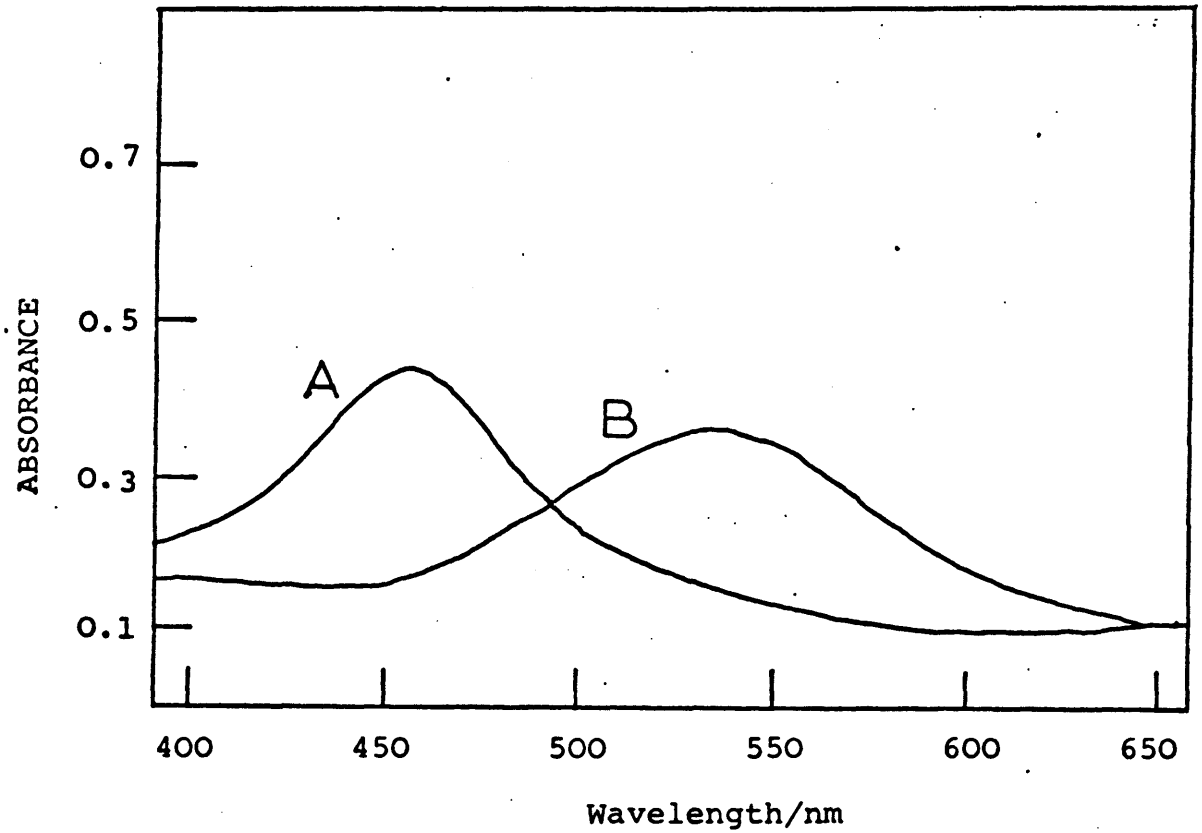

FIGURE 5.6 : A: Visible spectrum of the iridium species obtained in 1.0 mol dm^{-3} H_2SO_4 by corrosion of iridium at potentials greater than 1.85 V.

B: Spectrum of the same solution two days later.

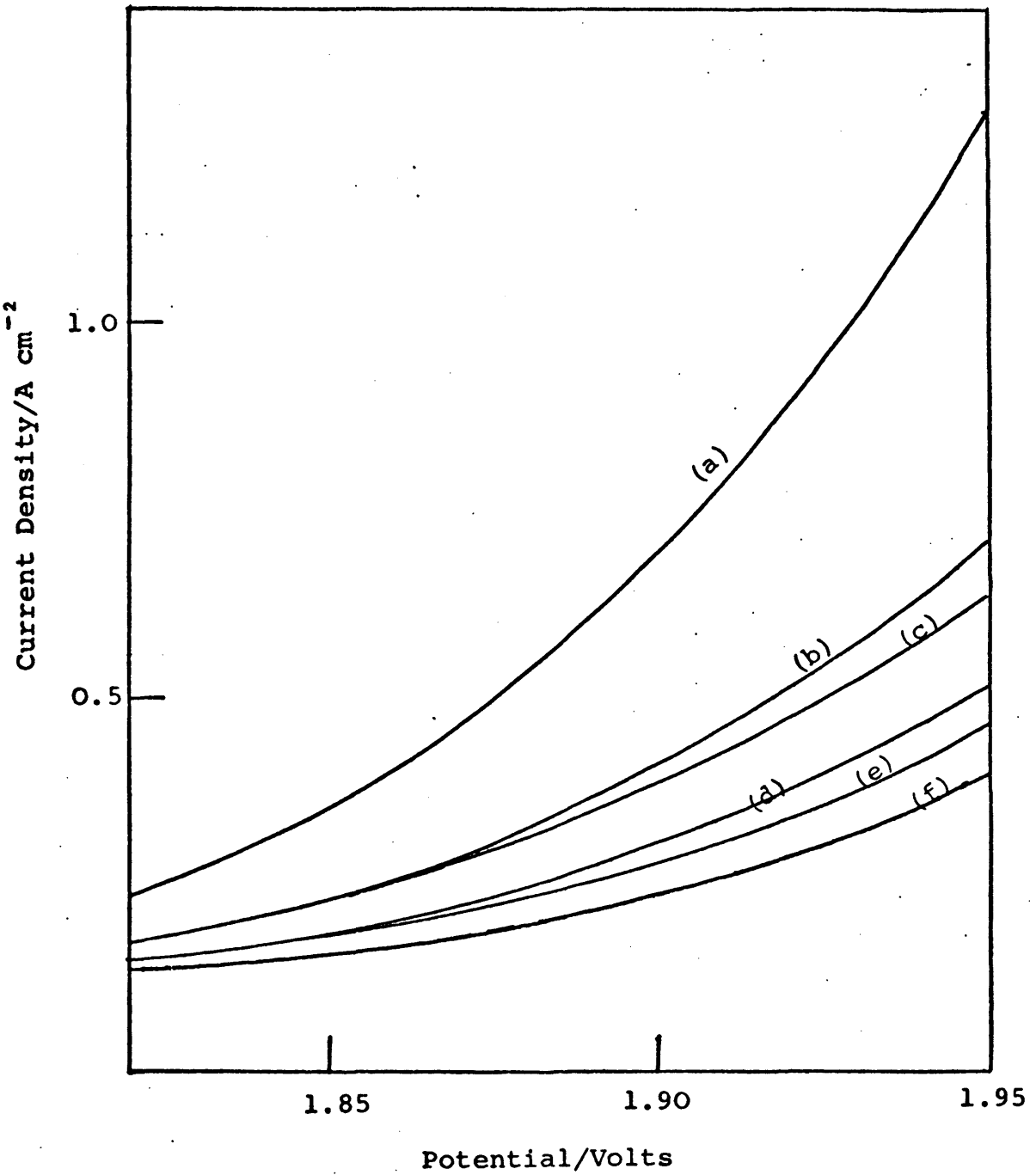

FIGURE 5.7 : Current potential curves for an iridium electrode in 1.0 mol dm^{-3} H_2SO_4 at 25°C and a scan rate of 0.5 V min^{-1}; in the absence of chloride (a), and in the presence of added HCl; (b) $5x10^{-4}$ mol dm^{-3}, (c) $1.0x10^{-3}$ mol dm^{-3}, (d) $2.0x10^{-3}$ mol dm^{-3}, (e) $3.0x10^{-3}$ mol dm^{-3}, (f) $5.0x10^{-3}$ mol dm^{-3}.

decreased by the progressive addition of chloride. Compared with corrosion into chloride-free electrolyte, corrosion into chloride containing electrolyte did not occur as readily and it resulted in a brown species with an absorbance maximum λ_{max} = 480 nm, whose colour did not change on standing.

DISCUSSION

5.10. Oxygen Evolution Mechanisms

There is at present no generally accepted mechanism for the oxygen evolution reaction. This lack is scarcely surprising in view of the complexity of the process which may involve electrochemical, adsorbed radical, and oxide film decomposition steps,[133] as well as taking place at an interface where the extent of metal oxidation can vary with both potential and time.[74] Attempts to use Tafel slopes ($\delta V/\delta$ log i) as an unambiguous criterion of reaction mechanism in the case of the oxygen evolution reaction[97] have been criticized by Breiter[133] and the fact that the reported Tafel slopes for this reaction at low current densities on iridium vary from 40 mV[97,169] to 80 mV[170] per logarithmic unit of current density reinforces the need for caution.

As mentioned earlier thermodynamic calculations by Hickling and Hills[81] suggest that hydroxyl radicals produced according to the equation

$$2H_2O \longrightarrow OH_{ads} + H_3O^+ + e^- \qquad 5.1$$

play a central role in the oxygen evolution process. The idea is supported by the observed[75] correlation between experimental oxygen overvoltage values and the estimated strength of the M-OH bond for a range of metals. This correlation is borne out by the present investigation where the Tafel plots (Figure 5.2) show that the rates of oxygen evolution, over the potential range investigated, are much higher on iridium as compared with the less strongly chemisorbing platinum.

5.11. Processes Occurring at Lower Potentials

There is ample evidence from cyclic voltammetry (see Chapter IV) that an iridium surface in aqueous solution is covered with an oxide film at potentials well below the reversible oxygen potential of 1.23 V. It seems reasonable, therefore, to assume (as have Damjanovic and co-workers[97,169] that at low over-potentials (< 1.57 V) there is a small equilibrium avtivity of adsorbed hydroxyl radicals on the oxidized electrode surface, and that the rate of oxygen evolution is determined by the reaction of these with other surface species such as oxygen. The break in the Tafel plot at 1.57 V (Figure 5.2) clearly indicates a change of mechanism at this potential, and it is possible that at this stage the reaction of the adsorbed radicals is so rapid (due to their high activity) that their rate of formation, according to equation 5.1 becomes rate determining. Although IrO_2 is quite a good electronic conductor there is, as seen in Chapter IV, evidence from cyclic voltammetry that over the region 1.4 V to 1.6 V the anodic film on iridium

can take up considerable quantities of oxygen and this increase in oxide stoichiometry may impede electron transfer. It is assumed, therefore, that above 1.57 V there is a non-equilibrium concentration of hydroxyl radicals on the oxide surface and an appreciable charge-transfer component in the total overpotential. Some evidence linking the change in oxygen evolution behaviour with changes in the properties of the oxide film is provided by the fact that the thick anodic film produced on an iridium surface by cycling the potential in a triangular manner (e.g. 0.01 V to 1.50 V at 10 Hz) corrodes off the surface above 1.57 V.

The decrease in oxygen evolution current with time under potentiostatic conditions at potentials less than ca. 1.8 V (Figure 5.1) is probably due to slow transformation, possible with further slow uptake of oxygen, of a thin layer of surface oxide resulting in lower reactivity or electron mobility in this region.

5.12. Processes Occurring at Higher Potentials

A sharp increase in current density occurs with an iridium electrode in acid solution at ca. 1.8 V (Figure 5.2). Above this potential it was also observed that the current density time behaviour at constant potential (Figure 5.1) differed from that at lower potentials as described earlier. These facts seem to indicate a change in the mechanism of oxygen evolution in this region. The onset of continuous iridium corrosion at about this potential

suggests a major change in the properties of the metal ions in the anodic film. It is possible that above 1.8 V a higher oxidation state of iridium is produced in the outer region of the oxide layer; this can react with water to yield an unstable oxide species which decomposes with evolution of oxygen gas and regeneration of the lower oxidation state of the metal ion. This type of cyclic mechanism involving participation of an ionic species in two valence states is well established in electrochemistry, a well-known example being the reduction of hydrogen peroxide at a mercury cathode in the presence of ferric ions.[131] The rate of reduction of hydrogen peroxide on mercury tends to be rather slow. However, on addition of a ferric salt the ferric ions are reduced to ferrous ions and the latter reduce the hydrogen peroxide and are thereby converted back to the ferric state to carry on the cycle. Some evidence in support of a mechanism of this type may be got from the work of Wöhler and Witzmann[142] who reported that by fusing iridium with sodium peroxide a compound of approximate composition IrO may be obtained, and that this liberates oxygen on treatment with sulphuric acid solution. Possibly a similar species is formed on iridium under anodic conditions. It is also interesting to note that while ceric sulphate is stable in sulphuric acid solution, it reacts with the water present to liberate oxygen gas when low concentrations of iridium ions are present in the solution.[171]

Both the oxygen evolution process and the corrosion process obey the Tafel relationship, and while the former is one million times faster than the latter, the observed slope values show that the corrosion rate is increasing with potential twice

as rapidly as the oxygen evolution rate. This result may be explained by assuming that the rate-determining step is the formation of the higher oxide species and that there is then competition between reaction with water, resulting in oxygen evolution, and the corrosion process. Of these two reactions, the former is a purely chemical process and is not expected to be greatly influenced by potential changes. The corrosion reaction on the other hand, since it involves electron transfer, is expected to increase with increasing anodic potential. Therefore, the more marked dependence of the corrosion process on potential can be explained in terms of this electrocatalytic mechanism involving formation of a reactive higher oxidation state.

It is likely that the hydroxyl radical is the intermediate in the oxygen evolution reaction not only at potentials below 1.8 V but also at short times after a potential step to values above 1.8 V. This would explain the initial decrease in current at these potentials. However, at longer times reaction via the higher oxidation state intermediate becomes more important than reaction via hydroxyl radicals and the current becomes almost constant since the species being oxidized is now within, and not simply on, the outer regions of the anode surface. A very slow increase in current density occurring above 1.8 V at these longer times probably reflects changes due to corrosion or rearrangement in the oxide film resulting either in an increase in the amount of oxide participating in the reaction or a lowering of the activation energy for the formation of the higher oxidation state.

The brown species formed in the bulk of solution during the course of the corrosion reaction is probably

IrO_2^{++}. This iridium VI species has been reported earlier by Dwyer and Gyarfas[172] who prepared it by oxidation of iridium(III) sulphate, perchlorate or nitrate at a smooth platinum anode. The purple solution obtained on addition of a reducible species to the brown solution was probably some form of quadrivalent iridium,[172] e.g. IrO^{++} or $(IrOOH)^{+}$.

The current obtained in base at potentials above 1.8 V is considerably smaller than the corresponding current in acid. Furthermore, it decays continuously with time (Figure 5.3). It appears, therefore, that even at these high potentials the oxygen evolution reaction in base occurs via a hydroxyl radical intermediate rather than by the type of oxide decomposition mechanism assumed in the case of acid. The difference could be explained either if the higher oxidation state of iridium was not formed or if it did not decompose readily in alkaline solution. Evidence in support of the latter is provded by the work of Wöhler and Witzmann[142] who observed that IrO is stable in alkaline solution. The possible formation of iridate species[152] ($IrO_4^{=}$) in solutions of high pH must also be borne in mind.

The chloride inhibition of the oxygen evolution reaction on iridium (Figure 5.7) is scarcely surprising since this anion is weakly hydrated and tends to displace water molecules in the inner region of the double layer.[173] It is capable of functioning as a ligand and by bonding to metal ions on the surface it can retard various electrode processes in the anodic region.[157]

It might appear at first that iridium is unsuitable as a substrate for oxygen evolution due to the corrosion reaction. However, this is not necessarily true since the current densities involved at the potentials where corrosion occurs are very large. Oxygen is evolved on iridium at 1.65 V at the same rate as on platinum at 1.95 V and a rate of oxygen evolution 30 times that on platinum at 1.95 V is obtained on iridium at a potential well below that at which detectable corrosion begins. This could be increased considerably by the use of iridized rather than bright iridium electrodes. From the viewpoint of industrial application, the high cost of iridium also dictates the use of thin iridium deposits on base metals such as titanium and the properties of such deposits, particularly those of high roughness factor, on such substrates would seem to merit investigation.

REFERENCES

1. E. A. Guggenheim, *J. Phys. Chem.*, 1929, 33, 842.

2. D. C. Grahame, *Chem. Rev.*, 1947, 41, 441.

3. E. Lange, *Z. Elektrochem.*, 1951, 55, 76; 1952, 56, 94.

4. J. O'M. Bockris and A. K. N. Reddy, *Modern Electrochemistry*, Vol. 2 (Macdonald, London, 1970), p.841.

5. *Ibid.*, p.702.

6. K. J. Vetter, *Electrochemical Kinetics, Theoretical and Experimental Aspects*, (Academic Press, London, 1967), p.82.

7. R. B. Whitney and D. C. Grahame, *J. Chem. Phys.*, 1941, 9, 827.

8. D. M. Mohilner, *Electroanalytical Chemistry*, Vol. 1, Ed. A. J. Bard (Arnold, London, 1966), pp.275-278.

9. D. C. Grahame, M. A. Poth and J. I. Cummings, *J. Amer. Chem. Soc.*, 1952, 74, 4422.

10. S. Levine, G. M. Bell and D. Calvert, *Can. J. Chem.*, 1962, 40, 518.

11. J. O'M. Bockris, M. A. V. Devanathan and K. Muller, *Proc. Roy. Soc. A* (London), 1963, 274, 55.

12. T. N. Anderson and J. O'M. Bockris, *Electrochim. Acta.*, 1964, 9, 347.

13. See ref. 8, pp.306-331.

14. *Ibid.*, pp.247-248.

15. W. J. Moore, *Physical Chemistry* (Longman, London, 1972), pp.205-206.

16. See ref. 6, p.17.

17. J. R. W. Warn, *Concise Chemical Thermodynamics* (Van Nostrand Reinhold, London, 1969), pp.99-100.

18. See ref. 6, p.121.

19. See ref. 4, p.959.

20. M. L. Tobe, *Inorganic Reaction Mechanisms* (Nelson, London, 1972), pp.129-133.

21. C. N. Banwell, *Fundamentals of Molecular Spectroscopy* (McGraw-Hill, London, 1972), pp.208-212.

22. P. Delahay, *Double Layer and Electrode Kinetics* (Interscience, London, 1966), p.182.

23. K. J. Vetter, *Z. Physik. Chem.* (Leipzig) A, 1950, 194, 284.

24. W. R. Grove, *Phil. Mag.*, 1839, 14, 127; 1842, 21, 417.

25. W. M. Latimer, *The Oxidation States of the Elements and their Potentials in Aqueous Solutions* (Prentice Hall, Englewood Cliffs, N.J., 1952) p.39.

26. G. Bianchi, F. Mazza and T. Muzzini, *Electrochim., Acta*, 1962, 7, 457; 1965, 10, 445.

27. J. O'M. Bockris and A. K. M. S. Huq, *Proc. Roy. Soc. A* (London) 1956, 237, 277.

28. N. Watanabe and M. A. V. Devanathan, *J. Electrochem. Soc.*, 1964, 111, 615.

29. J. P. Hoare, *J. Electrochem. Soc.*, 1962, 109, 858.

30. J. P. Hoare, *J. Electrochem. Soc.*, 1963, 110, 245.

31. J. P. Hoare, *J. Electrochem. Soc.*, 1964, 111, 610.

32. J. P. Hoare, *J. Electrochem. Soc.*, 1964, 111, 232.

33. J. P. Hoare, *J. Electrochem. Soc.*, 1964, 111, 988.

34. H. G. Bain, *Trans. Am. Electrochem. Soc.*, 1940, 78, 173.

35. L. Mond, W. Ramsay and J. Shields, *Z. Physik. Chem.* (Frankfurt), 1898, 25, 657.

36. A. N. Frumkin, A. Slygin and W. Medvedovsky, *Acta Physicochim.*, 1936, 4, 911.

37. M. Breiter, H. Kammermaier and C. Knorr, *Z. Elektrochem.*, 1956, 60, 37.

38. S. Schuldiner and R. M. Roe, *J. Electrochem. Soc.*, 1963, 110, 332.

39. S. Schuldiner and T. B. Warner, *J. Electrochem. Soc.*, 1965, 112, 212.

40. S. W. Feldberg, C. G. Enke and C. E. Bricker, *J. Electrochem. Soc.*, 1963, 110, 826.

41. K. J. Vetter and D. Berndt, *Z. Electrochem.*, 1958, 62, 378.

42. A. Hickling, *Trans. Faraday Soc.*, 1945, 41, 333.

43. A. D. Obrucheva, *Zh. Fiz. Khim.*, 1952, 26, 1448.

44. F. G. Will and C. A. Knorr, *Z. Electrochem.*, 1960, 64, 258.

45. A. K. N. Reddy, M. L. B. Rao and J. O'M. Bockris, *J. Chem. Phys.*, 1965, 42, 2246.

46. A. K. N. Reddy, M. Genshaw and J. O'M. Bockris, *J. Electroanal. Chem.*, 1964, 8, 406.

47. W. G. French and T. Kuwana, *J. Phys. Chem.*, 1964, 68, 1279.

48. F. C. Anson and J. J. Lingane, *J. Amer. Chem. Soc.*, 1957, 79, 4901.

49. H. A. Laitinen and C. G. Enke, *J. Electrochem. Soc.*, 1960, 107, 773.

50. W. Bold and M. W. Breiter, *Electrochim Acta*, 1961, 5, 145.

51. J. Giner, *Z. Elektrochem.*, 1959, 63, 386.

52. M. L. B. Rao, A. Damjanovic and J. O'M. Bockris, *J. Phys. Chem.*, 1963, 67, 2508.

53. A. Damjanovic, M. L. B. Rao and M. Genshaw, ASTIA Report No. AD405675 (November 1962).

54. J. A. V. Butler and G. Drever, *Trans. Faraday Soc.*, 1936, 32, 427.

55. F. G. Will and C. A. Knorr, *Z. Elektrochem.*, 1960, 64, 270.

56. W. Bold and M. W. Breiter, *Electrochim. Acta*, 1961, 5, 169.

57. M. W. Breiter, *Electrochim. Acta*, 1965, 10, 543.

58. G. Gruneberg, *Electrochim. Acta*, 1965, 10, 339.

59. H. A. Laitinen and M. S. Chao, *J. Electrochem. Soc.*, 1961, 108, 726.

60. G. P. Khomchenko, N. G. Ul'ko and G. D. Vovchenko, *Elektrokhimiya*, 1965, 1, 659.

61. L. Young, *Anodic Oxide Films* (Academic Press, New York, 1961), pp.4-5.

62. A. Guntherschultze and H. Betz, *Z. Phys.*, 1934, 92, 367.

63. Fr. Flade, *Z. Phys. Chem.*, 1911, 76, 513.

64. U. F. Franck, *Z. Naturf.*, 1949, 4a, 378.

65. K. J. Vetter, *Z. f. Elektrochem.*, 1958, 62, 642.

66. W. Schottky, *Halbleiterprobleme II* (Ed.W.Schottky,155),p.23

67. K. J. Vetter, *Z. Elektrochem.*, 1951, 55, 274.

68. K. J. Vetter, *Z. Elektrochem.*, 1954, 58, 230.

69. K. J. Vetter, *Z. Phys. Chem.*, 1953, 202, 1.

70. J. L. Ord and F. C. Ho, *J. Electrochem. Soc.*, 1971, 118, 46.

71. D. A. Vermilyea, *Advances in Electrochemistry and Electrochemical Engineering*, Vol. 3, Ed. P. Delahay and C. W. Tobias (Interscience, New York, 1963) p.258.

72. J. L. Ord and D. J. De Smet, *J. Electrochem. Soc.*, 1969, 116, 762.

73. V. V. Picheta, *J. Gen. Chem.*, USSR, 1931, 1, 377.

74. J. W. Schultze, *Z. Physik. Chem. N.F.*, 1970, 73, 29.

75. P. Ruetschi and P. Delahay, *J. Chem. Phys.*, 1955, 23, 556.

76. K. Y. Rosenthal and V. Y. Veselovskiy, *Dokl. Akad. Nauk. SSSR*, 1956, 111, 637.

77. F. P. Bowden, *Proc. Roy. Soc. A*, 1930, 126, 107.

78. M. A. Gerovich, R. I. Kaganovich, W. M. Vergelesov and I. N. Forochov, *Dokl. Akad. Nauk. SSSR*, 1957, 114, 1049.

79. P. C. Milner, *J. Electrochem. Soc.*, 1964, 111, 438.

80. A. Hickling, *Chem. Rev.*, 1949, 3, 95.

81. A. Hickling and S. Hill, *Trans. Faraday Soc.*, 1950, 46, 557.

82. L. D. Burke, F. McCarthy and T. O. O'Meara, *J. Chem. Soc. Faraday Transactions I*, 1972, 68, 1086.

83. J. P. Hoare, *The Electrochemistry of Oxygen* (Interscience, New York,1968) p.87.

84. R. Geriser and M. Gerisher, *Z. Phys. Chem.*, 1956, 6, 178.

85. J. O'M. Bockris and L. F. Oldfield, *Trans. Faraday Soc.*, 1955, 51, 249.

86. *Programmes of Research and Development Actions in the Field of Energy* (Commission of the European Communities COM(74) 2150, Brussels, 1975), p.19.

87. W. A. Titterington and J. F. Austin, *Extended Abstracts of the Electrochemical Society's 146th Meeting* (New York, 1974), pp.576,577.

88. M. L. B. Rao, A. Damjanovic and J. O'M. Bockris, *J. Phys. Chem.*, 1963, 67, 2508.

89. J. H. Sinfelt, *Catalysis Reviews*, Ed. H. Heinemann (Marcel Dekker, New York, 1970), p.195.

90. J. B. Goodenough, *Progress in Solid-State Chemistry*, Vol. 5, Ed. N. Reiss (Pergamon Press, 1971).

91. W. D. Ryden, A. W. Lawson and C. C. Sartain, *Phys. Lett A*, 1958, 26, 209.

92. J. Llopis and M. Vazquez, *Electrochim. Acta*, 1966, 11, 633.

93. L. D. Burke and T. O. O'Meara, *J. Chem. Soc. Faraday Transactions I*, 1972, 68, 839.

94. D. Galizzioli, F. Tantardini and S. Trasatti, *J. App. Electrochem.*, 1974, 4, 57.

95. L. D. Burke and T. O. O'Meara, *J. Electroanal. Chem.*, 1972, 36, App.25.

96. J.Llopis and L. Jorge, *Electrochim. Acta*, 1964, 9, 103.

97. A. Damjanovic, A. Dey and J. O'M. Bockris, *J. Electrochem. Soc.*, 1966, 113, 739.

98. J. Llopis, *Catalysis Reviews*, Vol. 2, Ed. H. Heinemann (Marcel Dekker, New York, 1969), p.172.

99. J. Llopis, J. M. Gamboa and V. Menendez, *Collection Czechoslov. Chem. Commun.*, 1971, 36, 528.

100. A. T. Kuhn and C. J. Mortimer, *J. Electrochem. Soc.*, 1973, 120, 231.

101. S. Puschaver, *Chem. and Ind.*, 15 March, 1975, p.236.

102. L. Meites, *Polarographic Techniques* (Interscience, New York, 1965) pp.59-61.

103. D. Britz and W. A. Brocke, *J. Electroanal. Chem.*, 1975, 58, 301.

104. B. R. Sundheim, *J. Electrochem. Soc.*, 1968, 115, 158.

105. A. Hickling, *Trans. Faraday Soc.*, 1942, 28, 27.

105a. J. Newman, *J. Electrochem. Soc.*, 1970, 117, 507.

106. J. D. E. McIntyre and W. F. Peck Jr., *J. Electrochem. Soc.*, 1970, 117, 747.

107. R. Bezmann, *Anal. Chem.*, 1972, 44, 1781.

108. E. R. Brown, D. E. Smith and G. L. Booman, *Anal. Chem.*, 1968, 40, 1411.

109. G. W. Osann, *Phil. Mag.*, 1827, 2, 391.

110. V. M. Goldschmidt, *Geochemistry* (Oxford, University Press, 1954).

111. R. W. G. Wyckoff, *Crystal Structures*, Vol. 1, (Interscience, London 1965), Chapter II.

112. W. P. Griffith, *The Chemistry of the Rarer Platinum Metals* (Interscience, London 1967), pp.7-11.

113. H. Remy and M. Kohn, *Z. Anorg. Allchem. Chem.*, 1924, 137, 365.

114. See ref. 83, pp.28-29.

115. N. A. Shumilova, G. V. Zhutaeva, M. R. Tarasevich and R. Kh. Burshtein, *Zh. Fiz. Khim.*, 1965, 39, 1012.

116. See ref. 83, pp.47-61.

117. G. Gruneberg, *Electrochim. Acta*, 1965, 10, 339.

118. M. Pourbaix, *Atlas of Electrochemical Equilibria in Aqueous Solutions* (Pergamon, London, 1966) pp.343-349.

119. L. D. Burke and A. Moynihan, *Electrochim. Acta*, 1970, 15, 1437.

120. H. H. Uhlig, *J. Electrochem. Soc.*, 1950, 97, 2150.

121. H. H. Uhlig, *Z. Elektrochem.*, 1958, 62, 700.

122. H. Schafer, G. Schneidereit and W. Gerhardt, *Z. Anorg. Allg. Chem.*, 1963, 319, 372.

123. S. Pizzini, G. Buzzanca, C. Mari, L. Rossi and S. Torchio, *Mat. Res. Bull.*, 1972, 7, 449.

124. O. De Nora, *Chem. Eng. Tech.*, 1970, 42, 222.

125. V. De Nora and A. Nidola, *Ext. Abs. Electrochem. Soc. Meeting* (Los Angeles, 1970), paper No.270.

126. S. Trasatti and G. Buzzanca, *J. Electroanal. Chem.*, 1971, 29, App.1-5.

127. D. Galizzioli, F. Tantardini and S. Trasatti, *J. App. Electrochem.*, 1974, 4, 57.

128. See ref. 112, pp.146-147.

129. U. R. Evans, *The Corrosion and Oxidation of Metals* (Edward Arnold, London, 1960), p.665.

130. J. W. Schultze and K. J. Vetter, *Ber. Bunsenges. Phys. Chem.*, 1971, 75, 470.

131. I. M. Kolthoff and E. P. Perry, *J. Amer. Chem. Soc.*, 1951, 73, 3718.

132. R. E. Harmon, S. K. Gupta and D. J. Brown, *Chem. Rev.*, 1973, 73, 21.

133. M. Breiter, see ref. 71, Vol. 1, Ch.3.

134. T. J. Borisova and V. I. Veselovski, *Zh. Fiz. Khim.*, 1953, 27, 1195.

135. See ref. 112, pp.134 and 156.

136. Smithson Tennant, *Phil. Trans.*, 1804, 94, 411.

137. *Platinum Metals Rev.*, 1964, 8, 60; *Tech. Bull.* (Englehard Industries Ltd.), 1965, 61.

138. J. Llopis and L. Jorge, *J. Electrochem. Soc.*, 1963, 110, 947.

139. W. E. Bell, M. Tagami and R. E. Inyard, *J. Phys. Chem.*, 1966, 70, 2048.

140. See ref. 112, pp.246-251.

141. J. H. Norman, H. G. Staley and W. E. Bell, *J. Chem. Phys.*, 1965, 42, 1123.

142. L. Wohler and W. Witzmann, *Z. Anorg. Allgem. Chem.*, 1907, 57, 323.

143. M. W. Breiter, C. A. Knorr and W. Volkl, *Z. Elektrochem.*, 1955, 59, 681.

144. A. Capon and R. Parsons, *J. Electroanal. Chem.*, 1972, 39, 275.

145. B. D. Kurnikov, A. I. Zhurin, V. V. Chernyi, Yu. B. Vasil'ev and V. S. Bagotskii, *Elektrokhimiya*, 1973, 9, 833.

146. M. W. Breiter, C. A. Knorr and R. Meggle, *Z. Elektrochem.*, 1955, 59, 153.

147. P. Stonehart, H. A. Kozlowska and B. E. Conway, *Proc. Roy. Soc. A*, 1969, 310, 541.

148. See ref. 83, p.59.

149. T. Biegler, *J. Electrochem. Soc.*, 1967, 114, 1261.

150. M. Bonnemay, G. Bronoel and M. Haim, *Compt. rend. C*, 1973, 277, 903.

151. R. Woods, *Proc. Symp. Electrocatalysis* (The Electrochemical Society, New Jersey, U.S.A., 1974), p.302.

152. See ref. 118, pp.373-377.

153. K. S. Kim, C. D. Sell and N. Winograd, see ref. 151, pp.242-257.

154. *Handbook of Chemistry and Physics* (The Chemical Rubber Co., Cleveland, Ohio, 51st edn., 1970), p.F-152.

155. A. Damjanovic and M. K. Y. Wong, *J. Electrochem. Soc.*, 1967, 114, 592.

156. R. Breyer and H. H. Bauer, *Alternating Current Polarography and Tensammetry* (Interscience, New York, 1963).

157. M. W. Breiter, *Electrochim. Acta*, 1963, 8, 925.

158. J. M. Otten and W. Visscher, *J. Electroanal. Chem.*, 1974, 55, 1.

159. J. M. Otten and W. Visscher, *J. Electroanal. Chem.*, 1974, 55, 13.

160. D. A. J. Rand and R. Woods, *J. Electroanal. Chem.*, 1974, 55, 375.

161. G. W. O. Briggs, *Specialist Periodical Reports, Electrochemistry*, Vol. 4 (Chem. Soc., London, 1974), Ch.3.

162. D. M. MacArthur, *J. Electrochem. Soc.*, 1970, 117, 422 and 729.

163. J. P. Gabano, J. Seguret and J. F. Laurent, *J. Electrochem. Soc.*, 1970, 117, 147.

164. K. R. Newby and A. B. Scott, *J. Electrochem. Soc.*, 1970, 117, 152.

165. L. Glasser, *Chem. Rev.*, 1975, 75, 21.

166. G. A. Perley and J. B. Godshalk, *U.S. Patent*, No. 2,416,949; British Patent No. 567,722, June 10th, 1942.

167. D. J. G. Ives and G. J. Janz, *Reference Electrodes*, (Academic Press, London, 1961) pp.376-377.

168. A. V. Boiko and L. I. Kadaner, *Elektrokhimiya*, 1973, 9, 1437.

169. A. Damjanovic and M. K. Y. Wong, *J. Electrochem. Soc.*, 1967, 114, 592.

170. J. P. Hoare, *J. Electroanal. Chem.*, 1968, 18, 251.

171. S. I. Ginzburg and M. I. Yuz'ko, *Zh. Anal. Khim.*, 1966, 21, 79.

172. F. P. Dwyer and E. C. Gyarfas, *Proc. Roy. Soc.*, N. S. Wales, 1950, 84, 123.

173. B. E. Conway, *Theory and Principles of Electrode Processes* (The Ronald Press, New York, 1965), Ch.3.

174. E. W. Berg and H. L. Youmans, *Anal. Chim. Acta*, 1961, 25, 470.

APPENDICES

APPENDIX 1

The following table which refers to the most recent data on the General Electric Company's solid polymer electrolyser[87] is included to illustrate the various sources of energy loss associated with the electrolytic production of hydrogen from water. Current density i = 2.15 A cm^{-2} (2000 A ft^{-2}); temperature, T = 82.2°C (180°F).

Theoretical Voltage (82.2°C)	=	1.18 volts
Oxygen Overvoltage	=	0.38 volts
Hydrogen Overvoltage	=	0.04 volts
Electrolyte Resistance Losses	=	0.45 volts
Leads Losses	=	0.05 volts
Operating Cell Voltage	=	2.10 volts

APPENDIX 2

PUBLISHED WORK

1. Lowering of the Overvoltage for Oxygen Evolution at Noble Metal Electrodes in the Presence of Ruthenium Salts.

   D. N. Buckley and L. D. Burke, *J. Electroanal. Chem.*, 1974, 52, 433-442.

2. Enhancement of Charge Capacity of an Iridium Surface in the Anodic Region.

   D.N. Buckley and L. D. Burke, *J. Chem. Soc. Faraday Trans. 1*, 1975, 71, 1447-1459.

3. Oxygen Evolution and Corrosion Behaviour of Iridium under Anodic Conditions.

   D. N. Buckley and L. D. Burke, *Extended Abstracts of the Electrochemical Society's Fall Meeting*, New York, 1974, 580-581.

The following articles have been submitted for publication to the Faraday Division of the Chemical Society (London).

4. Oxygen Evolution and Corrosion at Iridium Anodes.
   L. D. Burke and D. N. Buckley.

5. Factors Effecting the Enhancement of the Charge Storage Capacity of an Iridium Anode.
   D. N. Buckley, L. D. Burke and J. K. Mulcahy.